Highly Filled, Durable, and Sustainable Wood-Plastic Composites from Recycled Thermoplastics

by

Dylan Fernand Jubinville

A thesis

presented to the University of Waterloo

in fulfillment of the

thesis requirement for the degree of

Doctor of Philosophy

in

Chemical Engineering

Waterloo, Ontario, Canada, 2022

Examining Committee Membership

The following served on the examining committee for this thesis. The decision of the examination committee is by majority vote.

External Examiner:	Patrick Lee Professor, Mechanical and Industrial Engineering Department, University of Toronto
Supervisor:	Tizazu Mekonnen Associate Professor, Chemical Engineering Department, University of Waterloo
Internal Examiner:	Alex Penlidis Professor, Chemical Engineering Department, University of Waterloo
	Costas Tzoganakis Professor, Chemical Engineering Department University of Waterloo
Internal-External Examiner:	Giovanni (John) Montesano Associate Professor, Mechanical and Mechatronics Engineering Department, University of Waterloo

Author's Declaration

I hereby declare that I am the sole author of this thesis. This is a true copy of the thesis, including any required final revisions, as accepted by my examiners. I understand that my thesis may be made electronically available to the public.

Abstract

The increasing concern for environmental sustainability and the accumulation of solid waste (e.g. single-use plastics) has led to an increased interest in the utilization of renewable feedstocks and recycling of plastics to produce sustainable products, such as wood plastic composites (WPCs). As such, the first two stages of this thesis investigated reprocessing polypropylene (PP) as well as maleated PP (MAPP) to simulate recycling as a potential matrix for highly filled WPCs (70 wt.% wood). The extent of PP and MAPP recycling was analyzed using high temperature gel permeation chromatography (H-GPC), light scattering, nuclear magnetic resonance (NMR), rheology, microscopy, and other physical/mechanical properties. Successive thermo-mechanical reprocessing caused noticeable chain scission, shown by the melt viscosity and the slight reduction in the average molecular weight. Furthermore, other properties like tensile strength and modulus did not change significantly with respect to recycling. The repeated reprocessing allowed to incorporate high loading of wood fiber to produce highly filled WPC. This indicates that the recycling of PP could be of great importance to reduce waste accumulation and produce highly filled WPCs. As well, the recycling of MAPP could be an important and effective strategy to reduce virgin and petroleum-based MAPP manufacturing while revitalized mechanical properties for WPCs.

The last stage of this project involved the chemical modification of WF with dodecenylsuccinic anhydride (DDSA), in order to enhance the hydrophobicity of the wood, as well as the recycling and maleation of poly(lactic) acid (PLA). The successful modification of the WF was evaluated using X-ray photoelectron (XPS) and Fourier transform infrared (FTIR) spectroscopy as well as solvent dispersibility analysis. Recycling of PLA had a profound effect on PLA's crystallinity and modulus as other properties were not affected. The recycling of PLA had a considerable effect on PLA's crystallinity and modulus even though other properties were not affected. The addition of WF more significantly affected PLA's crystallinity; all the while, also increasing the storage and loss modulus of the fabricated biocomposites. Moreover, the modified wood flour (mWF) WPCs had greatly enhanced water repellent capabilities. Lastly, the maleation of the recycled PLA allowed better interaction with the WF, which further aided in controlling the dimensional stability of the WPCs even as tensile properties were not affected. Overall, this study aimed to develop highly-filled, more durable, and recycled WPC for both the construction and packaging industries and the success of this project has many benefits to the emerging circular economy and closed loop recycling.

Acknowledgements

First and foremost, I would like to express my sincerest gratitude for my supervisor, mentor, Dr. Tizazu Mekonnen who at his core is a very compassionate, patient, driven, intelligent person who helps his team to work for absolute success. Thank you for fighting to get me into the program and putting your trust in me. I would also like to extend my thanks to Dr. Costas Tzoganakis who provide valuable resources and access to equipment that I might not have been able to complete my PhD otherwise as well as always providing way to strength the research and elevating it. I'd also like to thank Dr.'s Ahmed Ghavami and Neil McManus who took me on as a TA and allowed me to grow my leadership skills all the while being valuable sources of information. Lastly, I would like to thank my committee for being a part of the journey with me and helping become a better researcher.

I want to thank the office staff on the third floor, especially Judy, who has always gone completely out of her way to ensure students are comfortable, on track, and taken care of. Even during COVID lockdown, Judy would call students if needing to explain something and to help whatever need be. As well, the technical staff especially Bert Halbert, Charles Dal Castel, and Ralph Dickhout for all of the support and technical expertise that I could not have gone without. I'd also like to thank Dr. Tizazu Mekonnen's research in its entirety for being there for moral and intellectual support when needed. Lastly, the financial support for this body of work was provided by Natural Resources Canada (NRCan) through the Clean Growth Program and both Ingenia polymers and Total Corbion for the generous donations of PP, HDPE, and LDPE as well as PLA, respectively, for this research to be conducted.

Dedication

I'd like to dedicate this work to my sister for all she has done to help me and for who the person she has become since we were kids. I'd like to dedicate this to my friends who has been there since the start of this crazy academic obstacle course I have undertaken and all of whom are part of my chosen family. You have always provided means of relaxation, closure, and you are all always your truest of selves. Lastly, I dedicate this work to my partner and our dogs, Gryphon and Dexter, who has helped see me through at every step and always being my support to fall on to.

I can't fully express my gratitude to every person but to everyone who has been there along the way,

Thank you.

List of Figures

List of Appendix A Figures and Tables

List of Appendix B Figures and Tables

List of Appendix C Figures and Tables

List of Schematics

List of Tables

List of Abbreviations/Nomenclature (Alphabetical)

%	percent	**Deg.**	Degree
%Abs	%Absorbance	**DI water**	Deionized water
%TS	Percent Thickness Swelling	**DLS**	Dynamic Light Scattering
$\%W_0$	Weight loss at 0%	**DMA**	Dynamic Mechanical analysis
$\%W_{50}$	Weight loss at 50%	**DMT**	Dimethyl Terephthalate
%WA	Percent Water Absorption	**dn/dc**	Specific Refractive Index Increment
$\%\chi_{CR}$	Percent crystallinity (DSC)	**DSC**	Differential Scanning Calorimetry
(G)(M)Pa	(Giga)(Mega)Pascal	**dTCE**	1,1,2,2-tetrachloroethane-d2
(L)LDPE	(Linear) Low-Density Polyethylene	**DTG**	Derivative Thermal Gravimetric Analysis
(m)WF	(Modified) Wood Flour	**EC**	European Commission
°C	Degree Celsius	**EPA**	Environmental Protection Agency
3D	Three Dimensional	**EPS**	Expanded Polystyrene
ABS	Acrylonitrile Butadiene Styrene	**EU**	European Union
AF	Almond Flour	**eV**	Electron Volts
ANOVA	A one-way analysis of variance	**FTIR**	Fourier Transformed Infrared
aPP	Atactic Polypropylene	**G'**	Storage Modulus
ASTM	American Society for Testing Materials	**G"**	Loss Modulus
atm	Standard Atmospheric Pressure	**GDP**	Gross Domestic Product
Au	Gold	**h**	Hours
BHET	Bis(Hydroxyethylene) Terephthalate	**H**	Hydrogen
Bt	Billion Tonnes	**HB**	Herschel-Buckley
C	Carbon	**HB**	Herschel-Buckley
-C=O	Carbonyl	**H_C**	Enthalpy of crystallization
C^{13}	Carbon-13	**HDPE**	High-Density Polyethylene
CAD	Canadian Dollar	**H-GPC**	High Temperature Gel Permeation Chromatography
-CH-	Methine	**H_M or H_F**	Enthalpy of melting
$-CH_2-$	Methylene	**hr**	Hours
$-CH_3$	Methyl	**HSI**	Hyperspectral Imaging
CI	Carbonyl Index	**Hz**	Hertz
CO	Carbon Monoxide	**iPP**	Isotactic Polypropylene
CO_2	Carbon Dioxide	**ISID**	International Dismantling Information System
CPS	Counts per second	**J/g (m)**	Joules/gram or Joules/meter
D	Diffusion Coefficient	**KDal**	KiloDaltons
DCP	Dicumyl Peroxide	**kPa s**	Kilopascal seconds^n
DDSA	Dodecenyl Succinic Anhydride	**LVR**	Linear Viscoelastic Region

m	Consistency index	**REACH**	Registration, Evaluation, Authorization and Restriction of Chemicals
MA	Maleic Anhydride	**rePP3**	Recycled PP 3 times and maleated
MAPP1	Recycled MAPP	**S**	Sorption Coefficient
MFR(I)	Melt Flow Rate or Index	**SA**	Succinic Anhydride
mins	Minutes	**SAA**	Surface Area Analysis
MPLA1	Maleated recycled PLA	**sc-CO_2**	Super Critical Carbon Dioxide
Mt	Million Tonnes	**SCF**	Stress Concentration Factor
MW	Molecular weight	**SEM**	Scanning Electron Microscope
M_W	Weight-average molecular weight	**sPP**	Syndiotactic Polypropylene
MWD	Molecular Weight Distribution	**T_C**	Crystallization Temperature
N	Nitrogen	**T_{CC}**	Cold Crystallization Temperature
n	Power index	**T_G**	Glass Transition Temperature
NA	North America	**TGA**	Thermal Gravimetric Analysis
NAFTA	North American Free Trade Agreement	**T_M**	Melting Temperature
NAFTA	North American Free Trade Agreement	**UEAtc**	European Union for Building Products Approval
NMR	Nuclear Magnetic Resonance	**UHMWPE**	Ultra-High Molecular Weight Polyethylene
O	Oxygen	**UK**	United Kingdom
P	Permeability Coefficient	**US(A)**	United States (of America)
PC	Polycarbonate	**UV-**	Ultraviolet-
PDI	Polydispersity Index	**WPC**	Wood Plastic Composite
PE	Polyethylene	**Wt.%**	Weight Percent
PET	Polyethylene Terephthalate	**XPS**	X-ray photoelectron spectroscopy
PLA0	Virgin Poly(lactic) acid	**Z-N**	Ziegler-Natta
PLA1	Recycled PLA (1 time)	**α**	Alpha
PMA	Poly(maleic anhydride)	**β**	Beta
PMMA	Poly(Methyl Methacrylate)	**δ**	Delta
PO	Polyolefin	**η**	Viscosity
POM	Polarized Optical Microscope	**η_0**	Zero Shear Viscosity
PP	Polypropylene	**η_∞**	Infinity Shear Viscosity
ppm	Parts per million	**µL**	Micro-litre
PS	Polystyrene	**µm**	Micro-meter
PTFE	Polytetrafluoroethylene	**ρ**	Density
PUR	Polyurethane Rubber	**τ_0**	Yield Stress
PVC	Polyvinyl Chloride	**ω**	Angular Frequency
Rad/s	Radians per second	**ω_B**	Critical Angular Frequency

Chapter 1 – Introduction

1.1 Biomass and its Constituents

Over the course of human history, culture changing innovations (e.g. domestication of livestock, agriculture practice and adaption, and the industrial revolution) have aided in expanding the human population while, consequently, having severe ecological impacts. Biomass may be defined as a renewable resource of organic material that originates from both plants and animals and in 2021 provided ~5% of the total primary energy that the US used that year [1,2]. Typically, biomass is reported by its mass of carbon since that property is independent on moisture content, but other methods may also include measuring the dry weight [1]. It has been estimated that the sum of biomass across all taxonomic groups, on Earth, is approximately 550 gigatons of carbon (Gt C) with 80% being taken up by land plants and another 15% representing bacterial biomass. The last 5% is contributed to groups such as fungi, protists, animals, and viruses (in descending mass of carbon order) [2].

For the purposes of this work, biomass is defined as a plant derived material, which is generated from the reaction of CO_2 in the presence of air, water, and sunlight (i.e. photosynthesis) in order to produce carbohydrates [1]. Plant based biomass may be divided into aboveground biomass, representing 320 Gt C, and belowground biomass (e.g. roots and microbes) accounting for ~160 Gt C [2]. Furthermore, plant biomass is mostly woody (~70%) and metabolically inert as it comprised mostly of stems and tree trunks. Plant biomass is also typically localized to terrestrial environments with <1 Gt C being in marine environments (e.g. algae and seagrass) [2]. Moreover, plant biomass used as harvest crops, are generally categorized as first-, second-, third-, and fourth-generation biomass; where the first-generation

refers to food grade sources (i.e. starch crops and sugars), the second-generation biomass is residual and non-food fraction crops with higher lignocellulosic, while the third- and fourth-generation biomass is derived from algae and microalgae [3,4].

Outside of using biomass as fuel and energy resources, there has been increased focus over the past few decades on creating composites derived from lignocellulosic materials (i.e. wood). As displayed in **Figure 1**, the chemical composition of most plant-based biomass is in the forms of cellulose, hemi-cellulose, and lignin. Furthermore, the elemental breakdown for those groups, on average, is made up of 50% carbon, 5% hydrogen, 40% oxygen, and the remaining fractions (5%) are nitrogen and various metal salts [5]. The lignocellulosic components all have active functional groups as primary and secondary hydroxyls, carbonyls, carbon-carbons, ethers, and acetal linkages [6]. Other compounds that may also be found within lignin-based polymers are ethylenic and sulfur-containing groups [6]. Cellulose is a biopolymer and carbohydrate which is produced initially as glucose from water and carbon dioxide during photosynthesis. It is the principal constituent of wood and other natural fibres, which forms the structural framework of plant cells [4]. Cellulose (see **Figure 1**) contains glucose ($C_6H_{12}O_5$) bound together by β-glycosidic linkages which form linear chains that are stable and resistant to chemical attack due to the large number of hydrogen bonds between the cellulose chains [3]. Hydrolysis and other degradation mechanisms may render cellulose down to cellobiose repeating units ($C_{12}H_{22}O_{11}$) and eventually back to its monomer unit, glucose. Cellulose's heat resistance will differ depending on its original biomass source but literature reports that it typically decomposes between 300 to 400 °C in an inert atmosphere [7,8].

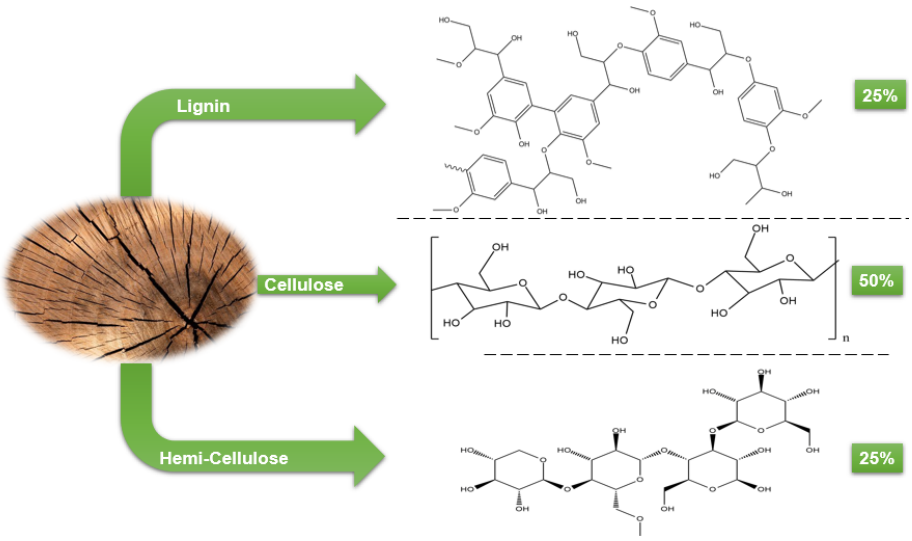

Figure 1. Structural components of wood derived products. (Adapted from S. Borysiak et al (2006)) [9].

Hemi-cellulose, shown in **Figure 1**, is a short and highly branched chain with five different sugars. It contains two 5-carbon sugars (i.e. D-xylose and L-arabinose) and three 6-carbon sugars (i.e. D-galactose, D-glucose, and D-mannose) as well as uronic acid [3]. The branched structure of hemi-cellulose gives it an amorphous property which makes it considerably more vulnerable to be hydrolyzed into individual sugar components compared to cellulose. In hard wood, hemi-cellulose will hydrolyze into more five-carbon sugars while soft wood yields more six-carbon sugars [3]. In terms of thermal stability, hemi-cellulose is the weakest as it typically decomposes between 200 to 300 °C and through pyrolysis it will mainly produce non-condensable gases. Lastly, lignin (see **Figure 1**) is the non-carbohydrate polyphenolic portion of wood and other biomass sources that helps to cement the cells together and supports the cell wall. Lignin is a highly complex, crosslinked, aromatic structure with a typical molecular weight of approximately 10,000 g/mol and it is the biggest contributor to the bio-charcoal end product [3].

1.2 Biocomposites

Conventional polymeric composites have been around for the past century and longer with the systems reaching commodity status by the 1940's [10]. Polymer composites are usually made from thermoplastic or thermoset polymers that are primarily reinforced with synthetic fillers like glass fibres or talc making them much more durable and stronger than an unfilled polymer [11]. These material types are usually constructed for desired properties (*i.e.* electrical conductivity, toughness, heat deflection etc.) and not solely just to increase the material's strength. However, due a number of sustainability factors and strict environmental policies, an emerging trend towards biobased and sustainable fillers is ever increasing helping to turn the tide away from non-sustainable practices in both academia and industry. This trend to go towards sustainability brings forth and empowers a more green and circular economy. A circular economy helps to promote the capitalization of natural and renewable resources, their recyclability, other end of service life option (i.e. reuse) as well as the potential to offset fossil fuel consumption [12]. The rapid depletion of natural and non-renewable resources across the globe has helped to drive the demand and search for innovation with regard to renewable resources that continues to drive industries to investigate the utilization of biobased alternatives [10]. As biobased materials are becoming more mainstream, research and markets tend to follow the evolving societal demands. **Figure 2** highlights the relative research areas, from 2007 to 2016, that investigate and produce composites containing wood or lignocellulosic fillers with the three biggest consumers being in material sciences, engineering, and polymer science [12]. As **Figure 2** displays, the number of publications focusing on wood and lignocellulosic materials has significantly increased year over year from 2007 to 2018.

Table 1. Relative research interests related to wood and other lignocellulosic as reinforcement materials. (Adapted from A. Gallos et al.)[12]**.**

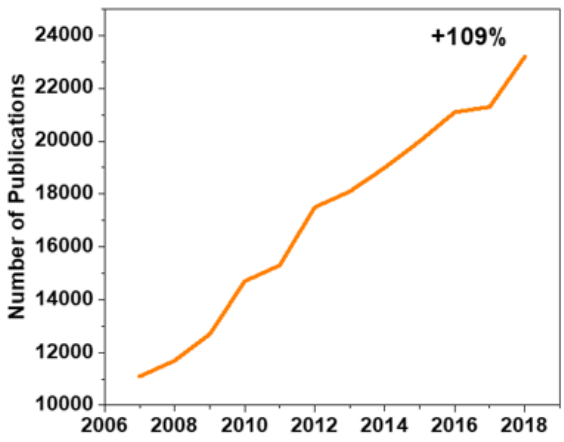

Industry	Research interest (%)
Material Science	45
Ecology	4
Engineering	25
Polymer Science	17
Forestry	13
Chemistry	11
Agriculture	9
Bio-Tech	8
Energy/Fuels	7
Plant Science	4

Figure 2. Publication related to wood and other lignocellulosic fibres from 2007 to 2018. (Data taken from Google scholar search).

Biocomposites are a form of materials that strive to be fully biodegradable and "green" by means of combining both natural fibers with a biodegradable resin (preferably bio-based). The main advantages to the use of green composites sourced from renewable sources are that they are more environmentally friendly and in many cases biodegradable making them green as their cradle to crave is more of a continuous cycle as opposed to a start/stop like most post-consumer plastic products. Biocomposites can be either plant based, comprised mostly of cellulose, or animal based, which contains mostly protein. Additionally, plant fibers may further be divided into 6 sub-groups based on the part of the plant the fiber is yielded from (*i.e.* core, seed, leaf, bast, grass or reed grass, and agriculture residues/other types) [13]. Major drawbacks to the use of natural fibers are geographic availability and variability, high moisture absorption, complex and inefficient supply and transport chain as well as their low thermal stability (< 200 °C) compared to synthetic fibers and some polymer resins [13].

In general, biocomposites are attractive materials because of their low cost, light weight, can be biodegradable, with high specific moduli, and being more environmentally sustainable compared to the synthetic-fiber-reinforced polymer composites [14]. The performance of biocomposites depends on several factors, including fiber chemical composition, cell dimensions, microfibril angle, defects, interaction, and both physical and mechanical properties of the fiber within the matrix [13]. Compatibility of wood fibers has been studied quite extensively with a range of thermally suitable polymer resins and they are typically enhanced through a few techniques, for example chemical and/or physical modification as well as the addition of a coupling agent or compatibilizer. For the remainder of this thesis, wood-plastic composites will be the main biocomposite of focus.

1.2.1 Wood-plastic composites (WPC)

Wood composites encompasses a wide range of different derivative wood products and can also be sub-categorized as engineered ("man-made") wood or WPCs [15,16]. Manmade or engineered wood employs the process of binding and reforming wood strands, flour or even whole boards together in a layered fashion, termed ply, through heat, glue, and pressure. Both engineered wood and WPCs are products that are typically used as replacement for natural wood products and show usage in wet working environments due to the hydrophobic polymer encapsulating and protecting the hydrophilic wood and other natural materials. This in turns aids in the durability of these composites and decreasing the amount of time and money for maintenance, which is especially appealing for the construction, automotive, and acoustics industries.

As previously mentioned, due to the tailorable nature of WPCs they are used in many different applications with most widespread usage being in home and industrial construction mainly as outdoor decking, railings, fencing, benches, windows, and doorframes, and even to replace steel joists and beams. Specifically, in the North Americas (NA) there is phenomenal growth of WPCs usage in the construction and automotive industries driven by weight reduction benefits, fuel saving advantages in automotives, and overall ecological benefits. Other factors include stricter environmental regulations, demand for the usage and recovery of chemicals, increase consumer (end user) education and awareness, changes in lifestyle, and more [17]. Due to this phenomenal growth, governmental agencies have provided financial resources for research and innovation within this market sector. Such agencies include the US Department of Agriculture (USDA), the US Department of Energy (DOE), the Forest Products Laboratory (FPL), Natural Resources Canada (NRC), and the Agricultural and Agri-Food Canada (Ag-Canada). In the United States (US) and Canada, there are more than 30 main WPCs producers and of that, the top 20 maintain 97% of the overall market value, between 2004 and 2008 [17]. Currently, some of the major WPC manufactures and sellers that are helping to bolster the market share of this product are TimberTech Limited, Trex Company Inc., Fibreon LLC., and WPC-wood plastic A.S., to name a few. In 2007, the global production of WPCs was ~ 0.9 Mt, with NA producing about 97% of that total quantity. More recently, a few reports on the WPC global market had capitalized on ~4.4 billion USD in 2016 at ~4.2 million tonnes (Mt) and expected to gross up to 8.8 billion USD by 2022 with a compound annual growth rate (CAGR) of 12.3% [18]. From 2007 to 2016, the WPC global production grew 367% [17,19].

One of the earliest patents for WPCs was assigned in the 1970's to *GOR Applicazioni Speciali SPA* from Turin, Italy who compounded a 50:50 wt.% mixture of polypropylene (PP) and wood flour (WF). A short while afterwards, 1983, a company called *American Woodstock* located in Sheboygan, Wisconsin began the first major production of WPCs within NA [19]. They began producing interior panels out of PP and 50 wt.% WF for the automotive industry using the Italian extrusion technology. The company compounded the WPC in-line and extruded a flat sheet and formed into various interior components [19]. Although *American Woodstock* had the first reported major production of WPCs, the existence of WPCs has been known and used since the start of the 20th century when the automotive company *Rolls Royce* implemented wood gear boxes and side paneling in 1916 [19]. The next major spike for WPC manufacturing occurred in the 1990's where international conferences regarding WPCs began to grow steadily in the hopes to bring together both researchers and industrial representatives from the plastics and forestry sectors. In 1991, the first *International Conference on Woodfibre Plastic Composites* occurred in Madison, Wisconsin as well, similar conferences began to appear in Toronto, Canada throughout the 1990's [19]. At the end of the 20th century, multiple companies began to produce and capitalize on WPC across the global especially in Asia-Pacific and Europe [17]. Also, *Advanced Environmental Recycling Technologies* (AERT) from Junction, Texas and a division of Mobil Chemical Company from Winchester, Virginia brought to market solid WPCs consisting of Polyethylene (PE) and 50 wt.% wood fibre for applications of deck boards, landscape timbers, picnic tables, and industrial flooring [19].

1.2.1.1 Factors effecting the extrusion and overall performance of WPCs

The performance of WPCs, once produced, also depends on several factors which includes aspect ratio of the wood fibre, type of wood (soft or hard), chemical composition, wood cell dimensions, wood microfibril angle, wood fibre defects, resin type, and resin to fibre ratio/interaction [13]. Thus, in order to effectively fabricate wood like structures it is essential to understand the shortcoming and underlying issues involved with the extrusion of these materials. For WPCs, the two most important factors are the WPCs melt viscosity and wood/polymer interaction and dispersion.

1.2.1.2 Filler/Resin interaction and dispersion

The interfacial bonding between the wood and the polymer matrix is important for stress transfer and the overall mechanical properties of the composite. In fact, most research on these materials results in poor interfacial bonding between the matrix and filler. Overall, the compatibility of these fillers has been studied extensively by means of chemical and/or physical modification, pyrolysis as well as the addition of a coupling agent or compatibilizer [20]. In terms of the dispersion of wood derived fillers within a polymer matrix and their interaction with each other, careful study must be conducted to overcome this concern.

It is well known that wood is hydrophilic in nature due to its polarity which typically causes it to agglomerate when used in a hydrophobic polymer matrix (apolar) and therefore chemical modification and coupling agents are typically utilized to facilitate dispersion and bonding. Common coupling additives include stearic acid, maleated polymers, titrates and more [21–24]. A study conducted by D.G Dikobe et al., (2017) investigated the efficacy of

blending maleated PP (MAPP), as a main phase, with PE in the presence of WF against that of a PP/PE WPC. The researchers used a batch mixer at a temperature and speed of 190 °C and 30 rpm and held for 15 mins to ensure proper mixing. The generated WPCs were then compression molded at 190 °C in order to produce test specimens. They used a scanning electron microscope (SEM) on cryo-fractured surfaces to evaluate the effectiveness on MAPP/PE WPC against that of the PP/PE WPC. The morphology of the MAPP/PE WPC is much smoother with minimal to no noticeable boundary layers and pullout regions, unlike, the PP/PE WPC which has clear evidence of particle pull out, breakage, and poor particle/matrix interaction. This is a result of the hydrophilic nature of wood and the hydrophobic nature of PP and PE, unlike with the MAPP/PE WPCs system which was able to produce hydrogen bonds between the PE and the WF. Upon examination of the tensile properties, it was determined that the MAPP/PE WPCs had better tensile strength and elongation properties; however, the PP/PE WPC systems had a better Young's modulus which was attributed to the nature of the base polymers forming a co-continuous matrix [24]. They concluded that the better properties were a result of interaction between MAPP and the Wood content due to the formation of hydrogen bonds between functional groups giving rise to better properties while indicating that PP could be removed entirely from the process [24].

Another study looking at the influence of chemical modification on WF with regard to the mechanical properties of PP/MAPP WPCs compounded by a batch mixer was a study by M. Farsi (2010). In this study, the WF was pre-treated with sodium hydroxide, benzoyl chloride, acrylic acid, and silane in order to observe how these treatments influence the

interfacial strength between PP and the WF. The results found that the inclusion of pre-treated wood content increased the tensile strength and modulus in all cases to varying degrees depending on the conditioning [22]. The most significant increase in tensile modulus was after the benzoyl chloride treatment as a result of the wood becoming more reactive due to benzoyl attachment caused by benzoylation reaction [22]. While the most significant increase in tensile strength was noted after the alkaline treatment the increase in the crystalline content of cellulose while removing impurities producing a more texturized and rougher surface resulting from the treatment [22]. Both of these studies showcased why manufactures often utilizes the aid of additives or treatments to enhance the overall performance but at greater overhead and materials cost.

1.2.1.3 WPC melt viscosity

The melt viscosity is the other major limitation to the manufacturing of these composite systems and a proper study/understanding of its material flow is essential. With that, the two most common methods for measuring the physical melt properties of WPCs are rotational and pressure driven rheometer evaluations. A pressure-driven rheometer forces a fluid through a narrow circular (capillary) or rectangular (slit) die by means of an externally applied pressure gradient. An issue with this method, with regard to WPCs, is the sieving phenomenon which occurs as wood particles tend to aggregate in clusters and separate from the polymer at the capillaries or slit's entrance while the passageway narrows. As well, an oscillating pressure may also be observed due to the fluttering phenomenon [25]. With that in mind, a particular advantage to these machines is that they do not need an inert atmosphere as they work with

low oxygen which reduces oxidative degradation [25]. With rotational rheometers, a layer of fluid is placed between two plates where one plate is fixed and the other rotates creating a torsional flow. The particular advantage to the use of these rheometers is that they are simple to use, no fibre deterioration issues, and minimal wall slip while also obtaining additional information regarding the materials interface and dispersion properties [25]. The main difference with these two methods is the range of shear rate that can be observed as pressure-driven focuses on high shear rates while rotational rheometers work with medium and low shear rates [25].

As it is known, the viscosity ($\eta = \frac{\tau}{\dot{\gamma}}$) of a given fluid is described as the ratio between the shear stress (τ) and the shear rate ($\dot{\gamma}$). The drastic increase in viscosity for WPCs generates large pressures during processing giving rise to flow issue which is exacerbated with increasing wood content. For WPCs it is well documented that with increasing wood content the apparent viscosity of the material increases drastically and at sufficiently high levels of wood the counteracting pressures on the melt are too high to overcome and no flow will occur [25]. There is little corrections one can apply to this issue as it is not possible to increase the temperature due to the thermal stability limitations and increasing the shear rate would add excess heat accelerating polymer degradation. In most cases, processers employ lubricants to assist with the materials wall slip and flow or they will only use polymers of high melt index to assist flow but the overall strength of the material will be lowered.

A study evaluating the rheological and mechanical characterization of PP based WPC by V. Mazzanti et al., (2016) recorded the changes in the viscosity with increasing wood

content as well as varying temperatures. The findings showed that as the wood filler content increased from 30 to 70 wt.% the melt's viscosity has also significantly increased from 80,000 to 1,000,000 Pa·s [26]. Their other pertinate finding in the study was obtained by varying the testing temperature from 170 to 200 °C with neat PP. They noted that with increasing processing temperature the ability for the polymer to flow more "fluid like" has increased as a result of decreasing viscosity due to chain scission and thermal degradation [26]. These results showed how increasing the tempature assists in flow but will begin to degrade the wood content especially when shear was introduced.

An interesting solution to potentially overcome the melt viscosity limitation without solely relying on processing additives and pre-treatments was to employ recycled/degraded polymers for their reduced viscosity. A common trend with WPC manufacturing was the use of recycled plastics as a complete replacement or a partial offset to virgin polymers to further its environmental sustainability impact. Globally, the biggest plastic users and hence waste generators are the construction, packaging, and automotive products/industries creating an enormous stockpile of discarded plastic waste as only about 9% of recyclables are actually recycled due to innovation limitations [27,28]. To illustrate this, a study conducted by S. Saikrishnan et al., (2020) examined multiple reprocessing of the same polymer blends to observed how many times a plastic component may be recycled while still holding onto their properties. From their results, the researchers noted that the melt flow index (MFI) had a drastic increase while generally maintaining the baseline properties [29].

To show recycled polymer's effectiveness within a composite, a study by I. Turku et al., (2016) sought out to characterize WPC derived from recycled plastic blends. The investigators compounded composites from waste generated from construction applications and manually sorted out PP and PE, which was further divided into flexible packaging and hard non-packaging plastics. The plastic waste was compounded in a twin screw extruder with maleated PE (MAPE) and WF from a spruce tree following which the newly compounded materials were injection molded. Although no treatment was performed on the WF beforehand, they found that the WF was still effective at increasing the composites overall stiffness and potential replacement for virgin material depending on the application [27]. The hardness increase they noticed was partially attributed to the inclusion of non-plastic and non-wood contaminants, found under SEM, that could not be sorted out [27]. There were clear signs of inclusion of foreign matter noted during the thermogravimetric analysis [TGA] as there was inorganic residue ranging from 2 to 8%. As well, the researchers observed multiple melting peak using differential scanning calorimetry [DSC] indicating the different types of packaging from the construction waste.

As discussed, conventional composite materials are typically made with non-renewable reinforcing fillers such as glass fibres, carbonaceous particles, and synthetic fibres that prevent or lower the recyclability of the composites resulting in its disposal in a landfill. This is still due to inorganic fillers being intrinsically stronger than a natural filler and polymer. With both the matrix and filler traditionally being non-renewable, the biodegradability and environmental sustainability concern remains, which is causing and forcing manufacturers to look for partial

or fully biobased alternatives. Over the past 20 to 30 years, WPCs demand has been increasing due to its widespread functionality, tailorability and sustainability.

However, the manufacturing and production of WPC is not as straightforward as one would think or hope especially at relatively high loading of wood derived fillers. This is due to the inherent limitations of the material as it tends to form poor interaction with apolar matrices as well as the drastic increase in the material's apparent viscosity. Common industrial practice is to employ additives and pre-treatments to help combat these concerns and limitations. The additives and pre-treatment are used to enhance interfacial interactions, dispersion, and the overall repeatability of the process leading to better mechanical properties. As well, lubricants and high melt index materials may be used to help overcome the material's viscosity up until a significant enough level of filler. For excessively high loadings of wood derived fillers (>70 wt.%) other means need to be investigated which may include sc-CO2 extrusion and recycled/ degraded thermoplastics. Although WPCs have been around for a while and continue to thrive in today's markets, they still require more innovation to optimize their properties and biocontent.

1.3 Problem Statement

The increasing concern with the continued use of petroleum feedstock associated with global warming and air pollution in conjuncture with solid waste accumulation as a result of single use plastics, has led to a substantial interest in the utilization of renewable feedstock for the production of sustainable plastics that offsets the petroleum based plastic industry [1,2]. The use of solid wood as a substitute to plastics in multiple applications has gained momentum.

However, the direct use of solid wood also has drawbacks including limitations in geographic availability, high moisture absorption, complex and inefficient supply chain, and most importantly low thermal stability (< 200 °C) compared to synthetic fibres and various polymer resins [1,2]. With that, hybrid biomaterials such as wood plastic composites (WPCs) have been gaining more popularity with each passing year mainly for environmental, cost, and social reasons [3].

Presently, environmental problems and regulations have caused a heightened awareness of producer liability with regard to plastic recycling while maintaining global demand [4–7]. In Canada, specifically, the utilization of recycled plastics is in dire need after the recently implemented Chinese ban on the importation of plastic waste for recycling. Process-induced degradation during recycling (e.g. extrusion and injection molding) will, over time, lead to irreversible changes in the physio-chemical properties and structure of the material. Thus, it is important to understand the magnitude and mechanisms of property deterioration during the recycling process via either chemical, thermo-mechanical, or high-temperature processes while, looking into possible utilizations, applications, and solutions for the existing global accumulated polymer waste. The utilization of recycled plastics for WPC application could provide a sustainable solution to reduce waste plastic accumulation while also reducing the need to utilize virgin plastics [8].

WPCs are generally composed of plastic resin, wood biomass, compatibilizers, and other additives (e.g. UV-stabilizers). The performance of WPCs depends on several factors, including biomass chemical composition, plastic resin characteristics, cell/particle dimensions,

aspect ratio, defects, particle/resin interaction, etc. [3]. WPC materials have been substituting entirely pure plastic, wood, and steel products in a range of applications due to their low cost (manufacturing, transportation, etc.), improved performance (reduced density, high modulus, etc.), and are more environmentally sustainable. WPCs have high demand in furniture and furnishing applications due to their close resemblance with pure wood (colour, texture, and scent) leaving the impression of high quality but at a much lower cost to pure live edge wood pieces and at a lighter weight for saving the fuel economy. For Canada, the forestry industry is a large contributor to the Canadian economy and provides jobs in several communities. Moreover, there is an ever-increasing societal demand on the plastic industry to develop environmentally sustainable materials coupling that with a continuous interest in diversifying the Canadian forestry products.

The compatibility of wood fibre with polymer resins has been studied quite extensively; and they are typically enhanced through several techniques, including chemical and/or physical modification of the wood fibre as well as the addition of a coupling agent or compatibilizer. Wood biomasses are not very suitable with engineering thermoplastics that have melting points > 200 °C (i.e. polyamide 6 or poly(butylene terephthalate)) due to wood's inferior thermal stability [3]; other means must be sought out by researchers in order to utilize them for broader applications to continue to offset the petroleum resource on plastics. With that, to date the combination of recycled polyolefins with extremely high loading (> 70 wt.%) of wood biomass via a twin-screw extrusion operation has yet to be fully studied and monetized. Therefore, this

study aims to develop and optimize thin-structured WPC for the construction and automotive industries utilizing recycled municipal waste plastics with forestry byproducts.

1.4 Objectives

1.4.1 General Objective

The thesis's overall objective is to study the effect of thermo-mechanical reprocessing on thermoplastic material and optimize high performance wood-based bio-composite materials from polypropylene (PP), polylactic acid (PLA), and wood particles or wood flour. The specific objectives are:

- To investigate the potential of utilizing reprocessed PP, which simulates recycled PP which would generate varying degrees of degraded PP, for the fabrication of highly filled WPCs free of other lubricants and compatibilizers. This study looks to recycle PP up to six times to see how the degradation of properties translate when compounded into composites. Additionally, this study looks to successfully compound 40 to 70 wt.% filled composites from batch mixing.
- To evaluate the effect of recycling of MAPP to study the potential degradation mechanisms that may translate to polymer and composite functionality and performance and the effectiveness of maleating recycled PP (e.g. revitalized polypropylene (rePP)) to retain properties. This study looks to recycle PP and MAPP up to three times to see how the property deterioration translates when compounded into composites.

- To evaluate the applicability and performance of thermo-mechanically reprocessed PLA, which simulates recycled PLA, in combination with pristine and DDSA modified wood. This is in hopes to significantly inhibit water absorption capabilities and enhance the WPCs durability.

1.5 Outline of Thesis Chapters

This PhD thesis is composed of six main chapters each of which contributes to achieve the overall objective of the project. **Chapter 1** is the introductory chapter where the motivation behind this work and the core objectives of the project are described. The remaining and subsequent chapters provide detailed literature reviewing the current state of polymeric recycling and experimental research performed to achieve each objective.

→ **Chapter 2:** This chapter reviews and compiles the past and current literature on the recycling on thermoplastics, with a specific focus on polyolefins (PO) by showcasing global production rates with a breakdown per resin and industry. This chapter also highlights and defines circular economy as well as polymeric waste collection means and breakdown of rates and routes (e.g. landfill, recycling, energy recovery) on a global level. Finally this chapter will illustrate potential applications for polymeric waste.

→ **Chapter 3:** In this chapter, polypropylene (PP) was reprocessed at various cycles to simulate recycling to be used as a matrix for moderately to highly loaded (40 to 70 wt.% wood flour) woo- plastic composites (WPC). The neat and composite samples were produced using a batch mixer and injection molder. The extent of PP recycling

was analyzed using chromatography, rheology, microscopy, and other physical/mechanical properties.

→ **Chapter 4:** In this chapter, PP and maleated polypropylene (MAPP) were reprocessed from one to three times to simulate recycling. 30 wt.% of the reprocessed PP and MAPP were compounded with 70 wt.% wood filler to fabricated highly filled wood plastic composites [WPC]. The neat and composite samples were produced using a batch mixer and injection molder. The effect of recycling and maleation of PP was analyzed using light scattering, nuclear magnetic resonance, rheology, microscopy, and other physical/mechanical properties.

→ **Chapter 5:** This study investigated the effects of simulated recycling of PLA using thermo-mechanical processes on its structure and physico-chemical properties. The recycled PLA and its maleated counterpart were then combined with pristine and modified wood flour (WF) to fabricate biocomposites. The WF modification entails a base (NaOH) catalyzed reaction of dodecenylsuccinic anhydride (DDSA) with WF's surface – OH groups to reduce its polarity and enhance its compatibility with both poly (lactic acid) (PLA) and maleated PLA (MPLA) in biocomposites. The successful modification of the WF was evaluated using X-ray photoelectron (XPS) and Fourier transform infrared (FTIR) spectroscopy as well as solvent dispersibility analysis. The simulated recycling, maleation of PLA, and composite processing were all conducted using a reactive batch mixer followed by injection and compression molding.

→ **Chapter 6:** The final chapter will provide an overall conclusion showcasing the main points from the preceding chapters and how it all links together for a greater picture. Finally, this section draws attention to future directions this research can go in.

Chapter 2 - literature review[1]

As the global population continues to grow, everything from food security to the increasingly growing concern of environmental impact of human activities has steered research and legislation towards more sustainable and circular economies. With an alarming rise in natural disasters, from uncontrollable wildfires in Australia and North America to the thousands of displaced refugees, environmental impact due to greenhouse gas emission are much more apparent. Some legislation and regulations examples to help alleviate environmental impact include REACH [(EC) No. 1907/2006] from the European Union [30], the Paris Agreement by the United Nations [31], and the Carbon Pricing Policy of Canada ("carbon tax") introduced in 2018 [32]. Also, the depletion and slow disappearance of fossil fuels across the globe highlights the necessity for finding uses for existing material waste. For example, 4 to 6% of fossil fuels were devoted to plastic production in 2017, which could be reduced with the adoption of a circular economy (i.e. using sustainable materials and processes) [33].

Since the 1950s, global production or conversion of polymer resin has grown by about 1,182% from 28 to 359 Mt in 2018 [34,35]. Examining the years of 2017 and 2018 more closely, there was a 9% growth in production from 348 to 359 Mt [33,36]. Of the 359 Mt of produced plastic, NAFTA, Asia, and the EU contributed 18, 51, and 17% respectively. Canada specifically, had estimated sales of 10 billion dollars (CAD) in polymer resin and 25 billion

[1] A version of this chapter has been published on peer-reviewed journal as a review article: D. Jubinville, et al. (2020). A comprehensive review of global production and recycling methods of polyolefin (PO) based products and their post-recycling applications. *Sustainable Materials and Technologies*, *25*, e00188. https://doi.org/10.1016/j.susmat.2020.e00188

dollars (CAD) in plastic manufacturing in 2018 with an average of 4.6 Mt entering the domestic market per annum [37]. **Figure 3(A)** graphically depicts a correlation between raising plastic production amounts against that of an ever-growing global population. This correlation clearly shows that the increasing production levels are dependent on the global population since manufacturers are required to meet the demand. A deeper investigation into the overall EU contribution to the global production is that the higher converting countries, Germany>Italy>France>Spain>United Kingdom>Poland, produced ~80% (> 3 Mt) [36]. **Figure 3(B)** shows another way in which the components may be dissected, by industry, of plastic production which combines to form the 359 Mt global production quantity. As it is shown, the largest elements are packaging (34%), construction (19%), and transportation (14%) for plastic production as well as the largest potential plastic waste generation [36,38].

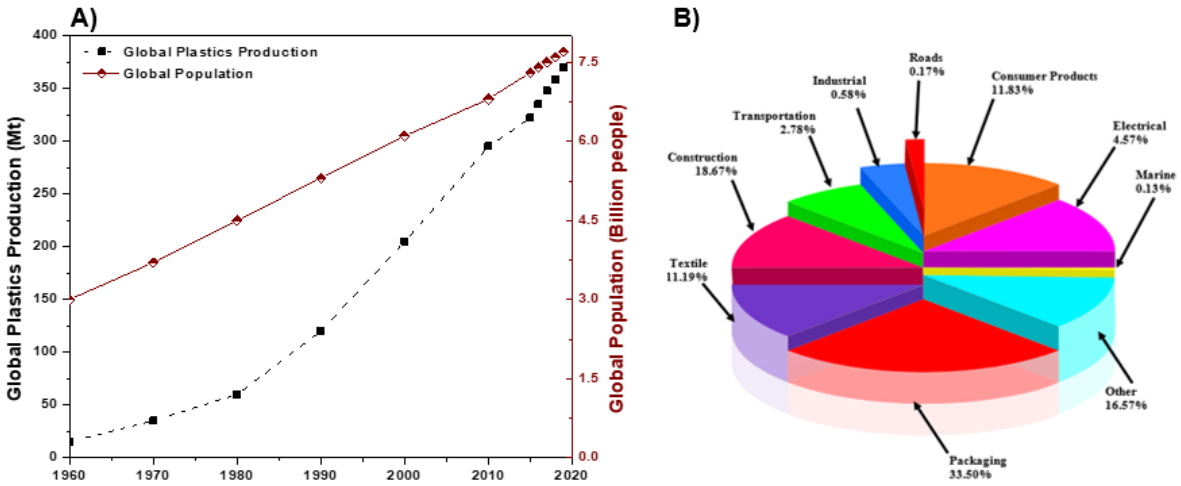

Figure 3. (A) The global plastics production (per million tonnes) against that of the global population (per billion people) from 1960 to 2019 and **(B)** A graphical breakdown, by sector, for the major resin converters in 2018 (taken and adapted from D. Jubinville et al. (2020)) [28].

2.1 Polyolefins (PO)

POs, examples shown in **Figure 4(A)**, are polymers that are produced from compounds having at least one carbon-carbon double bond commonly known as olefins or alkenes. POs typically consist of polymers produced from ethylene, propylene, 1-butene, and other α-olefins monomers. The PO family of polymers includes HDPE, LDPE, LLDPE, UHMWPE, PP, as well as other α-olefins and combination of these polymers. PP was first commercially produced in the 1950s by G. Natta who produced PP by polymerizing propylene in the presence of an organometallic catalyst, such as titanium and aluminum. Following 1957, the Montecatini company along with Professor Natta produced the first stereoregular PP. Four other processes have been developed since then for the manufacturing of PP which includes slurry, bulk, gas-phase, and solution techniques [39].

LDPE is manufactured by free radical polymerization typically using an initiator of either an organic peroxide or oxygen and the overall process is carried out in either an autoclave or tubular reactor at very high pressures and temperatures [40]. The initiator is injected at different points in the reactor than the feed and thus is at a higher temperature while the heat is removed along the tube by the ethylene/polymer mixture [39]. The conversion of ethylene to PE is higher in tubular reactors than in autoclaves as a result of more efficient heat transfer. The number average molecular weight of LDPE processed is less than 100,000 g/mol and the PDI is between 3 to 20 [39]. LDPE has both short and long branches that relate to their lower crystallinity reducing the density of the macromolecule. As a result of the lower crystallinity

and density, there is an increase in the ductility or toughness and transparency of LDPE allowing it to be used in applications such as food packaging.

In contrast, HDPE is a linear PE polymer with very little to no branching formed by a polymerization reaction using a Z-N catalyst (e.g. a mixture of titanium tetrachloride and alkyl derivative of aluminum) or supported chromium–phillips [41]. HDPE cannot be made by free radical mechanisms in order to generate short and controlled branching. The low degree of branching and subsequently high ordered chains give higher crystallinity compared to LDPE resulting in increased tensile strength, stiffness, chemical resistance, and opacity. The molecular weight of HDPE is controlled during the heterogeneous catalyst polymerization process thus a wide range of HDPE may be obtained with varying molecular weights. HDPE is used in many day-to-day products such as milk bottles, detergent bottles, fuel tanks, piping application for sewage and water circulation, beauty product containers, and many more.

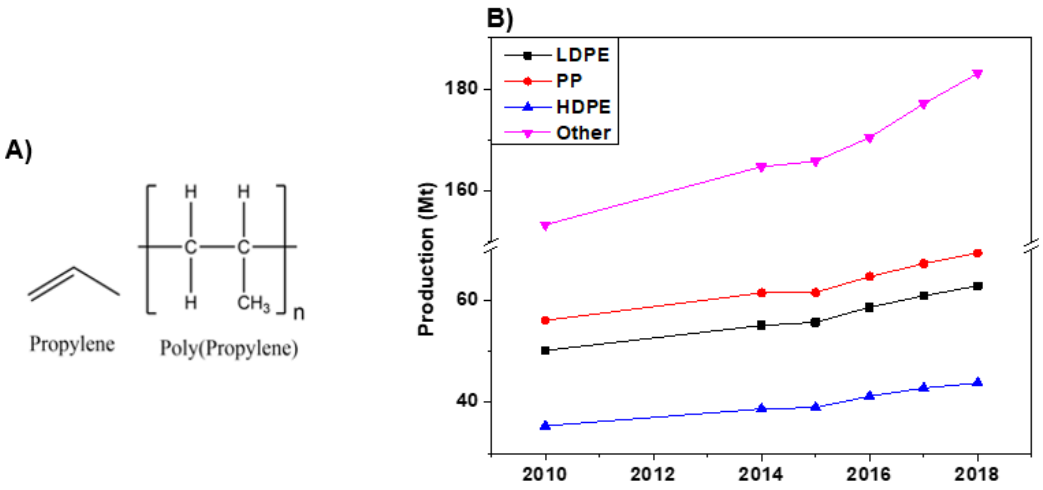

Figure 4. (A) Schematics of propylene and polypropylene and **(B)** Polyolefin production breakdown over the past four years (taken and adapted from D. Jubinville et al. (2020)) [28].

2.1.1 Properties of polyolefins and applications

PO resins consist of weak Van Der Waals forces which result in their low melting and crystallization temperatures, thus making it inappropriate for applications that may require higher temperatures and pressures without further modification [40]. The monomers, olefins, are synthesized by the cracking of crude oil (i.e. the breaking of carbon-carbon double or pi-bonds in complex organic alkanes) into simpler hydrocarbon molecules.

The properties of PP depend on the crystallinity, molecular weight, and distribution as well as the type of co-monomer used. The increase in crystallinity improves properties like stiffness, flexural strength, and yield stress, but also decreases the material's toughness like impact strength [42]. PP is more versatile when compared to other POs due to its superior properties (e.g. its chemical superior abrasion resistance). The aforementioned properties of PP can be controlled in many ways during its polymerization and its crystallinity is determined by the internal structure which gives different properties as well (e.g. mechanical and thermal properties). The tacticity of PP generates three sub-classes for it: isotactic, syndiotactic, and atactic. iPP is most widely used when compared to its other stereoisomer configurations (e.g. sPP and aPP) because of its exceptional mechanical and thermal properties. Atactic PP finds application in adhesives and some low-cost applications. The melting point of iPP is 165 °C due to the stereoregularity while a non-stereospecific PP has a melting temperature window of 160 to 170 °C. PP finds application in many areas including, but not limited to, the automotive and textile industries. In the automotive industry, PP finds use in bumpers, gas cans, and internal components (e.g. dashboards) [43]. When PP is spun into fibres containing a high molecular weight, it is successfully used as ropes, upholstery, and carpets in the textile

industry. In the food industry, it is used in the form of disposable food containers that are made by a thermoforming process. Similar to PP, PE is a thermoplastic polymer with high chemical resistance, toughness, remarkable insulating properties, low coefficient of friction, etc. [44]. There are many forms of PE that differ in the nature of branching [43].

The various PO types, differentiated by the degree of crystallinity and associated physical properties, are used for producing a wide range of commercial products like pipes, packaging films, household bottles, automobile parts, disposable diapers, food containers, and many more [40,45]. The main factors responsible for the success of PO production are the availability of monomer units, the low cost of the raw materials (e.g. petroleum prices), recent advancements in polymerization reactor technology, and chemistry. As shown in **Figure 4(B)**, PP in 2018 held the largest PO market share of 19% (69 Mt) which is an increase of 24% from 2010 (56 Mt) in applications of food packaging, snack wrappers, hinged caps, microwaveable containers, thermoplastic pipes, interior automotive components, banknotes, etc. [36,46]. On the other hand, HDPE and LDPE held a global market share of 12% (44 Mt) and 18% (63 Mt), respectively, in 2018 [36]. Since 2010, HDPE production increased by 23% in the products of toys, milk bottles, shampoo bottles, thermoplastic pipes, houseware appliances, etc. [36]. LDPE has also increased in the amount converted since 2010 by 25% in the finished consumer goods of reusable bags, food trays, and containers, agricultural films, food packaging, cling wrap, etc. [36]. Lastly, all other studied polymers (e.g. PVC, PET, PUR, PS as well as EPS, ABS, PC, PMMA, and PTFE) combined have shown a substantial increase as well year over year. These polymers also contribute greatly to the waste disposed of the ecosystems each year

but some are more difficult to recycle [47]. This is due to their high stability and resistance to degradation; thus, increasing pollution and landfill all over the world. The plastic material not only affects the environment during article production but also its chemical and biological inertness after the product's life cycle possesses a greater threat [40].

2.2 Circular Economy

Since and even before the industrial revolution the linear cradle-grave economic model greatly depends on easily accessible materials and energy from non-renewable and/or slow to replenish sources. Due to environmental concerns as well as price volatility, supply chain interruptions/hindrances, and pressure on valuable resources have thus compelled companies to look for alternative and sustainable materials and energy supplies. According to the Ellen Macarthur Foundation, "A circular economy is one that is restorative and regenerative by design and aims to keep products, components, and materials at their highest utility and value at all times, distinguishing between technical and biological cycles" [48].

The goal of this new economic model is to separate economic development from non-renewable resource consumption, on a global scale. A common theme with a circular economy is sustainability, which arises from the assumption that the modern economic production and consumption cycles systematically have led to a depletion of natural resources while ignoring the socio-economic costs of overuse [49]. Sustainability is generally governed by three principles: efficiency, consistency, and sufficiency as shown in **Figure 5(A)**. The sufficiency principle relies on lifestyle changes that shift from a very materialistic society with superfluous consumption activity to a more post-materialistic and minimalist attitude [49]. The efficiency principle aims to reduce as much waste as possible while also producing the desired product

or service for the end-users. The last principle, consistency, relates to having the material and production as well as their associated energy costs being completely integrated into natural cycles. In other words, the consistency and efficiency principles are dependent on innovations in technology and company incentive direction while, sufficiency is human consumer-mentality which is based on trends and societal views.

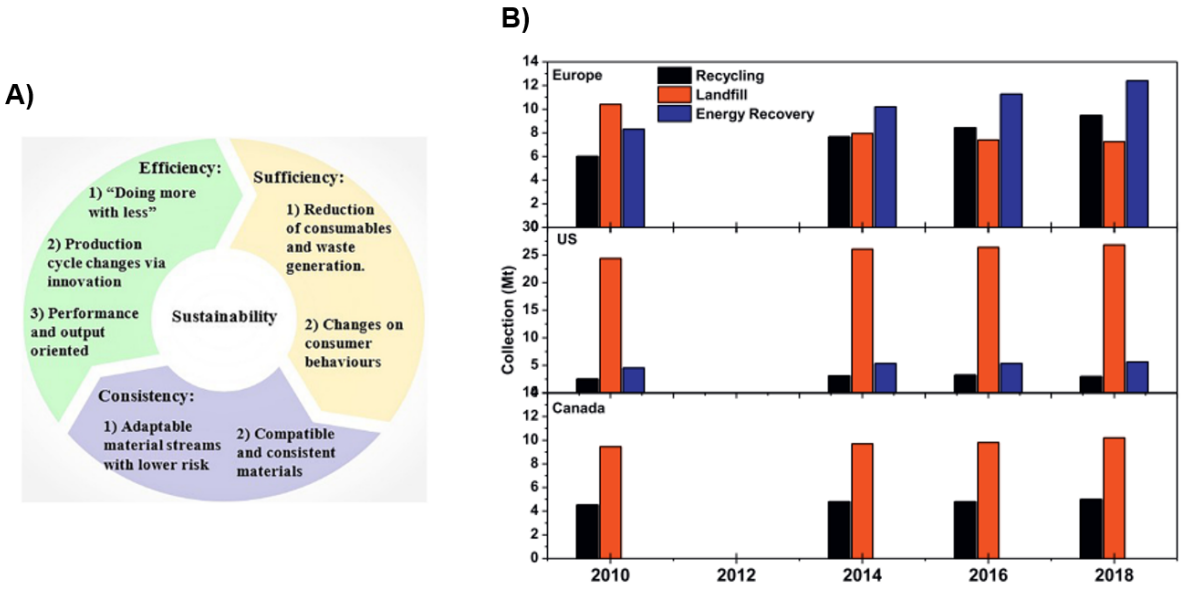

Figure 5. (A) Graphical representation of the nature of sustainability and its components and **(B)** Polyolefin waste collection amount in Europe, the United States, and Canada by method, over the past decade (taken and adapted from D. Jubinville et al. (2020)) [28].

2.3 Plastic waste collection

The production and conversion of raw materials into plastic feedstock (i.e. extraction, refining, and transportation) are some of the main contributors to plastic waste accumulation. Pollution due to plastic waste accumulation is an ongoing and everlasting battle as the amount of waste increases each year as plastic conversion rates also increase due to population demands (see **Figure 3(A)** and **Figure 5(B))**. Plastic waste or debris is often characterized by

their size into macro- (> 22 mm), micro- (< 5 mm), and nano-debris (> 100 nm). Macro-debris encompassed all large size plastic waste from macro- to mega-debris [50], with the most abundant type of product in this category being packaging materials. Micro-debris is usually a product of environmental pollution created by discarded plastic and eventual disintegration [50]. Microplastics are usually a mixture of size, shape, colour, density, etc. [51]. Lastly, nano-debris is generated mostly from cosmetics and personal hygiene products as well as the breakdown of post-consumer waste [50].

Each year, 2.01 billion tonnes (Bt) of municipal waste is generated with the higher-earning countries contributing 34% (689 Mt) of that [52]. It has been reported that the global recycling rate is approximately 18% with the EU, NAFTA, and China representing 30, 25, and 9% of the main contributors [53]. Breaking down global plastic waste accumulation in terms of polymer types, LDPE and PP are the two biggest contributors with 57 and 55 Mt being collected each year; while HDPE is close behind with 42 Mt generated. In Canada alone, 87% of plastic "waste" will end up in a landfill as opposed to being recycled which represents about 9.7 Mt of plastic resin and an estimated loss of 7.8 billion dollars (CAD) capital [54,55]. Another source has reported that the USA has generated an average of 20.8 Mt of plastic resin in landfills between 1990 and 2017 [56]. Packaging (mainly POs) material is one of the major contributors towards plastic waste with about 40% (276 Mt) single-use packaging in 2018 [57,58]. As shown in **Figure 5(B)**, Europe accounts for 6.5% (17.8 Mt) of the packaging waste collected [36] while another study reports that Australia accounted for 0.33% (0.91 Mt) of the total [59]. It can also be observed in **Figure 5(B)**, that both Canada and the US are both behind

the EU in both recycling and incineration or energy recovery rates. It should also be noted that Canada's landfill data, in **Figure 5(B)**, is combined with its incineration data due to their methods of collection so the values are a little inflated.

Most of the polyolefin products on the market have shorter life cycles while in use and is usually thrown away after their usage. The different types of plastic typically have different service life expectations, usages, and environments. Other important considerations with plastic components are that some finished goods are products consisting of only one component (e.g. a bottle cap); while others are a part of a system of products (e.g. a sealed bottle (cap + bottle) or an assembled vehicle) which are harder to recycle. In terms of service life, some polymers will only have an active service life of one to two years (e.g. filters) and some products may have a service life of 10 or more years (e.g. automotive components).

The depletion of resources and environmental concerns due to plastic waste have pushed researchers and government legislators towards studying the recyclability and reusability of plastic waste. As different polymers break down at many different rates, the collection in a landfill is difficult to correlate with the demand in the same timeline**.** Recycling is the process in which municipal and industrial waste is collected, segregated/separated, cleaned, and reprocessed to yield a new product or become a secondary raw material by offsetting virgin plastic [60]. The current recycling methods implemented globally to reduce plastic waste include thermo-mechanical, -chemical processes, devulcanization, and energy recovery. There is also an alternative to the outlined recycling methods which is the most economical, i.e. reuse.

2.3.1 Current recycling and reuse practices

Different techniques of recycling and the reuse technique are presented in the following sections. Mechanical recycling is collecting the waste and then reprocessing it. This technique is widely used worldwide. Chemical recycling technique converts polymers back into monomer units by changing the chemical structure. Energy recovery is a process wherein energy is recovered from the plastic through controlled combustion and conversion into liquid fuel. Lastly, reusing of plastic waste is the most preferable end of life option as plastic produced for a specific application or multicomponent plastics may not possess the required specifications for regular municipal recycling. General keys to successful polymer recycling are:

1. Recycling the material generates business incentives by obeying the laws of economics. Quite often the recycler is faced with an uncertain consistent material supply; changing governmental policies (e.g. curbside pickup frequency and material allowance); and competitive and more reliable products [53].
2. Recycled material must be able to be sorted and based on good science and technology [53,61].
3. Recycling must be compatible with modern infrastructure and population density [61]. For example, the recycling needs of New York City, New York, USA would be much greater than that of Kyoto, Japan.

2.3.2 Thermo-mechanical recycling

Thermo-mechanical recycling, also known as primary recycling, is where the municipal wastes are collected and processed into a product with similar or comparable properties with those of the original one. Thermo-mechanical recycling of polymers is a crucial component of reducing the consumption of non-renewable resources that are needed for the synthesis of the corresponding monomer units. Also, recycling takes less energy than producing new versions of the product [62]. A major limitation in thermo-mechanical recycling is the potential for contamination of waste streams which makes sorting and separation costly and next to impossible without sophisticated equipment. All types of thermoplastics known to mankind can be recycled mechanically and this process is also known as re-extrusion or closed-loop process [63]. Primary recycling method usually involves reducing the size and separating different polymer wastes from a mixture without changing the chemical structure of the recyclates. This method uses lower temperatures and energy compared to chemical, thermal, and enzymatic techniques, allowing the recyclates to retain their structure and most of their molecular weight/ length [62].

The most important step in mechanical recycling is the sorting of various plastics according to the resin type. The process describing this type of recycling begins with segregating the plastics either manually or by automated machines. The steps involved in mechanical recycling are separation and sorting, baling, washing, grinding, and compounding and pelletizing [64]. After the collection of plastic waste, sorting of these wastes is done based on density, chemical composition, size, and colour. Wastes which include plastic bottles, fluid containers, metal cans, and Tetra Pak® are first sieved by rotary mechanism and then blown

with wind sifter for removing the loose paper. Magnetic separator is used to remove ferrous articles followed by a ballistic separator. These are then placed in the sorting cabin for manual labor checks for some inconsistency and sorts it. Contaminants are removed by magnetic separation or complex spectrophotometric distribution technologies [63]. Separation and identification of plastics can be done in many ways: FTIR, magnetic density separation, HSI technology, froth floatation method, X-ray fluorescence, laser-induced breakdown spectroscopy and triboelectric separation [65]. The froth floatation method is used for the segregation of plastics from one another [66]. This technique was first discovered by Alter in 1978 citing the difference in the critical surface tension between plastics. The separation of PVC, PET (similar density) by this method was studied by many researchers and it was concluded that around 95 to 100% of PVC and PET can be separated [67–71]. FTIR technique is another characterization technique used to identify the plastics. FTIR gives the spectra of the sample and compares it to different models present in the database. This is used to identify the type of polymer and segregate it for further processing. Carvalho et al. 2010, presented a paper about the identification of plastics using FTIR. In this paper, PVC, PET, and PS were identified using FTIR and separated by froth floatation method [72]. Warren and Burns, 1988, concluded that primary recycling is very easy and can be done without many precautions, but the waste collected must be clean and segregated properly [73,74].

The final step in thermo-mechanical recycling, compounding, and pelletizing of recyclates, is usually carried out by using either a twin-screw extruder or single screw extruder depending on the amount of mixing required. Once the extruded product is obtained it is passed

onto the molding process. The challenges with the recycling of plastics are the low value of the material and additives and fillers present in the plastics [63].

Recycling has many advantages but the more important ones for this context are: its ability to reducing energy consumption and decrease landfill accumulation (ideally); allows for the implantation of a circular economy model to offset slow and non-replenishing resources (e.g. petroleum); it is reported that the recycling industry, globally, tends to create 9 to 30x more jobs than landfills and incinerators [75]; lastly, it has also been reported in 2018 by Toronto, Canada that curbside or municipal recycling is more cost effective at 79.8$/unit (CDN) than landfill at 119.9$/unit (CDN) [76]. However, the disadvantages, although fewer, are rather challenging and expensive to overcome. The need to precisely separate plastic waste, amongst a mass of other waste, continues to be the biggest downfall in the industry. Which is a result of over production and inadequate technology to keep up with product design complexity. The difficulty in separation increases the cost when recycling some products (e.g. multi component or multilayered) not equitable making closed loops systems and/or circular economies in general all the more valuable. The last disadvantage to recycling deals on the side of the consumer or end-user as there is often a preconceived notion that recycled products are inherently worse than their virgin counterparts causing the demand to decrease while the supply is forever increasing. The bias of recycled materials is not completely correct as it ultimately depends on how the material was recycled (i.e. chemical recycling vs. thermo-mechanical recycling) and how it was re-engineered into a suitable design (e.g. use of compatibilizers and fillers) and application (e.g. asphalt, WPC, concrete filler, etc.). Overall,

there is a very evident need for more innovation within the recycling area so more sophisticated and, more importantly, robust technologies and methods can be created, all the while, educating the global market to practice re-use and recycling.

2.4 Potential applications for polymer waste

As it is known, recycling may alter the physical, chemical, mechanical, and rheological properties of POs that control the property of the final product. It should be noted that the main goal of utilizing recycled polymers in design besides economic value is that, in use, they should be close in properties to virgin grades. To what extent this goal is achieved depends on the careful engineering of both employed design of the product and the manufacturing processes [77]. One possible avenue for the application of recycled plastic waste in to use them within composite applications. WPCs, as the name suggests, are composite materials containing a wood component and polymer in the matrix. The wood component in WPCs can be either a wood fibre or wood flour. The polymer matrix can be either thermoplastic or thermosetting polymers. The first WPC produced was a composite made of phenol-formaldehyde resin and wood flour for use as gearshift knob in automobile [78]. Wood generally degrades around 220 °C and thus it is important that the polymer used does not thermally degrade the wood component during thermomechanical processes. The preparation of polymeric composites based on recycled polymers with nature-based materials is an interesting alternative that contributes to the preservation of natural resources, a decrease of pollutant waste, and the production of low-cost materials [79]. Most PO and other commodity polymers such as PE, PVC, PP, etc., are used in the production of WPCs. The manufacturing techniques of recycled PO based WPCs' do not differ from those of other polymeric composites [80] and they are

commonly produced by extrusion, injection molding, compression molding, thermoforming [81], layer modelling and laser sintering [82].

Gardner et al., 2015 [81] have reviewed WPC technology with thermoplastic resin and wood flour/fibres. In the study, the manufacturing processes, advances in WPCs materials, and also the new developments in the field are briefed [81]. WPCs are advantageous for a variety of reasons. It is a cheaper alternative to products produced with only plastics as its main component, better compression properties, lower maintenance, and water absorption than solid wood. Another advantage of WPCs is that plastic is produced from fossil fuel feedstock. Thus, including wood into plastic reduces the carbon footprint as compared to pure plastic-based products. WPCs are recyclable (melting and reprocessing), sustainable material as wood flour or fibre is a by-product of many industries that use renewable wood as raw material. Furthermore, the flexibility of shaping WPCs to any form for a wide range of applications stands out as an excellent alternative for plastics only product [83]. Wood absorbs moisture and decays over time, and these are the two main limitations of using wood as fibre or flour in WPCs for long term use. Even though the water penetration is less as compared to solid wood, it still leads to decays and structural weakening over time. Decking is the main application of WPCs currently in the market. Furniture like benches, chairs, and picnic tables are also some examples of products made from WPCs [84]. Decking made from WPCs are available in different colours and shapes [85]. The utilization of recycled POs has been considered for the manufacture of WPCs by a plethora of research [86–90]. There is no doubt that recycling procedure influences the properties of POs used as WPC matrix and thereby controlling the

final composite material. Thus, the effect of the recycled POs on the performance of WPCs needs to be identified and compared to that of virgin POs. Ares et al. showed that despite other plastics, recycled PP maintains the optimal rheological properties and processing parameters after recycling that makes it easier to be processed for WPC production by extrusion [89].

The trend for the influence of the number of re-extrusion cycles on the properties of PO-based WPCs is similar to that of the recycled POs without wood [87]. Flexural modulus variation showed that sawdust filled recycled PP composites exhibit about two times higher flexural modulus than unfilled PP due to considerably higher flexural modulus of wood as a component [91]. Lignin as a low-molecular-weight component of wood exhibited an antioxidant effect for recycled PP [90]. The critical drawbacks of WPC based on recycled PO are low mechanical properties and high flammability which can limit them to meet specific end-use requirements. One of the effective efforts has been made to improve such properties in the formation of WPC composite using various kinds of reinforcing fillers. Nano clay minerals have been reported as the most widely chosen naturally available nanofiller for reinforcing WPC increasing their strength and stiffness, thermal stability, gas barrier property, and flame retardancy [92–94]. Improved mechanical properties were also observed in testing and analysis conducted on hybrid WPC containing other reinforcement such as glass fibres [95]. Significant improvement in the mechanical properties of recycled PP based WPCs was shown in composites containing MA-grafted PP [91] and MA-grafted POE [96], as a reactive coupling agent, which can efficiently improve fibre-matrix bonding by the formation of

covalent linkages and hydrogen bonds between the MA and the hydroxyl groups of the wood fibre [87].

Kazemi-Najafi et al. have published a series of works, where they examined long term water absorption properties of recycled PO based WPC and proved that the absorption mechanism followed the kinetics of a Fickian diffusion process[97,98]. The water absorption of WPCs from recycled-PP and HDPE plastics are higher than those made from virgin plastics. WPCs from the mixture of recycled-PP/recycled-HDPE have the highest water absorption and diffusion coefficients [98]. They also reported that the presence of the MA-grafted PP as a coupling agent enhanced long term water resistance wood flour/PP composites based on recycled-PP. The ester linkages formed between the hydroxyl groups of wood flour and the anhydride part of MA-grafted PP, which reduce the amount of free OH^- in the wood cellulose, improved the adhesion between wood and PP that decreased the interfacial gaps and block association with water [97].

2.5 Summary of Chapter 2

In summary, POs are the most versatile class of polymers with appealing physical and chemical properties. As a result, they are by far the most used plastics in a range of single-use commodity and engineering applications and consequently the most abundant plastics present in the waste. In 2018, PO globally collected waste reached a record 154 Mt, while; 176 Mt was produced representing a 25% increase from 2010 (137 Mt). One main challenge against fully exploiting recycled polymer is that of achieving the level of properties available for virgin ones in a cost- effective approach. It is important to ensure that the end property of recycled material

is sufficient for a suitable application and also economical. Another main challenge facing recycling is the cost and difficulty of sorting and separation of complex plastic components (e.g. polymer blends, multilayered plastics with each layer composed of different polymer types or even metal-based layers, etc.) compared to their virgin plastic counterparts. With that, it is important to consider how to design for the material's end of life stage when materials, more specifically polymers, are becoming more and more complex. The huge potential of recycled POs has become apparent in different fields of research and industry such as automotive, electronic appliances, construction, WPCs, and fuels. However, other possible applications of recycled-POs such as food packaging have yet to be fully studied profoundly to get suitable protocol before commercialization. Incorporating the recycled plastic to produce a valuable article with better properties and at a lower cost should be the aim of industries and researchers. Recycling of plastics is not the end step but redesigning the process to input the recycled powder/flake/pellets or article to produce a product completes the circular economy. Furthermore, re-designing and simplifying the existing polyolefin-based products with a deliberate intention of recyclability such as reducing or avoiding multi-layering, combining non-plastics with plastics is an integral part of the success of plastic recycling.

Chapter 3 – Highly loaded wood plastic composites[2]

3.1 Introduction

In North America (NA), the utilization of recycled plastics is in dire need of reform due to a lack of overall process innovation and the 2018 Chinese ban on plastic waste importation [28,99]. In 2018, it was recorded that 2.01 billion tonnes (Bt) of municipal waste were collected with a global recycling rate of 18% (362 Mt) while the rest of the waste was sent to composting/energy recovery and landfill [28]. Of all waste plastics, polypropylene (PP) is one of the most converted polymers, with a market share of ~20% in 2018, but it is also one of the least recycled (0 to 1%) mainly due to its rigidity and its use in multilayered products [100]. PP has a great importance in commercial applications with the most commonly used compounding processes being thermo-mechanical techniques (e.g. extrusion and injection molding). In these processes, polymers are exposed to high shear and heat leading to process induced thermo-mechanical degradation much like what a polymer would experience during primary (thermo-mechanical) recycling [29]. Although the effect and use of recycling has been studied [8,29,101–106], there is little to no research focusing on the direction of using thermo-mechanical recycling on PP to facilitate the fabrication of highly filled composites free of lubricants and other processing aids. As mentioned in the previous chapter, hybrid biomaterials have been gaining more and more popularity with each passing year resulting from environmental, economic, and societal (e.g. perception) reasons [14,98]. Specifically, the

[2] A version of this chapter has been published on peer-reviewed journal as a review article: D. Jubinville, et al. Thermo-mechanical degradation of polypropylene (PP) and low-density polyethylene (LDPE) blends exposed to simulated recycling. Polym. Degrad. Stab. 2020, 109390.
As well as D. Jubinville, et al. Thermo-mechanical recycling of polypropylene for the facile and scalable fabrication of highly loaded wood plastic composites. Composites Part B: Engineering 2021;219:108873.

use of wood derived fillers as a substitute to synthetic reinforcements in some applications has gained momentum in the past decade even though the practice is long standing [19].

Wood plastic composites (WPC) materials have been substituting entirely pure plastic, wood, and steel products in a range of applications due to their low cost (e.g. manufacturing, storage, and transportation), improved performance (e.g. reduced density and high modulus) and increased environmental sustainability [107]. These hybrid materials also have high demand in furniture and furnishing applications due to its close resemblance to pure wood (e.g. colour, texture, performance, and scent) leaving the impression of a high-quality product but at a much lower cost to pure live edge wood pieces and at a lighter weight. The forestry industry aids many rural economies across the globe by creating jobs and wealth within populations with few non-farming alternative forms of employment. Globally, forests produce more than 5000 types of wood-based products and generate an annual gross profit of $240 billion USD (about 3% of global GDP) [108,109]. Some countries like Canada, Singapore, and Cameroon contribute much more to the forest economy achieving, in some cases, 3 to 5% of their own GDP [108]. Moreover, the increasing societal demands on the plastic industry helps to develop new environmentally sustainable materials coupled with a continuous interest in diversifying forestry products across many sectors.

WPCs are generally composed of plastic resin, wood biomass, compatibilizers, and other additives (e.g. UV-stabilizers) [110]. As mentioned in ***1.2.1 Wood-plastic composites (WPC)*** section, the performance of WPCs depends on several factors, including biomass composition, filler modification, plastic and resin characteristics, geographic availability and

variability, humidity, cell/particle dimensions, aspect ratio, defects, and particle/resin interaction [9,22,111–113]. Of those issues, the most limiting factors, in term of processing, are polymer/filler interactions, decomposition temperature of the natural filler, and melt viscosity especially at sufficiently high level of wood content. The melt viscosity of a polymer is an important aspect in the manufacturing of these materials making a proper understanding of the polymer flow necessary to produce the best preforming product [12,25]. For WPCs it is well documented that with increasing wood content the apparent viscosity of the material increases drastically and at sufficiently high levels of wood no flow may occur due to the generated pressures during extrusion operations [25]. There are few corrections to resolve this issue since increasing the temperature and/or shear rate would add excess heat and shear accelerating polymer degradation. In most cases, lubricants are added to assist with the materials wall slip and flow or the use of polymers with particularly high melt flow rates are selected to assist with the overall flow but the overall strength of the material will diminish [114].

3.2 Materials and methods

3.2.1 Materials

The PP used in this study was produced by LyondellBasell (Houston, TX, USA) and supplied by INGENIA Polymers (Brantford, ON, CA) under the trade name of Pro-fax 6301. The supplied PP had a density (ρ) and melt flow rate (MFR) of 0.90 g/cm^3 and 12 g/10 min (at 230 °C and 2.16 kg), respectively. The wood flour (WF) (mesh 600) was of Maple tree decent and was obtained from Ontario Sawdust Supplies (East Gwillimbury, ON, Canada). Prior to

processing and characterization, the WF was dried overnight at 80 °C and the final moisture content of the WF was 1.5 ± 0.02%.

3.2.2 Methods

3.2.2.1 Melt mixing

The PP and WPCs compositions, shown in **Table 2**, were prepared by using a HAAKE Rheomix 3000 batch mixer (Thermo-Fisher Scientific Inc., Waltham, MA, USA) at a mixing temperature and screw speed of 180 °C and 100 rpm, respectively. For the simulated recycling, the material was heated to its set temperature and when a constant torque value was obtained the sample was cooled to room temperature and the applied torque was removed. Following this, the material was then heated back to up to its set temperature and the torque was re-applied until a new constant value was obtained which is denoted as one reprocessing cycle. Once the desired number of reprocessing cycles have been run, the WF was then added into the batch mixer to produce clumps of WPCs. Cycle one is to denote one cycle of simulated recycling while cycle six is six cycles of simulated recycling. The temperature of the polymer melt ranged from 190 to 210 °C depending on the level of wood filler content added (40 to 70 wt.%) due to the increased friction. The PP and WPC samples were then ground to obtain small uniform particles using a laboratory mill for injection and compression molding purposes.

Table 2. Sample compositions and code names of the virgin PP and the WPCs.

Name	PP (wt.%)	WF (wt.%)	Recycling cycle
PP100	100	0	1,3,6
PP60W40	60	40	1,3,6
PP50W50	50	50	1,3,6
PP40W60	40	60	1,3,6
PP30W70	30	70	*,3,6

* - exceeded equipment maximum torque value.

3.2.2.2 Injection molding

A HAAKE Mini-Jet Pro (Thermo-Fisher Scientific Inc., Waltham, MA, USA) was used to injection mold the samples. The injection temperature was set to 200 ℃ with a pressure of 650 bar to produce type V tensile specimen (ASTM D638-14). A set of at least five specimens were produced for each sample to test the changes in the mechanical properties.

3.2.2.3 Compression molding

Both PP and WPC granules were compression molded into flat sheets of (L × W × T) 76 × 75 × 2.5 mm and 76 × 75 × 0.002 mm using a hydraulic press (Carver, Inc., Wabash, IN, USA) for rheological testing and optical microscopy, respectively. The sheets were molded between two plates heated to 190 °C and subjected, incrementally, to six metric tons force for five minutes (5 min). After forming, the sheets were cooled to ambient temperature and the thicker sheets were later laser cut to form the parallel disk samples.

3.3 Characterization methods

3.3.1 High-temperature gel permeation chromatography (H-GPC)

The polymer molecular weight distribution (MWD), number average molecular weight (M_n), and weight average molecular weight (M_w) for the virgin and re-processed PP were collected on a H-GPC (Polymer Char, Valencia, Spain) at 145 °C using trichlorobenzene (TCB) as a mobile phase at a flow rate of 1 mL/min. The GPC was calibrated using standard polystyrene (PS) narrow standards and was equipped with three detectors in series (infrared, 15° angle light scattering and differential viscometer). The three columns of PLgel Olexis 13 μm mixed pore type (300 × 7.5 mm) were used for GPC separations.

3.3.2 Parallel plate rheometry and melt flow rate (MFR)

The ASTM D4440-15 standard was followed to study the rheology of the specimens using a parallel plate rheometer with a specimen thickness and diameter of 2.5 and 25 mm, respectively. A TAI AR2000 parallel plate rheometer (TA Instruments, New Castle, DE, USA) was employed to study the rheology of the PP and its WPC derivatives. A frequency sweep of 0.1 to 100 rad/s at 180 ℃ was performed on all samples at a constant strain of 0.01% (within the linear viscoelastic region) at a gap of 1.5 mm. The MFR for the virgin and recycled PP was measured using a Dynisco–Kayeness Polymer Test System (Franklin, MA, USA) in accordance with ASTM D1238 at a temperature of 230 ℃ and a load of 2.16 kg.

3.3.3 Fourier transform infrared spectroscopy (FTIR)

FTIR spectra for virgin PP and its recycled derivatives were obtained by using a Nicolet 6700 model unit (Thermo-Fisher Scientific Inc., Waltham, MA, USA). To accomplish this, PP films of thickness 20 μm were produced via compression molding using a Carver press. The spectra were collected in absorption mode between 600 to 1800 cm^{-1} with a resolution of 4 cm^{-1} at 64 scans.

3.3.4 Polarized optical microscopy (POM)

The crystal structure of the virgin PP and its recycled derivatives were investigated using an Olympus BX53M POM (Melville, NY, USA) optical microscope equipped with a 20× objective lens and a polarized light filter. All samples were prepared as 20 μm thick films from compression molding as previously described.

3.3.5 Scanning electron microscopy (SEM)

The surface morphology of PP and its WPCs were examined using an Oxford Instruments Quanta FEG 250 Environmental SEM coupled with an energy dispersive X-ray system (EDX) capability (Abingdon, Oxon, UK) without any sputter coating. The micrographs were taken from broken tensile samples to investigate the material failure under load.

3.3.6 Tensile properties

The tensile test was conducted on a Mandel-Shimadzu (AGS-X) tensile testing unit (Shimadzu corp., Japan) at a constant crosshead speed of 50 mm/min for the virgin and recycled PP systems as well as its corresponding WPCs in accordance with ASTM D638-14 Type V.

3.3.7 Shore hardness

The hardness of PP and its composites were measured with a Shore-A hardness tester (Shore Instrument & MFG. CO. INC., Freeport, NY, USA) following ASTM D2240-15. The hardness was measured at three different points on the specimens and the average was reported.

3.3.8 Water absorption (%WA) and thickness swelling (%TS)

The %WA and %TS for the PP and its WPCs were tested in accordance with the ASTM D570-98 standard. Three samples of each specimen of dimensions (L × W × H) of 18 × 9 × 3 mm were dried at 80 °C until a constant weight (W_0) prior to testing. The dried sample's thicknesses were also measured, using a digital caliper with accuracy of 0.05 mm, at all four corners and an average thickness (ΣT_0) was calculated. The dried samples were then

submerged into a container filled with deionized water at room temperature and monitored for seven days (7 d). Both the weight change (W_n) and the thickness of the swollen samples (T_n) were recorded at various intervals within the pre-described time frame. All samples were tapped dry with blotting paper to remove any surface moisture and consequently weighed. The %WA and %TS values were then calculated using **Eq. 1** and **Eq. 2**.

$$\%WA = \frac{(W_n - W_0)}{W_0} \cdot 100\% \qquad \textbf{Eq. 1} \qquad \%TS = \frac{(\Sigma T_n - \Sigma T_0)}{\Sigma T_0} \cdot 100\% \qquad \textbf{Eq. 2}$$

3.3.9 Bond durability test

The bond durability measurement of the WPCs was accomplished by soaking five tensile samples in boiling water for two hours (2 hr) followed by drying until a constant weight prior to tensile testing. For this, WPCs at 40 and 70 wt.% WF was selected, to illustrate the extremes of our systems, and dried overnight at 80 °C. Finally, the samples were then left in an ambient environment at relative humidity (50%) for 40 hr prior to tensile testing.

3.3.10 Differential scanning calorimeter (DSC)

The thermal analysis of the samples was conducted using a differential scanning calorimeter (DSC Q2000) with an autosampler manufactured by TA instruments (New Castle, DE, USA). The DSC experiments were conducted under a nitrogen flow at a rate of 50 mL/min. About 7.5 mg of ground PP and WPC particles were placed in an aluminum T_{zero} pan which was then heated at 5 °C/min up to 210 °C, held there for five minutes before cooling down at 5 °C/min to -20 °C, and heated again at 5 °C/min up to 210 °C. For this study, the melting temperature (T_m), crystallization temperature (T_c), and melt enthalpy (H_f) were taken during the second heating cycle to remove the thermal history of the processing and any residual

moisture. For comparison, the neat PP and all WPCs were tested using the same method and the percentage crystallinity of PP ($\%\chi_{cpp}$) within the WPCs was determined using **Eq. 3** ($H^0_{f_{PP}} = 207.1\, J/g$) [115,116].

$$\%\chi_{c_{PP}} = \left(\frac{H_{f_{PP}}}{H^0_{f_{PP}} * (PP\ wt.\%)}\right) \cdot 100\% \qquad \textbf{Eq. 3}$$

3.4 Results and discussion

3.4.1 Effect of repeated recycling on PP matrix on chemical structure changes

In this work, the effect of process-induced degradation in terms of the number the recycling (thermo-mechanical) cycles was analyzed using H-GPC, FTIR, optical microscopy, rheology, and mechanical property analysis techniques. The MWD and the molecular weight averages for the samples were examined in order to study the change or shift in the H-GPC results that is indicative of the type and degree of polymer-chain degradation [117]. It is established that if the main degradation mechanism is dominated by chain scission then MWD shifts to lower values; while, if crosslinking is dominating the MWD will shift to higher averages [117].

As shown in **Figure 6(C)**, there is a clear shift in the molecular weights to smaller sizes with repeated processing of PP indicating that chain scission has increased as noted from the loss in both number and weight average molecular weights ($\overline{M_w}$ and $\overline{M_n}$). Moreover, the curves are seen to slightly narrow down indicating that the polydispersity index (PDI) is also reducing as the re-processing cycle increases from cycles one to six. These results display that chain scission assists in making PP more homogeneous with respect to the molecular weight distribution (as shown in **Figure 6(D))**. However, the change in MWD was not severe under

the studied reprocessing cycles. These results corroborate with data reported in the literature, in that, PP degrades preferentially by chain scission due to the hydrogen that is bonded to a tertiary carbon along the polymer's backbone [118]. A thermo-mechanical kinetic study, dynamic and static, of PP reprocessing is reported in another study conducted by Esmizadeh et al. (2020) [8]. The proposed structural changes because of chain scission were further analyzed with FTIR spectrometry. Comparison of the virgin PP and the counterparts are presented in **Figure 6(A)**. The most significant observation made was the change from cycle three to six at 1713 to 1765 cm^{-1} which corresponds to C=O symmetric and asymmetric stretching [119,120].

The increase in peak intensity signifies the onset of oxidative degradation, which was most likely prolonged until cycle six due to stabilizers added in the virgin PP by the manufacturer. Oxidative degradation is not desired in polymer recycling applications due to its ability to rapidly radicalize weak points (e.g. tertiary hydrogens) along a polymer backbone as well as the potential to produce volatile compounds like hydro-peroxide radicals and alkyl radicals [121]. As a means to quantify and observe the progress of oxidative degradation and chain scission within a polymer system the carbonyl index (CI) was calculated (see **Eq. 4**).

$$\mathrm{CI} = \frac{\mathrm{abs}(1756\ cm^{-1})}{\mathrm{abs}(1375\ cm^{-1})} \qquad \textbf{Eq. 4}$$

The reference bands were taken at 1376 cm^{-1} (CH_3 stretching) as it is known to be non-changing to photo- or thermo-degradation was compared against the 1756 cm^{-1}, which represents the formation of carbonyl groups [122]. **Figure 6(B)** shows an overall increase in the formation of carbonyl content with each successive processing cycle illustrating that

oxidation is not the primary mechanism until after cycle three leaving chain scission as the dominating mechanism.

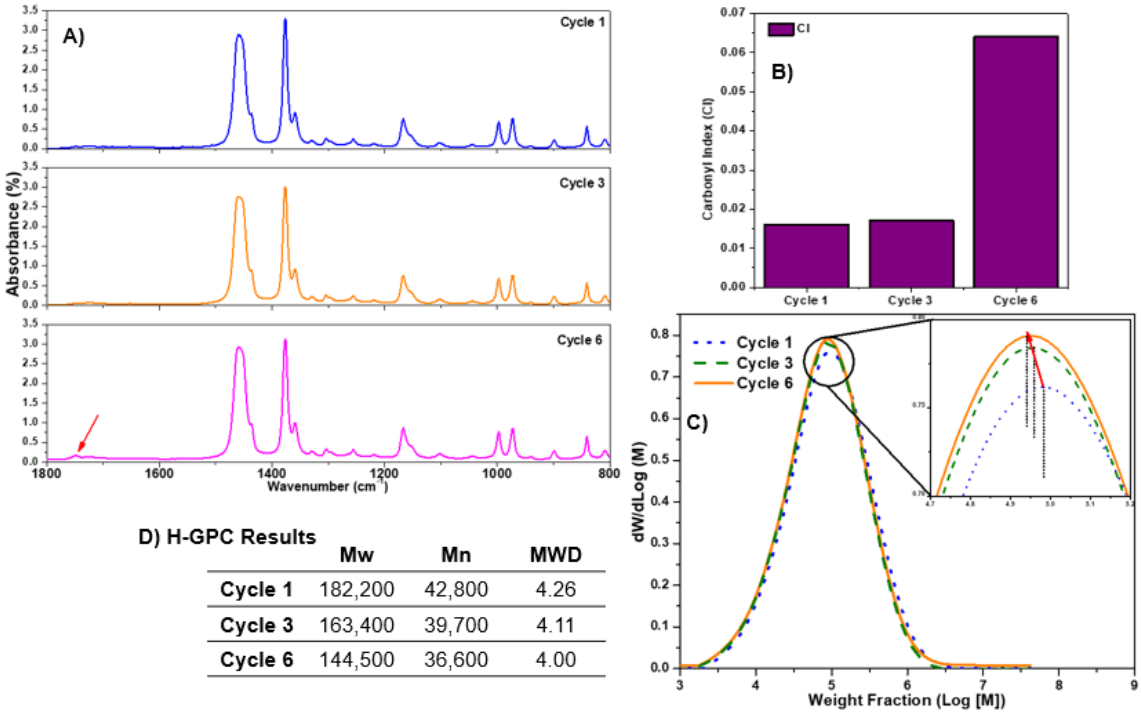

D) H-GPC Results

	Mw	Mn	MWD
Cycle 1	182,200	42,800	4.26
Cycle 3	163,400	39,700	4.11
Cycle 6	144,500	36,600	4.00

Figure 6. (A) FTIR spectra of PP and recycled counterpart by means of process induced thermo-mechanical; **(B)** Carbonyl index for the recycled PP specimens; **(C)** MWD curves of PP and its recycled derivatives taken by H-GPC; and **(D)** H-GPC results associated to each cycle.

3.4.2 Effect of repeated recycling on PP matrix on rheological and mechanical properties

The combination of the H-GPC and FTIR results indicated that the use of thermo-mechanical recycling could be a viable option to recover an acceptable quality of that can be used for composite applications including WPCs. As chain scission is the primary mechanism, it was expected that PP's viscosity could significantly reduce, which would help in flowability. A polymer's viscosity is associated to an irreversible bulk deformation by means of molecular chains slipping past one another. As such, the most important structural parameter in determining the flow properties of a given polymer is its MWD or rather its chain length.

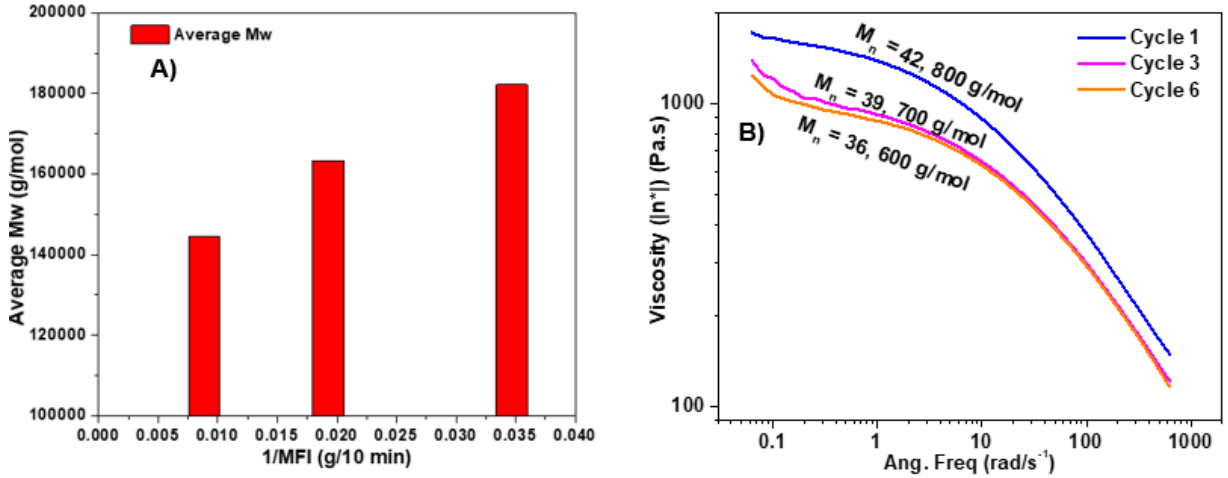

Figure 7. (A) Mw values in correlation to the equivalent MFR values and **(B)** Viscosity data of PP and recycled PP overlaid Mw data obtained from H-GPC.

A common method for evaluating the flow properties of a polymer is to calculate its MFR as it is related to a polymer's physical and chemical properties. MFR, specifically, is a measure of the polymer's viscosity or rather its ability to flow, under pressure, through a narrow orifice while in a molten state [123]. MFR tests offer an approximation for the zero-shear viscosity and a relative measurement of M_w for a given polymer system due to these experiments being conducted at comparably low shear rates [104]. A number of studies have been conducted in hopes to correlate Mw with MFR by means of various models such as the Mark-Houwink power law which describes an inverse relationship between the parameters [123]. **Figure 7(A)** shows that with increasing extrusion cycles the 1/MFR value decreases and when plotted against the $\overline{M_w}$ data, obtained by H-GPC, a near linear relationship can be seen where the highest Mw value has the lowest MFR value.

Although MFR is a measure of a polymer's ability to flow under a constant load and it correlates with Mw, it is not a clear representation of a polymer's overall viscosity curve. With that, parallel plate rheometry is often sought after in order to obtain the physical melt properties

over a range of frequencies. **Figure 7(B)** shows the change in viscosity for multiple processing cycles of PP. Although a Newtonian plateau was rather elusive, even at low shear rate, it can still be seen that with increasing extrusion cycles the melt viscosity of each PP sample decreased. Moreover, each individual cycle displayed shear thinning characteristics which was denoted by the linear slope at angular frequencies 10 rad/s and above. It was also noted that for all cycles at low shear (0.1 rad/s) there was a slight upward slope which is evidence of minor crosslinking as a result of recycling [124].

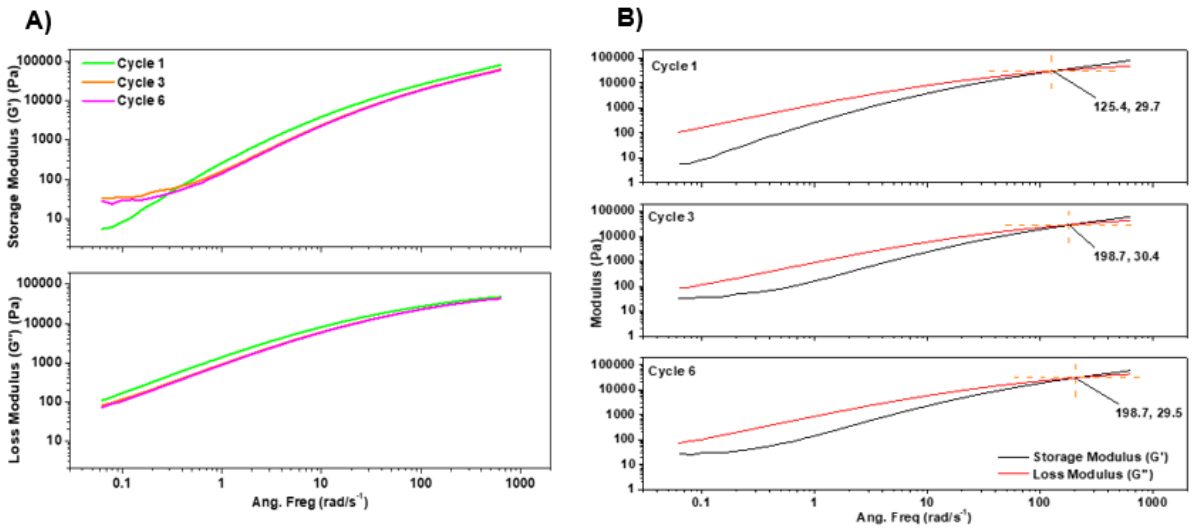

Figure 8. (**A)** Storage and Loss moduli of the virgin and recycled PP specimens and (**B)** Crossover moduli and frequencies of virgin and recycled PP.

Since the temperature was held constant, a decrease in viscosity cycle over cycle (one to six) is another indication of chain scission as the longer chains are preferentially broken first which agrees with the overlaid H-GPC M_W values as a relative trend. **Figure 8(A)** displays the associated storage and loss moduli for PP systems, which are measures of how the material stores energy in an elastic behavior as well as how the system dissipates said energy. As shown in **Figure 9(ii)-(D)** to **(F)** and **Figure 10**, the overall crystallinity of the polymer is greatly

affected from cycle over cycle in both crystallite size and quantity. In **Figure 10(A)** to (**B)**, it is shown that with each successive recycling process there is a decrease in crystallinity from ~46 to 33% [29]. Additionally, **Figure 10(C)** to **(I)** shows that WPCs also decreases slightly in crystallinity, from 37 to 35%, as the amount of WF increases. This is due to the crossover modulus being dependent upon the rheological PDI of the tested polymer. This indicates little to no change in the overall MWD or PDI [125].

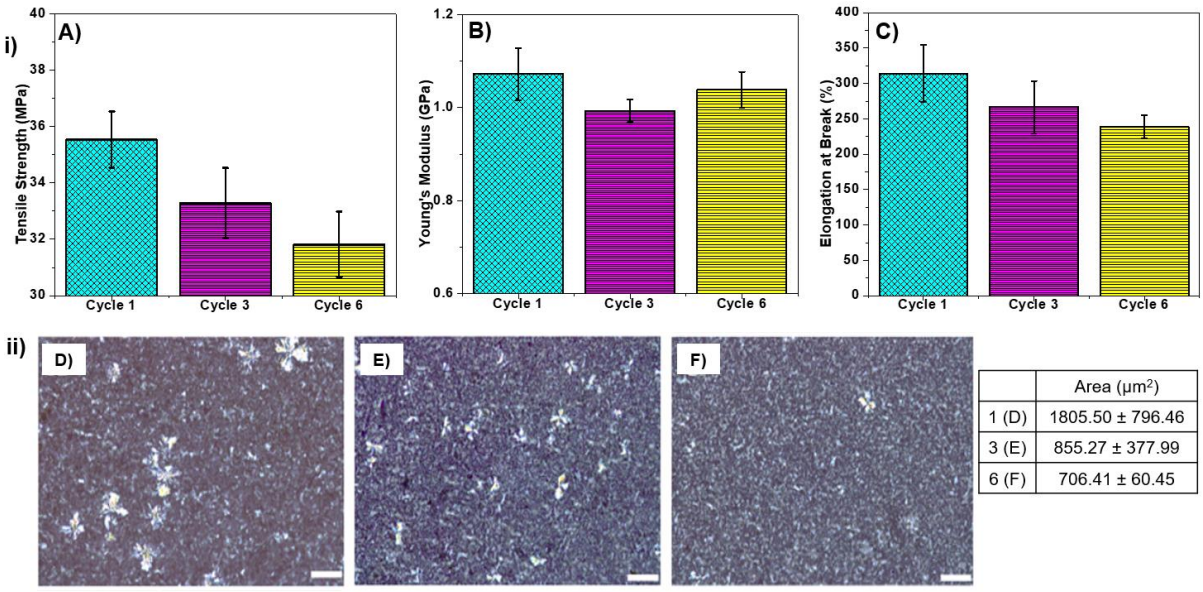

Figure 9. (**i)** Tensile properties of virgin PP and recycled PP. **(A)** Tensile Strength; **(B)** Young's Modulus; and **(C)** Elongation at break and **(ii) -** POM images (20× at 10 μm) of the virgin and recycled PP. **(D)** Cycle one; **(E)** cycle three; and **(F)** Cycle six.

Examining the cross modulus and frequencies of the various cycles in **Figure 8**(**B)**, it was observed that the crossover modulus does not change too significantly which correlates well with the H-GPC results on polydispersity. The final evaluation method conducted to study the effect of thermo-mechanical reprocessing cycles on the PP was tensile properties. As can be seen in **Figure 9(i) (A)** to **(C)**, both the tensile strength and modulus were relatively

unaffected by the reprocessing cycles (up to six cycles) employed in this study. One-way ANOVA ($p < 0.05$) indicated that the changes were not statistically significant. Unlike the strength and modulus values, the elongation at break value has decreased by 17%. Overall, the aforementioned results show signs of a decrease in the polymer's chain lengths resulting in less entanglement points and less slip resistance. Overall, the mechanical results along with the rheological results showed that the chain degradation as a result of the reprocessing cycles is not extensive enough to cause significant property deterioration. As such, the reprocessed PP can be utilized as a matrix for composite materials.

i)

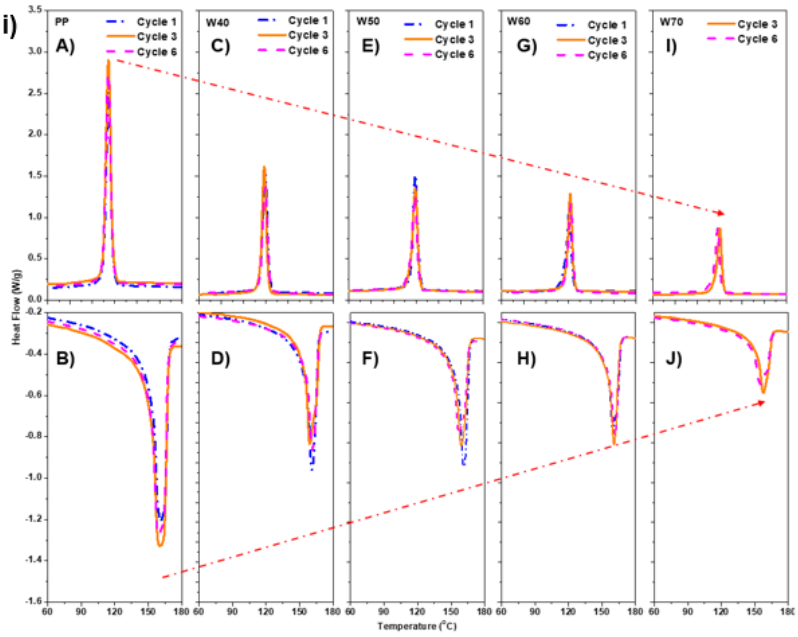

ii)

	Cycle #	ΔH_f (J/g)	$\%X_{cpp}$
PP	1	123.5	45.7
	3	106.1	39.3
	6	88.83	32.9
PP60W40	1	61.18	37.8
	3	50.65	31.3
	6	45.78	28.2
PP50W50	1	48.38	35.8
	3	47.46	35.1
	6	45.04	33.3
PP40W60	1	36.37	33.7
	3	38.01	35.2
	6	38.44	35.6
PP30W70	1	/	/
	3	28.65	35.3
	6	28.69	35.4

Figure 10. (i) - DSC thermograms of PP, its recycled derivatives, and its WPCs. **(A)** PP100W00 (cooling); **(B)** PP100W00 (2^{nd} heating); **(C)** PP60W40 (cooling); **(D)** PP60W40 (2^{nd} heating); **(E)** PP50W50 (cooling); **(F)** PP50W50 (2^{nd} heating); **(G)** PP40W60 (cooling); **(H)** PP40W60 (2^{nd} heating); **(I)** PP30W70 (cooling); **(J)** PP30W70 (2^{nd} heating) and **(ii) -** Crystallinity data obtained from DSC results.

3.4.3 Effect of WF loading (40 to 70 wt.%) on tensile and physical properties

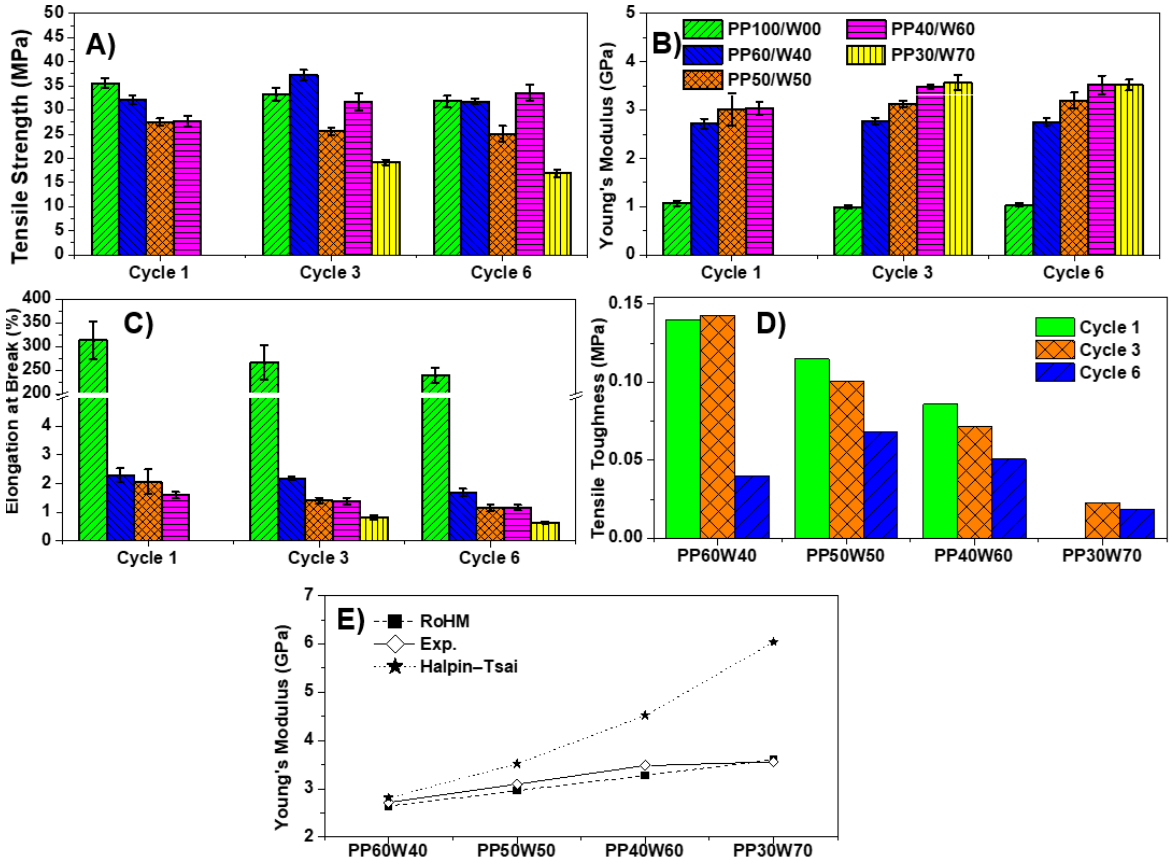

Figure 11. Tensile Properties of WPC after multiple recycling processes. **(A)** Tensile strength; **(B)** Young's Modulus; **(C)** Elongation at break; **(D)** Tensile toughness of WPCs; and **(E)** Comparison between real and predicted modulus values.

The effect of PP reprocessing and WF loading on the WPC properties was investigated via tensile and other physical properties testing, and results are presented in **Figure 11(A)** to **Figure 11(D)** as well as in **Table A1** in **Appendix A**. In all cases, the tensile strength has either remained unchanged or reduced likely due to the insufficient interaction between the non-polar PP and the mainly polar WF. Contrarily, the materials Young's modulus shows a positive effect with increasing WF due to the rigid and stiff nature of the wood and as expected, the WPC's elongation at break values has substantially reduced by the high WF loading. To

improve properties, it would be worthwhile to investigate more uniform WF particles as opposed to “as received” WF that had little to no pre-handling before compounding as well as studying the effects of surface modifications on the WF and PP. Finally, the tensile toughness was found by integrating the area under the stress-strain curve between the origin and the total extension of the sample. This value is a measure of composites crack’s resistance and in **Figure 11(D)** it is shown that with increasing wood content the toughness decreases as the material become more and more brittle. These results correlate with what has been found in literature [126]. To validate the experimental results, the data was compared with predicted values based off both the *rule of hybrid mixtures* (RoHM) and *Halpin-Tsai* (H-T) models. Results in **Figure 11(E)** calculated by **Eq. 5** to **Eq. 8** showed that the RoHM has accurately predicted the Young’s modulus (E_c) value even though it assumed full particle/matrix interaction which was not the case with these systems. Unlike the RoHM model, the H-T model predicted the modulus well to be substantially higher than the experimental values, which was likely due to the model being partially empirical and dependent on the particle’s dimensions, orientation, and packing/void spaces.

Although there are a few iterations of this model (e.g. Tsai–Pagano and Lavengood–Goettler modes) the H-T was chosen as it better represented short and randomly oriented fibres [127,128]. E_f and E_m are the known modulus values (GPa) for the fibre and matrix in the system; V_f is the volume fraction of the fibre; ‘ε’ is the fitting parameter, while ‘L’ and ‘D’ are the particle’s length and width. Similarly to the tensile properties, the density also experienced an increase by, initially, ~17% and increased with each subsequent addition of WF with the 70

wt.% WPC having a density of ~1.1 g/cm^3 as shown in **Figure 12(A)**. Preforming a reverse *rule of mixtures* (ROM) (**Eq. 5**) calculation, the density of the used WF was found to be ~1.20 g/cm^3 which was comparable to known literature [129].

$$E_c = \mathrm{E}_m V_m + \mathrm{E}_f V_f \qquad \textbf{Eq. 5}$$

$$\eta = \frac{\left(\frac{E_f}{E_m}\right) - 1}{\left(\frac{E_f}{E_m}\right) - \epsilon} \qquad \textbf{Eq. 6}$$

$$\mathrm{E}_c = E_m * \left(\frac{1 + \varepsilon\eta V_f}{1 - \eta V_f}\right) \qquad \textbf{Eq. 7}$$

$$\varepsilon = 2\frac{L}{D} \qquad \textbf{Eq. 8}$$

Using density values from literature for PP and WF and using the rule of mixture, the composites theoretical density was calculated to be 1.10 g/cm^3 [129]. Although there is an increase in density from the base, it is still well below that of more conventional fillers like glass fibre or talc which are ~2.2 to 2.4 g/cm^3 [130]. Additionally, it appears that recycling does not affect the overall density of the WPC. As it would be expected when adding a more rigid filler into a tough matrix the composite's hardness will increase. Hardness is a measure of a material's ability to resistant indentation, which reflects the material's overall stiffness. High hardness values will typically translate to composite having high flexural strength, an increased resistance to break while under stress, and a lower co-efficient of friction [131]. The Shore-A hardness value of the WPCs increased with each addition of WF loading as shown in **Figure 12(B),** which agrees with the density (**Figure 12(A)**) and torque data (see **Figure 13**). These results agree with what is already known in literature [132–134]; however, additional knowledge gained from this experiment is that recycling has little to no effect on the PP based WPC's ability to resist indentation. It should be noted that the PP30W70 cycle one specimen (denoted by '*') was not processible due to the mixer's maximum torque value so no data was

collected for it. As a result of the changing densities across the PP and WPC samples, the specific modulus otherwise considered the material's stiffness was found in terms of WF loading and recycling.

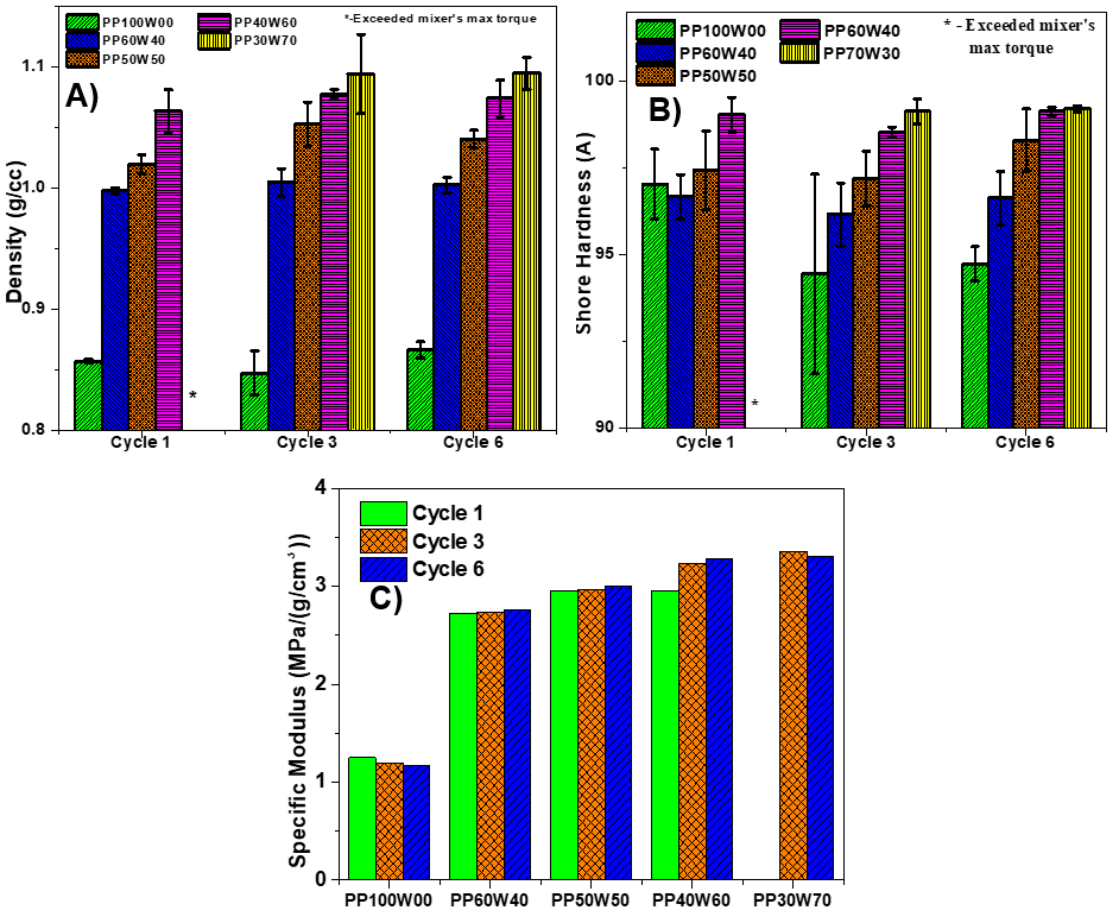

Figure 12. (A) Density comparison of WPCs with different degrees of recycled PP; **(B)** Shore hardness (A) values of produced WPCs from recycled PP; and **(C)** Specific Modulus of the neat PP and its WPCs.

In **Figure 12(C)**, it is shown that the specific modulus increases as the material becomes stiffer as the 70 wt.% WF being the stiffest (3.3 GPa/(g/cm^3)) and 40 wt.% having the lowest value of the composite systems (2.7 GPa/(g/cm^3)). The low values for WPCs have been attributed to wood type reinforcements being in a less compact state (i.e. porous) as compared to synthetic fillers like carbon or glass fibres [135]. Lastly, the WPCs were examined

using E-SEM to evaluate the effect of recycling on both the morphology of the composites but, more importantly, on how it affects the matrix's ability to flow and permeate through the WF. Shown in the middle (W60) and bottom (W70) rows of **Figure 14**, there were clear boundary layers between the filler and matrix resulting from a lack of compatibility between the polar WF and non-polar PP.

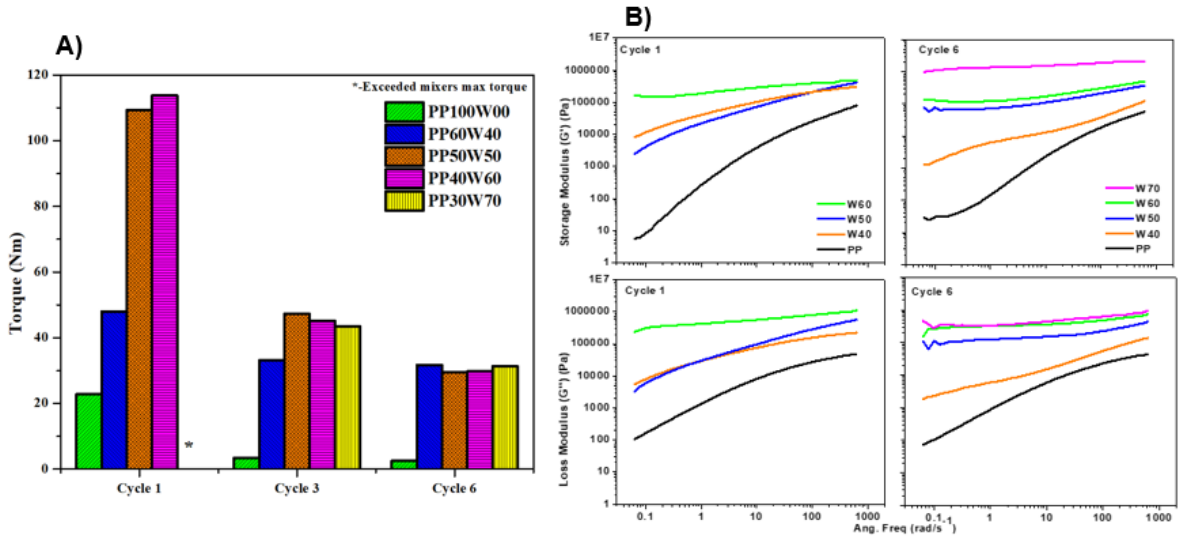

Figure 13. (A) Torque values before and after addition of wood at the three stages of recycling and **(B)** Storage and loss moduli of PP based WPCs.

For this reason, WPC producers often utilize coupling agents or other chemical modifications to help facilitate dispersion and interactions between the system's constituents but at a greater material cost [136]. Another noteworthy observation was the non-uniformity, filler pullout, and multiple SCFs all of which would result in the composite's catastrophic failure due to poor stress transfer. Looking at the top row (PP100), it was noted that simulated recycling had no effect on the composite's morphology attributed to the little oxidative deterioration. Due to the high amounts of WF in the composites as well as the large and

irregular particle sizes/shapes, it was difficult to examine extent of interactions resulting from the multiple reprocessing.

3.4.4 Effect of WF loading and recycling on rheological properties

The effect of wood derived filler concentration within a polymer matrix on rheological properties was examined using a parallel plate rheometer under inert atmosphere. For WPCs and other composites, it is well documented that with increasing wood content the apparent viscosity of the material increases drastically and at sufficiently high levels of wood content the counteracting pressures on the melt are too high to overcome and no flow will occur [12,25]. Due to the low thermal stability and inability to increase shear rates, lubricants and/or polymers with high melt indexes are typically incorporated to assist with wall slip but at a cost of the material's overall strength [114]. Results in **Figure 15(A)** showed that increasing WF loading caused drastic viscosity increase, which resulted in higher torque attributed to the WF restricting polymer mobility at the interfacial boundaries. In all cases, shear thinning was observed due to the polymer/filler interaction and the mechanical contacts between the filler particles themselves.

Particles that tend to cluster together and form aggregates, such as WF, are expected to remain bonded to one another due to cohesive forces. With increasing WF content the probability of direct interactions between fillers rises significantly and shear thinning becomes more pronounced. As expected, with increasing recycling the viscosity decreases as a result of the recycled PP chains having increased mobility (previously discussed). Finally, the shear stress (τ) of the PP based WPCs was found by fitting the viscosity data with a Herschel-

Buckley (HB) or yield power law model (**Eq. 9**) [137,138]. The HB model is an enhanced version of the power law model that contains both yield stress and the power equation. The model helps to provide a relationship to calculate rheological properties for materials that fall into the non-Newtonian, non-linear shear thinning fluid category [137,138].

$$\tau = \tau_0 + K\dot{\gamma}^n \qquad \textbf{Eq. 9}$$

Where τ_0 represents the yield shear stress; n is the power rate index; γ is the shear rate; and k is the consistency index. After applying and graphing the model (see **Figure 15(A)** and **(B))**, the predicted results fit nicely with the experimental data and clear trends were observed in terms of the composite's yield stress and power-law indexes. As it is shown in the result, with increase wood content the WPC's yield stress increases; however, with each successive recycling cycle the composite's yield stress decreases which agrees with the mechanical properties.

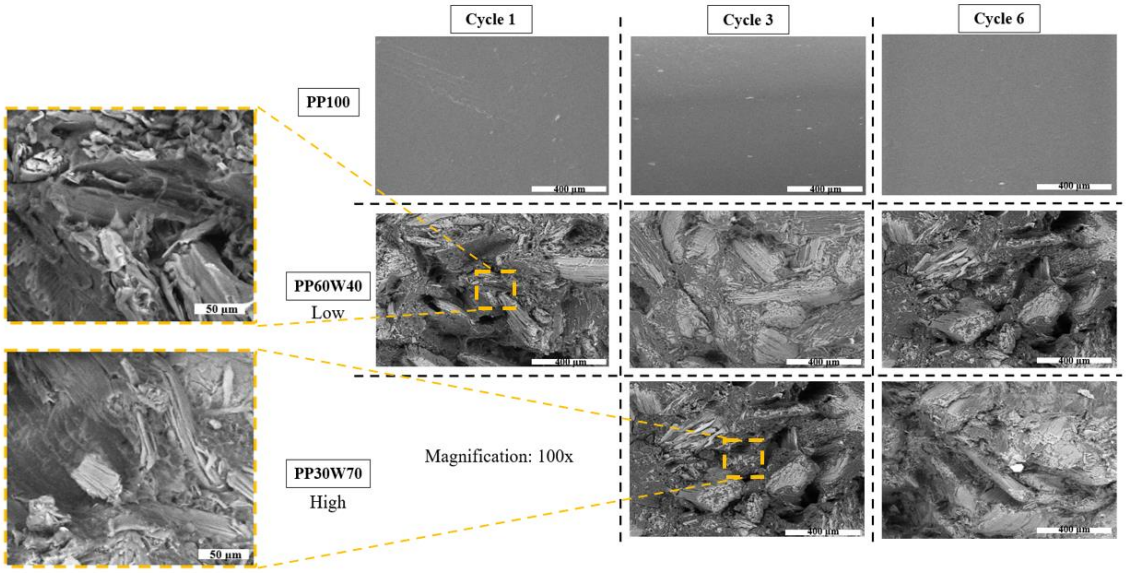

Figure 14. SEM micrograph illustrating the distribution, adhesion, and SCFs within the WPCs.

Similarly, the moduli of the WPCs (see **Figure 13**) increased with increasing wood content and decreased with recycling due the melt behaviour being filler dominated. Unlike the case with neat polymers, when wood derived fillers are added at a significant degree, the rheological properties are dominated by the filler meaning it acts as viscoelastic solid at low frequencies and switches to being polymer dominated at higher frequencies. Moreover, the crossover frequency and modulus have greatly decreased with the addition of wood, meaning the materials behaviour switches from a solid to viscous melt much more rapidly under elevated temperatures.

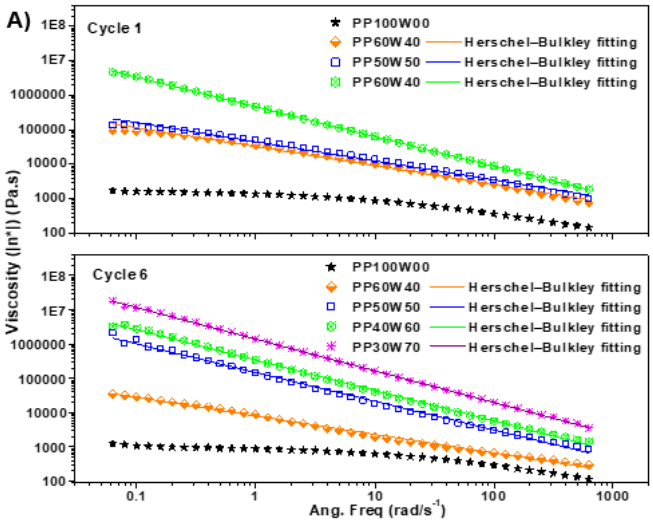

B)

Sample	Cycle #	n	m (KPa.s^n)	τ (Pa)
PP60W40	1	0.3166	30.7	7.97E4
	3	0.4036	33.4	5.17E4
	6	0.5718	37.7	1.56E4
PP50W50	1	0.3224	19.0	1.18E5
	3	0.3622	24.0	1.15E5
	6	0.4494	21.0	1.13E5
PP40W60	1	0.3231	31.9	3.10E5
	3	0.2618	44.8	2.80E5
	6	0.1716	68.9	1.08E5
PP30W70	1		*	
	3	0.1317	14.34	9.05E5
	6	0.1330	21.56	6.71E5

Figure 15. (A) Viscosity (Pa·s) of the WPCs in terms of shear rate and recycling count (top – cycle one; bottom – cycle six) and **(B)** Herschel-Bulkley model values and results from fitting.

3.4.5 Effect of WF loading and recycling on moisture absorption

The moisture uptake of WPCs is an important consideration for the applications of WPCs including outdoor versus indoor use, environmental degradation, and load bearing properties. In this study, %WA and %TS were used to investigate the moisture uptake of WPCs . %WA is the WPC's ability to absorb moisture from its surrounding environment as it may

act as a plasticizer leading to reduced glass transition, strength, and electrical performance due to irreversible degradation. As shown in **Figure 16**, the increase in the WF loading increased the %WA due to the association of water with the hydrophilic moieties of wood ingredients (e.g. cellulose, hemicellulose, lignin). The slope of water absorption versus time was noticeably steeper with the increase in wood loading in the WPC, and an equilibrium was reached much faster meaning water diffused more easily and quickly. This is a result of WPCs having two main driving forces behind water absorption, which are: 1) water's diffusivity ability (i.e. pores) and 2) the fillers hygroscopic nature (i.e. reactive sites) [139]. Conversely, pure PP samples had no inherent changes after 500 hr and increasing the amount of PP helped with the WPCs durability by encapsulating more wood and preventing water penetration and leaching (see **Figure 17(B)**).

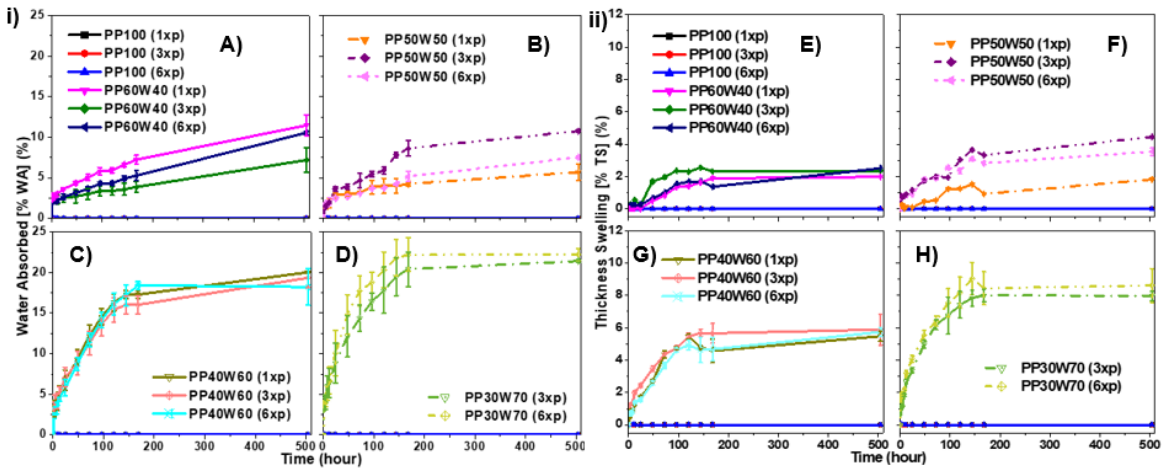

Figure 16. (i) %WA for WPCs as a function of time and recycling**. (A)** PP60W40; **(B)** PP50W50; **(C)** PP40W60; and **(D)** PP30W70 and **(ii)** %TS for WPCs as a function of time and recycling. **(A)** PP60W40; **(B)** PP50W50; **(C)** PP40W60; and **(D)** PP30W70.

It is known that PP is inherently hydrophobic and will not absorb water or swell, therefore, all absorption is governed by the WF content [134,140]. Lastly, the effect of

recycling on the material's ability to absorb water was not noticed due to the sheer amount of WF in the system. Similarly, %TS has the same trend as %WA, as shown in **Figure 16(ii)**, meaning that there is correlation between the swelling experience and the weight gain and by examining **Figure 17(A)** it is observed as a near-linear and increasing relationship. The increase in sample swelling is due to the presence of hydrogen bonding sites (hydroxyl groups) on the cellulose and hemi-cellulose when mixed with a non-polar polymer [141].

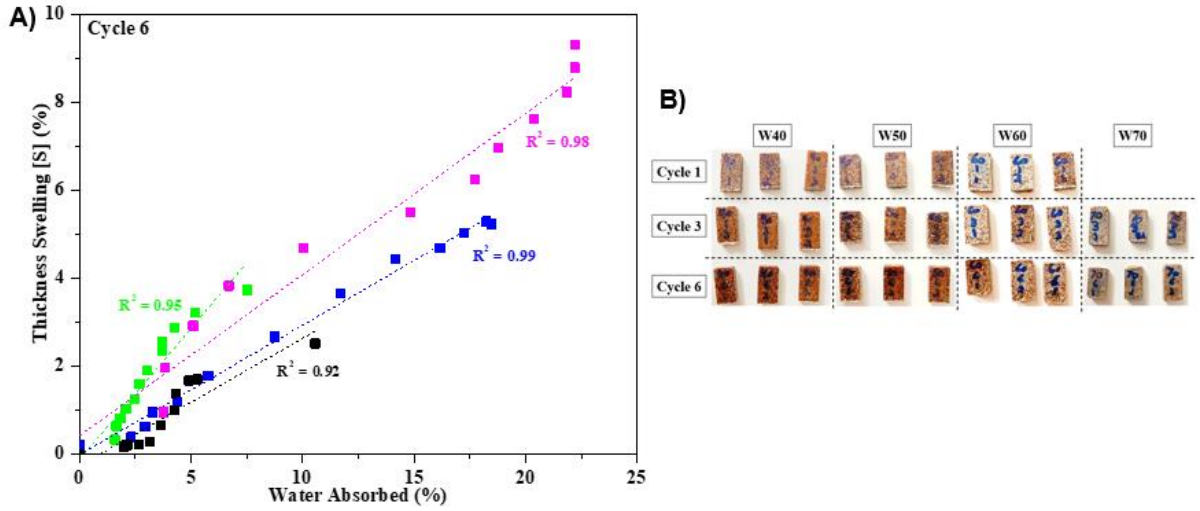

Figure 17. (A) Comparison between thickness swelling and water absorbed for cycle six specimens and **(B)** Water absorption specimens after seven days of conditioning.

Other studies have shown that compounding WPCs with additives reduces the thickness swelling; and reducing the WF particle, which provides a more compact systems provides lower %TS as compared to fibre systems [142,143]. It is important to study the effect of accelerated moisture sorption on the mechanical properties of WPCs, as many of these composites are used in marine and outdoor construction applications, such as decks and fences. The adhesive bonds between the PP matrix and the WF aids in the WPC's ability to withstand

mechanical forces and the bond strength is typically affected by moisture, chemical fluids, and outdoor weathering [144].

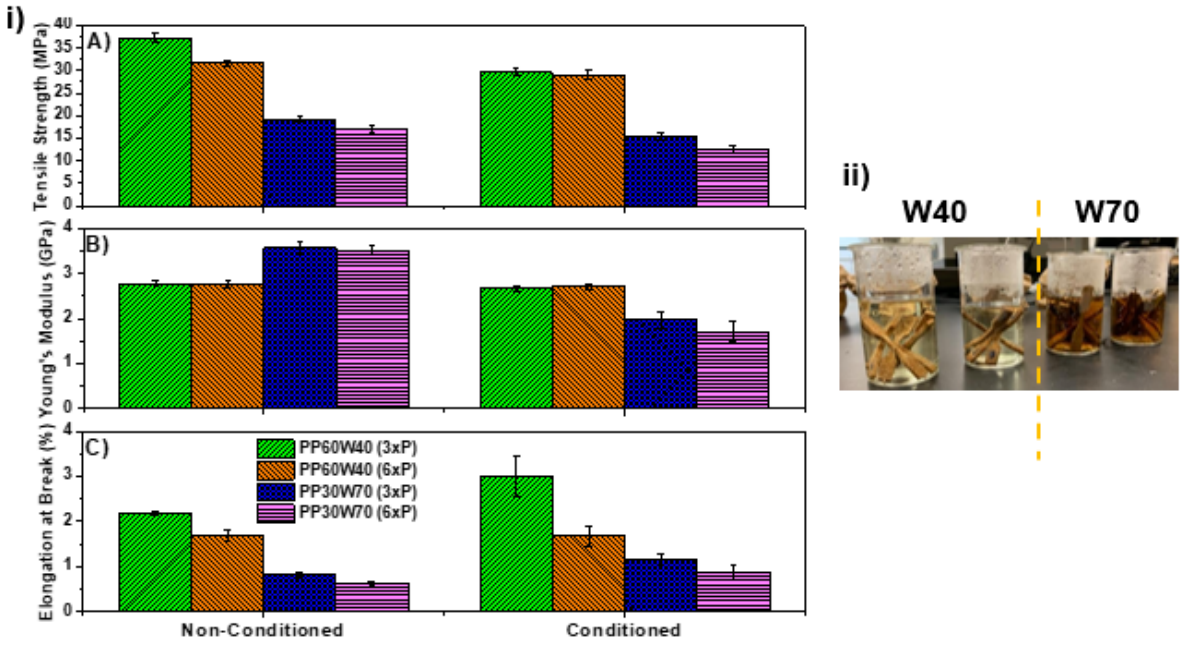

Figure 18. (i) - Bond strength of the WPCs. **(A)** Tensile strength; **(B)** Young's Modulus; **(C)** Elongation at break and **(ii)** - Colour bleed of the WPCs after bond durability test**.**

As shown in **Figure 18**, both the tensile strength and modulus show significant decrease after accelerated aging, which was expected as WF is inherently hygroscopic leading to particle swelling and voids between polymer and filler. Contrary to the strength and modulus, the elongation at break had the opposite trend, which could be due to the softening of the wood content leading to a less brittle failure while under stress [145]. **Figure 18(ii)**, shows the difference in colour leaching intensity from the 40 to 70 wt.% WF composites. The colour of wood is a result of the combination of lignin and phenolic extracts like tannins compounds that contain chromophore bonds which are predominately responsible for light absorption [146,147]. Thus intensity of "brown water" is due to the readily available tannins

and other bleeding compounds as a result of the higher wood loading at 70 wt.%. In terms of a commercial product, the leaching of tannins and other compounds may not be desirable as one of the most important selling points for WPCs in construction and furniture applications is its resemblance with high-quality pure wood products [147].

3.5 Summary of Chapter 3

This study has shown that PP can be reprocessed for at least up to six times, while retaining most of its essential material properties. The reprocessing of PP, which simulates recycling, has substantially decreased its viscous and elastic properties. This was validated through MFR and parallel plate rheometry and was attributed to chain scissions due to the thermo-mechanical process induced shear forces and not oxidative degradation. The chain scission and lack of oxidative degradation resulted in smaller and less perfect spherulite structures and overall crystallinity; all the while, having no noticeable changes on the surface morphology of the neat polymer. Due to the high viscosity of the virgin PP, the maximum WF loading achieved without over torquing the equipment was limited to 60 wt.%. Contrarily, WPCs with WF loading up to 70 wt.% was fabricated in all the reprocessed PP (cycles one to six) samples. This indicated that reprocessing can be beneficial to fabrication of highly loaded WPCs. Compounding WF into PP (70 wt.% loading) resulted in a ~17 and 9% increase in density and material hardness, respectively, which was to be expected due to the higher density of WF as compared to PP as well as the rigid nature of WF filler. As expected, the addition of WF into PP matrix has substantially increased the modulus while reducing the elongation and the trend continued with a further increase in the WF loading. The moisture absorption and

relative thickness swelling properties of WPCs are greatly affected by the levels of WF loading. Overall, it was shown that WPCs with WF loading of up to 70 wt.% can be fabricated with the use of reprocessed PP without the need of additional processing aids.

Chapter 4 – Recyclability of Maleated PP for WPC Fabrication[3]

4.1 Introduction

Polypropylene (PP) is one of the most widely consumed thermoplastics due to its ease of processibility, low density, good chemical stability, and low cost when compared to engineered polymers giving usage across many industries (e.g. automotive and medical) and applications (e.g., appliances, tubing, and packaging). However, there are a couple of caveats to the use of PP, which are its susceptibility to both oxidation and ultra-violet degradation, poor bonding with some fillers and polymers as well as high thermal expansion coefficients. One common application of PP is in composite materials, such as wood plastic composites (WPC), which are manufactured with wood reinforcements (e.g. flour/sawdust) along with a thermoplastic resin.

The popularity and high demand driving WPC production is due to the wood resembling aesthetics (e.g. smell, appearance, and touch); all the while, extending the durability and feedstock of natural wood. WPCs are also much more cost effective by using less wood and have the potential to be less dense compared to natural wood (depending on the wood genus, amount, and constituents of wood). Synthetic wood products or WPCs are extensively used in a range of products including decking, fencing, paneling, cladding, and furniture. Despite the popularity, after a substantial level of wood filler within a polymer matrix there will be several issues hindering the successful manufacturing of these products such as

[3] A version of this chapter has been published on peer-reviewed journal as a review article: Jubinville, D., et al. (2022). Simulated Recycling of Polypropylene and Maleated Polypropylene for the Fabrication of Highly-Filled Wood Plastic Composites. *ACS Applied Polymer Materials*, *4*(4), 2373–2383. https://doi.org/10.1021/acsapm.1c01671

the poor matrix/filler interaction and the material's high melt viscosity during extrusion type of operations [148]. When questions of compatibility arise, it is necessary to think in terms of how the components interact with respect to one another. For optimal properties, the filler material should disperse well and not agglomerate or form clusters in the resin. The constituent's polarity and overall chemical and physical interactions with each other is important to obtain composites with superior performance. It has been shown that the non-polar PP and polar lignocellulosic materials, such as wood fibers or flour, have poor compatibility leading to a distinct boundary layer formation between the resin and filler and inferior material properties [149–153].

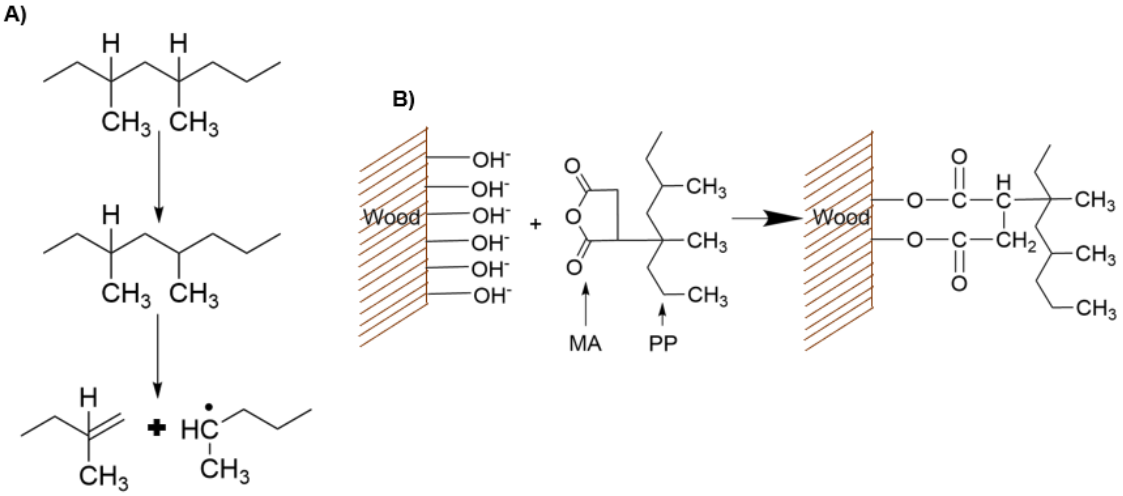

Schematic 1. A) Thermo-mechanical degradation pathway for the recycling of PP and **B)** Reaction schematic for MAPP and WF.

To mitigate the compatibility concern, compatibilizers, such as maleic anhydride (MA) and other modifiers, are often utilized to bridge the polarity gap (see **Schematic 1(B)**). In the case of PP based WPCs, maleic anhydride grafted polypropylene (MAPP) compatibilizers significantly enhance performance due to the interaction of the carbonyl groups of the MAPP

with the surface -OH groups of wood, and sometimes reaction to create ester bonds (**Schematic 1(B)**) [154].

To fabricate highly filled composites, the material's high viscosity during processing (e.g., extrusion operations) is among the main hindrances. This can be resolved by employing viscosity modifiers (e.g. lubricants) to some extent. It is also possible to employ controlled thermo-mechanical operations to reduce the polymer's melt viscosity resulting in lower processing forces while maintaining most mechanical properties, as shown in past studies [8,29,148]. Normally, when PP is reprocessed or recycled via a thermo-mechanical process, such as extrusion, it undergoes chain scission, which reduces its molecular size (see **Schematic 1(A**). In controlled thermo-mechanical process, the chain scission is sufficient to reduce the viscosity because of a reduction in chain entanglement from the reduced molecular size. All the while, not being severe enough to significantly affect some mechanical properties such as tensile strength and modulus while elongation at break may affected [28,29].

Although the reprocessing of PP as well as compounding MA with PP has been extensively studied [29,64,102,104,106,153,155,156], the effects of simulated recycling on MAPP's or its blends and composites have not been widely investigated. MA is a heavily supplied and demanded product having reached a US market size of 373 million USD in 2018, which is expected to grow to 398 million USD (6%) by 2050 due to increased usage in polymers, lubricants and 1,4-butanediol [157,158]. When MA is used in plastics as compatibilizer, it has been observed that the thermo-mechanical recycling of post consumer plastic waste containing MA based compatibilizer experiences a significant decrease in

properties [155,159–162]. At elevated temperatures (≥ 350 °C), MA is known to thermally break down into C_2H_2, CO_2, and CO compounds [163,164]; however, most thermoplastic extrusion operations do not reach those elevated temperatures. This means that it is unlikely that the chemical breakdown of MA is to blame for worsened properties, but it may still be converted to another form like polymaleic anhydride. A more plausible explanation for this is that the presence of MA compounds, along a polymer chain, results in more aggressive molecular chain fragmentation during reprocessing correlating to decreases in both molecular weight and viscosity.

4.2 Materials and Method

4.2.1 Materials

The PP used in this study was produced by LyondellBasell (Houston, TX, USA) and was supplied through INGENIA Polymers (Brantford, ON, Canada) under the trade name of Pro-fax 6301. The supplied PP had a density (ρ) and melt flow rate (MFR) of 0.90 g/cm^3 and 12 g/10 mins at 230 °C and 2.16 kg, respectively. Maleic anhydride (MA), 99%, dicumyl peroxide (DCP), 98%, and 1,1,2,2-tetrachloroethane-d2 (dTCE, 99.5%) were purchased from Sigma Aldrich. All chemicals were used as received without any further purification or modification processes prior to usage. A maple (*Acer pseudoplatanus*) wood flour (WF) with a particle range of 0.3 to 1.0 mm (20 to 60 mesh) was obtained from Ontario Sawdust Supplies (East Gwillimbury, ON, Canada) with no further refinement or sorting. Prior to processing and characterization, the WF was dried overnight at 80 °C and the final moisture content of the WF was 1.5 ± 0.02%.

4.2.2 Methods

4.2.2.1 Reprocessing (simulated/ thermo-mechanical recycling)

All formulations and compositions (**Table 3**) were prepared by using a HAAKE Rheomix 3000 batch mixer (Thermo-Fisher Scientific Inc., Waltham, MA, USA) at a mixing temperature and screw speed of 180 ℃ and 100 rpm, respectively. The recycling process is shown in **Figure B1(A)** in **Appendix B**, once the set temperature had been reached the PP was added and melt mixed until a constant torque was established and held for ~5 mins. This was followed by reducing the set temperature to a point below melting (60 ℃) to allow crystallization and then heated back up to the set temperature (180 ℃) denoting one reprocessing cycle. It should be noted that after each maleation and reprocessing operation the equalized torque value decreased, as in **Figure B1(B)**), due to changes in the sample's molecular weight and viscosity. Detailed explanations are provided in a previous publication [8,148].

Table 3. Specimen formulation breakdown.

Specimen code	Reprocessed count	Resin (wt.%)	MA (phr)	DCP (phr)	WF (wt.%)
PP1	1	100	-	-	-
PP3	3	100	-	-	-
MAPP1	1	100	5	0.1	-
MAPP3	3	100	5	0.1	-
rePP3	3	100	5	0.1	-
PP3(30)WF(70)	3	30	-	-	70
MAPP1(30)WF(70)	1	30	5	0.1	70
MAPP3(30)WF(70)	3	30	5	0.1	70
rePP3(30)WF(70)	3	30	5	0.1	70

4.2.2.2 Reactive compounding and WF addition

For the reactive mixing and generation of the maleated specimens from virgin (PP1) and recycled polymers (PP3, MAPP3, and rePP3), 5 phr of MA was first dissolved in 100 mL of acetone at room temperature and mixed with 190 g of PP powder to distribute the MA more evenly. Once the excess acetone was evaporated, the MA and PP dry mixture was placed in a kinetic mixer at 180 ℃ and 100 rpm for a moment before having added 0.1 phr of DCP to facilitate the radicalization of the PP backbone and allow for MA grafting. After 3 min of a stabilized torque the material was removed to in molten clumps and ground in a grinder for later compounding and characterization. The MAPP and recycled versions (e.g. rePP3 and MAPP3) granules were then washed in acetone and centrifuged (4500 rpm for 5 mins) three times followed by vacuum drying to remove unbound MA. Lastly, the addition of the 70 wt.% WF into the respective resins followed the same outline as previously mentioned and after 5 min of equalized torque the newly formed WPCs were removed as clumps and pulverized to form powder for injection molding and other analysis.

4.2.2.3 Injection molding

A HAAKE Mini-Jet Pro (Thermo-Fisher Scientific Inc., Waltham, MA, USA) was used to injection mold the samples. The injection molding machine used had two heating zones, the barrel, and the mold, which were set to 200 and 50 ℃ along with a pressure of 750 bar and a packing (i.e. holding) time of 10 sec to produce type V tensile specimens ASTM D638-14), impact bars (ASTM D256), and rheological discs (ASTM D4440). A set of at least five replicate test specimens were produced for each test method.

4.3 Characterization methods

4.3.1 Nuclear magnetic resonance (C^{13} NMR)

For the C^{13} NMR testing, 50 mg of PP1, MAPP3, and rePP3 samples were suspended in an NMR 500 grade glass tube that contained 0.70 mL of dTCE and placed in a heating block at 120 °C overnight. C^{13} NMR spectra of the samples were then collected at 120 °C in a DRX 500 spectrometer with a C^{13} spectra operating frequency of 125.76 MHz using a 5 mm QNP cryoprobe. ^{13}C inverse gated spectra were acquired with a pulse width of 90 set at 15 μs, and a relaxation delay of 2.9 s. The total experiment run time was ~15 h per sample.

4.3.2 Fourier transform infrared spectroscopy (FTIR)

FTIR spectra for virgin PP and its reprocessed derivatives were obtained by using a Nicolet 6700 model (Thermo-Fisher Scientific Inc., Waltham, MA, USA). To accomplish this, PP films of thickness 20 μm were produced via compression molding using a Carver press. The spectra were collected in absorption mode between 600 to 2000 cm^{-1} with a resolution of 4 cm^{-1} at 64 scans. To quantify and observe the progress of MA grafting onto PP, the carbonyl index (CI_{MA}) calculation was employed (see **Eq. 10**).

$$CI_{MA} = \frac{\%\text{abs of MA related species } (\sim 1775\ cm^{-1})}{\%\text{abs of CH3 stretching from PP } (\sim 1167\ cm^{-1})} \qquad \textbf{Eq. 10}$$

4.3.3 Dynamic light scattering (DLS)

To evaluate the weight-average molecular weight (M_w) of the PP and the MAPP specimens, a Malvern Zetasizer (Nano ZS90) was used by dissolving the neat samples in heated toluene (110 °C) under dynamic light scattering (DLS) operations. A refractive index

increment - dn/dc (ml/g) of 1.08 for PP in toluene was used in the calculations for M_w [165,166].

4.3.4 Shear rheometry and melt flow rate (MFR)

ASTM D4440-15 was employed to study the rheology of the PP and WPC specimens using a HAAKE Mars III parallel plate rheometer (Thermo-Fisher Scientific Inc., Waltham, MA, USA) with a sample thickness and diameter of 2.5 and 25 mm, respectively. A frequency sweep of 0.1 to 100 rad/s at 190 ℃ was performed on all samples under a constant strain of 0.01% (within the linear viscoelastic region (LVR)) at a plate gap of 1.5 mm. Additionally, the zero-shear viscosity of the polymer and the yield stress of the composites were investigated using the Carreau model (**Eq. 11**) and Hershel-Buckley (HB) rheological models (**Eq. 12**), respectively [167,168]. The Carreau model can predict the power law region for Newtonian fluids and is also able to extrapolate the viscosity (η_0) as the shear rate approaches zero. Finding the zero-shear viscosity provides insight of the polymer's M_w since they are proportional to one another; hence, when the M_w is changed the zero-shear viscosity will be affected. From **Eq. 11**, (η) is the viscosity, (η_∞) infinite-shear viscosity, (η_0) is the zero-viscosity, (ω) is the angular frequency, (ω_β) is the critical angular frequency, and (n) is the power law index. The HB model is used to represent the melt behaviour of composites and evaluate the yield stress (τ_0) as well as (γ) being the shear rate, (m) being the consistency index and (n) symbolizing the flow index.

$$\eta = \eta_\infty + \left(\frac{(\eta_0 - \eta_\infty)}{\left(1 + \left(\frac{\omega}{\omega_\beta}\right)^2\right)^n} \right) \quad \textbf{Eq. 11}$$

$$\tau = \tau_0 + m\dot{\gamma}^n \quad \textbf{Eq. 12}$$

The MFR for the unfilled specimens was measured using a Dynisco–Kayeness polymer test system (Franklin, MA, USA) in accordance with ASTM D1238 at a temperature and load of 230 °C and 2.16 kg.

4.3.5 Scanning electron microscopy (SEM)

The surface morphology of PP and its WPCs were examined using an Oxford Instruments Quanta FEG 250 SEM (Abingdon, Oxon, UK). The samples were coated for 120 s to obtain a 10 nm thick gold (Au) film and the micrographs of the broken impact samples were collected to investigate the materials' failure mechanisms under stress.

4.3.6 Mechanical properties

The tensile test was conducted using a Shimadzu - AGS-X tensile testing unit equipped with a 10 kN load cell (Shimadzu corp., Kyoto, Japan) at a constant crosshead speed of 50 mm/min for the MAPP and PP samples as well as the WPCs in accordance with ASTM D638-14 Type V. The notched Izod impact properties were measured using a TMI Monitor Impact Tester. All the samples were notched to a depth of 2 mm immediately following injection molding with TMI notching device (Testing Machines, DE) at 25 °C and relative humidity of 50% in line with ASTM standard D256. All the samples were conditioned for at least 40 h in the standard laboratory environment according to ASTM D618 before the test.

4.3.7 Thermal Analysis

The thermal analysis of the PP and MAPP samples was conducted using a DSC Q20 (TA instruments, New Castle, DE, USA). The DSC experiments were conducted under a nitrogen flow rate of 50 mL/min. About 6 mg of maleated and non-maleated PP powder were placed in separate aluminum T_{zero} pans which were then heated at 10 °C/min up to 200 °C, held isothermally for 5 min before cooling down at 10 °C/min to -20 °C, and heated again at 10 °C/min up to 200 °C. The melting temperature (T_m), crystallization temperature (T_c), and melt enthalpy (H_f) were taken during the second heating cycle to remove the thermal history of the processing. For comparison, the PP specimens were all tested using the same method and conditions as well the percentage crystallinity of PP ($\%\chi_{cpp}$) was determined using **Eq. 3** from ***3.3.10 Differential scanning calorimeter (DSC)*** with a $H^0_{f_{PP}}$ = 207.1 J/g [116].

Tan δ and the viscoelastic behaviour from all the specimens were evaluated using a DMA Q800 from TA instruments (New Castle, DE, USA) by using a dual cantilever clamp with a frequency of 1 Hz and a strain of 0.01% (within the LVR). The width and diameter of the samples were, 11.98 ± 0.03 and 2.99 ± 0.05 mm, respectively. The tests were conducted from −35 to 100 °C with a ramp rate of 3 °C/min.

4.3.8 UV accelerated aging

The WPCs were subjected to a controlled UV irradiation exposure. For this, a UV lamp used had an LSE Lighting bulb (120 V and 50 W) and was placed 25 cm above the samples. The samples were allowed to be irradiated with the UV for 0, 40, 80, 120, 240, 320 h (~13

days). The UV irradiated samples were then recovered and tensile testing was conducted to evaluate the effect of the irradiation exposure.

4.3.9 Statistical analysis

A one-way analysis of variance (ANOVA) test was conducted to evaluate any significant difference between the means between the different PP specimens (e.g. maleated and/or reprocessed) and the WPCs at 70 wt.% WF loading. The difference in means was considered significant at $p \leq 0.05$.

4.4 Results and discussion

4.4.1 Identifying and quantifying grafting potential of MA

The FTIR results, presented in **Figure 19(A)**, displays the grafting confirmation of MA onto PP chains. The spectra for the maleation of PP illustrated that new peaks are formed in the region of 1784 to 1791 cm^{-1} which have been related to the formation of either MA, succinic anhydride (SA), and residual polymaleic anhydrides (PMA) species [169]. Moreover, the change from the PP1 spectra around 1724 cm^{-1}, after simulated recycling, to all other species is an indicator of carbonyl groups (-C=O) brought on by chain scission of the main backbone [169–172]. As previously highlighted, depending on the form and the location of the grafted MA various compounds may be formed (e.g. n-octodecylsuccinic anhydride, poly(styrene-maleic anhydride), poly(maleic anhydride), maleic anhydride) whose peaks all lie within the region of 1650 to 1850 cm^{-1} adding to the analysis complexity [172]. More specifically, the presented peaked at 1791 and 1781 cm^{-1} are assigned to single grafted SA units and PMA, respectively. The form and locations of the anhydride containing compounds depend and vary

based upon the temperature used, mixing time, and the number of constituents. A complete FTIR spectra for all polymers can be found in **Appendix B** in **Figure B6.** Lastly, the CI_{MA} (**Figure 19(B)**) also validates the presence of relative amounts of grafted MA within the 3 systems. Although the amount of MA in the systems is minimal, ranging from 0.06 to 0.12%, the presence of grafted MA is still detected. It was found that commercially available grafted MA compatibilizers range from 0.5 to 3% MA content [155,159–162].

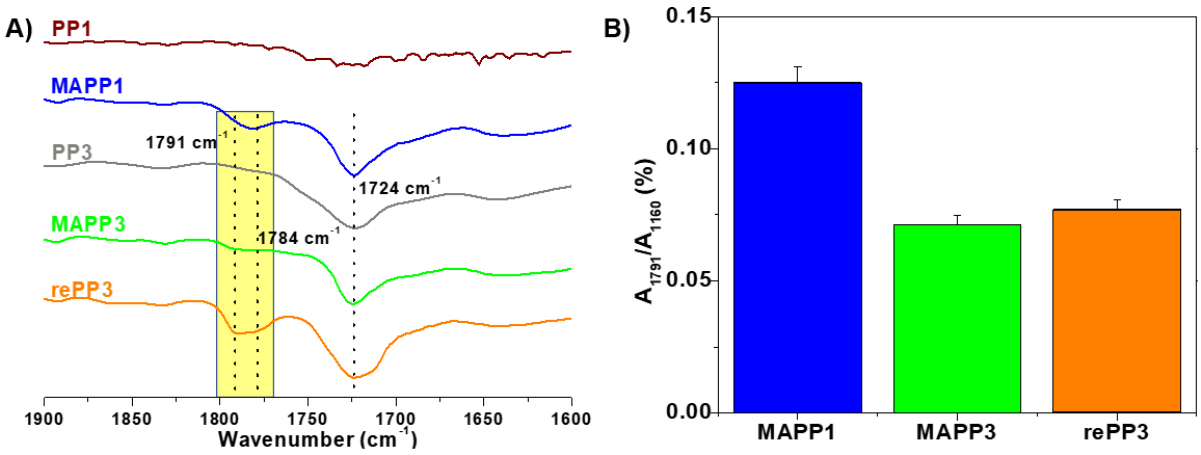

Figure 19. (A) FTIR (1600 to 1900 cm^{-1}) of PP and its maleates/reprocessed species and **(B)** MA amount (%) from FTIR spectra from carbonyl index calculation.

C^{13} NMR analysis was employed to obtain further insight into the possible grafting locations, chain information, and grafting amount for MAPP3, and rePP3 when compared to PP1. Examining **Figure B2** in **Appendix B**, the baseline spectra for PP have peaks at 21.0, 28.0, and 46.0 ppm, which are assigned to the $-CH_3$, $-CH_2-$, and -CH- groups of the PP backbone. Besides the normal peaks for PP, there is a lack of newly formed peaks at 5.0, 19.0 to 22.0, and 30.0 to 32.0 ppm which would indicate the absence of unsaturated ethylenic units, such as vinyl terminal groups at chain ends as well as vinylene units on the backbone chains [171]. As well, the absence of peaks at 44.0 to 45.0 ppm highlights an absence of oligomers or

small chain compounds [173]. Additionally, the presence of MA, or derivatives such as succinic, SA, and PMA at 31.0 to 31.2 and 49.0 to 49.5 ppm could not be detected by C^{13} NMR due to the minimal amount of grafted MA in the system also from poor resolution [174–177]. This could be enhanced by varying the amount of MA and peroxide introduced into the system, as shown by the study conducted by Yang (2003) [174].

4.4.2 Effect of recycling and maleation on the physiochemical and thermal properties of PP

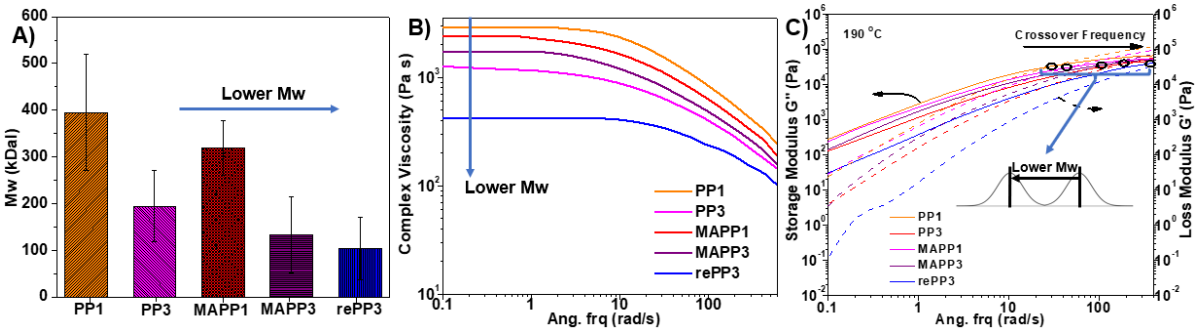

Figure 20. A) M_w measurement by dynamic light scattering for simulated recycling and maleated samples; **B)** Complex viscosity profile of the reprocessed and maleated specimens; and **C)** Crossover modulus and frequency for reprocessed and maleated specimens.

One way to investigate molecular weight (weight average - M_w) is through DLS, which is an optical technique that uses the relationship between a molecule's weight and size with the intensity of scattered light by the molecule following Rayleigh's theory. When this is coupled with multiple measurements at successively lower concentrations, linear interpolations may be used to determine the zero concentration from a Zimm plot to determine the M_w as well as the second viral coefficient that is related to the polymer's solubility parameter. As presented in **Figure 20(A)**, the effect of maleation caused a decrease in the

material's M_w due to the presence of peroxide which accelerated the rate of β-scission to facilitate the MA grating onto the backbone of PP.

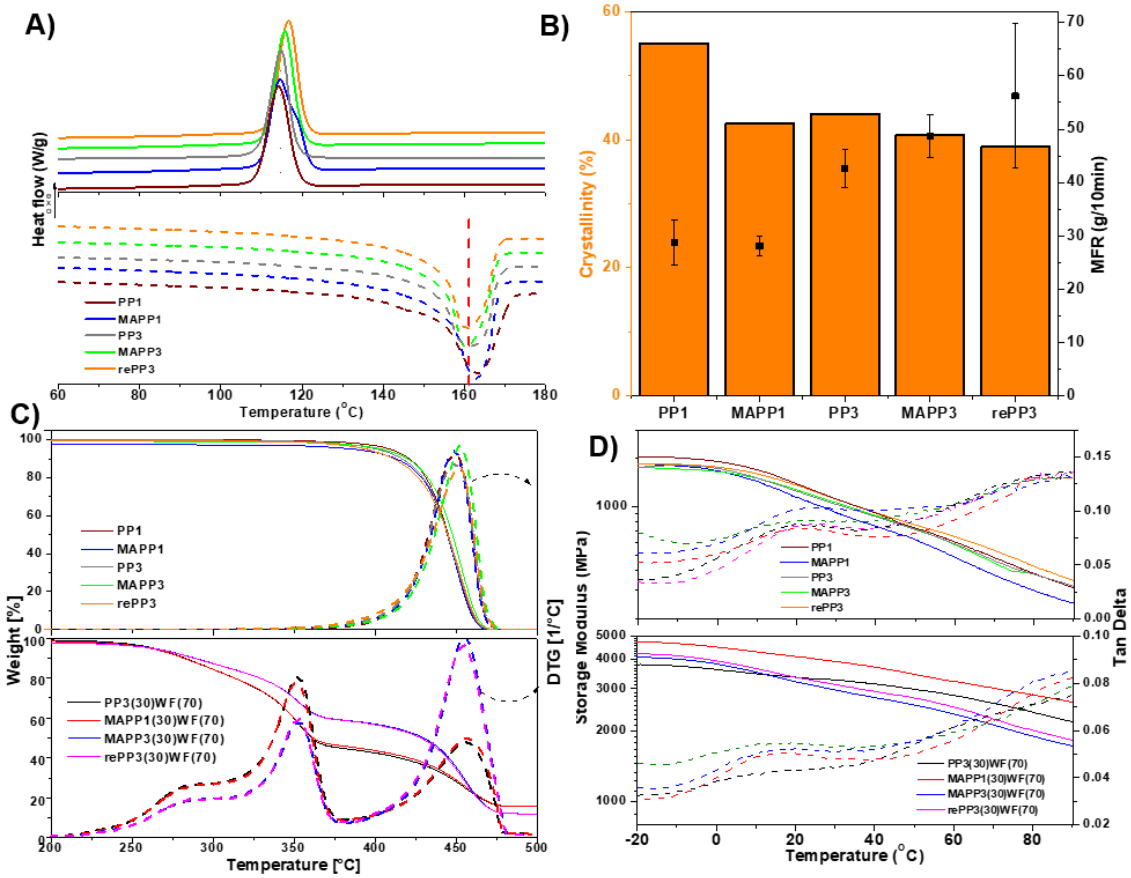

Figure 21. (A) DSC thermogram of the neat polymers; **(B)** MFR plotted against change in crystallinity (calculated by DSC); **(C)** TGA thermogram and derivative curves for the neat (top) and filled (bottom) samples; and **(D)** DMA storage modulus and Tan δ – α relaxation for the neat (top) and filled (bottom) samples.

However, the reprocessing of PP had a more substantial reduction effect on M_w (see **Schematic 1(A)**). The reprocessing of PP displayed a 51% M_w reduction from PP1 to PP3. Through either maleation or recycling, the trend remained similar in that the more processing the material experienced, the more M_w decreased, which are common trends in the literature [118,178,179]. As well, the error associated with each measurement could give insight into the distribution of M_w as PP1 has the largest range and as it becomes maleated or reprocessed the

error range decreased, i.e., narrower distribution is obtained, since larger chain compounds are preferentially segmented first.

Table 4. DSC thermogram tabulated values and crystallinity values.

	T_M (°C)	H_{fm} (J/g)	T_C (°C)	H_{fc} (J/g)	χ_{cr} (%)
PP1	161.52 ± 0.31	114.05 ± 3.61	118.67 ± 0.23	126.95 ± 5.16	55.1 ± 0.02
MAPP1	163.24 ± 0.16	88.06 ± 0.45	116.95 ± 0.33	93.71 ± 0.38	42.5 ± 0.00
PP3	161.25 ± 1.10	91.20 ± 3.69	116.36 ± 3.46	101.65 ± 3.46	44.1 ± 0.02
MAPP3	160.97 ± 0.76	84.23 ± 5.06	116.05 ± 0.42	88.98 ± 5.42	40.7 ± 0.02
rePP3	161.48 ± 1.06	80.46 ± 1.05	116.49 ± 0.19	86.12 ± 1.66	38.9 ± 0.01

As chain scission is the primary mechanism of polymer degradation during reprocessing, it was expected that PP's viscosity could significantly decrease, which could help in the material's flowability during processing but at the cost of its melt strength. The viscosity of a polymer is associated with irreversible deformation of molecular chains slipping past one another making molecular weight distribution (MWD) one of the most important structural parameters in determining polymer flow properties. Viscoelastic materials have a solid-like and liquid-like response to deformation since viscoelastic macromolecules under strain will tend to pull back to their original shape [104]. The dynamic modulus relates to the material's elastic behaviour while the loss modulus represents the amount of dissipated energy, and the crossover moduli and associated frequencies are measures of structural changes [104]. **Figure 20(B)** shows the change in viscosity for the maleation and recycling of PP polymers. In all the reprocessed and maleated polymers, a Newtonian plateau is clearly shown; moreover, each individual specimen displayed shear thinning characteristics which was denoted by the linear slope at angular frequencies ≥ 10 rad/s. Lastly, it is shown that as the material is reprocessed and/or maleated the melt viscosity decreases.

The storage and loss modulus were also affected negatively by reducing the material's capacity to store and release energy due to a reduction in M_w allowing for easier deformation. Looking at **Figure 20(C)** and **Table B1**, it was observed that with maleation and reprocessing the zero-shear viscosity decreased as well as the crossover frequency shifted to higher frequencies giving further confirmation that a reduction of M_w (by reduction in weight average molecular weight) had occurred. The lack of change in the crossover modulus also indicates a lack of change with respect to the MWD agreeing with the previous argument that not a substantial quantity of low molecular weight species (i.e. oligomers) had been generated. As was shown previously in **Figure 20(A)**, the most degraded species (e.g. MAPP3 and rePP3) still have M_w of >100,000 KDals. Similar conclusions to the viscosity were found when investigating the MFR of the neat polymer samples (**Figure 21(B)**) as the two properties are inversely proportional. The MFR increased significantly as PP is reprocessed and/or maleated signifying a reduction in M_w because of chain scission. This is because the experiments are conducted at low shear rates, which allows them to offer an approximation to the zero-shear viscosity and a relative measurement of M_w for a given polymer system [104,148].

Figure 21(A) and **Table 4** display the results from the DSC experiments. It was observed that recycling, from PP1 to PP3, had no effect on the overall melting temperature but had some effect (-2 °C) on the crystallization temperature [180]. As the M_w decreases and shorter chains are generated, the nucleating ability of the polymer is hindered which is reflected in the degree of crystallinity calculation where reprocessing caused a 20% reduction [181]. Finally, the maleated samples developed a shoulder on the melting peak which correlated to

the production of β-crystal structures which are imperfect and less ordered compared to the α-crystal structures [180].

In **Figure 21(D)**, the storage modulus values decreased with the simulated recycling and maleation like the rheological storage moduli. Additionally, the α-relaxation peak slightly decreased from PP1 (22 °C) to its derivatives (18 °C) because of the molecular segmentation as discussed earlier. With a reduction in the α-transition's temperature from 22 to 18 °C (18% decrease), the material's service temperature is lowered meaning that reprocessing and maleation impacts the polymer's performance or operating ability. The TGA thermograms and derivative curves in **Figure 21(C)** showed that neither reprocessing or maleation had a significant effect on the thermal stability of PP and it followed a single step degradation at ~400 °C [8]. No additional peaks from newly generated oligomers, low molecular weight compounds or residual unbound surface MA were observed in the TGA thermograms which corroborated with the results discussed earlier. Finally, both reprocessing and maleation processes had noticeable effects on the surface polarity, because of the chain scission, which can be interpreted through contact angle measurement shown in **Figure B3**. Both processes caused PP to switch from a more apolar structure (102°) to a slightly more polar structure especially after maleation and three cycles of reprocessing (73 to 83°), which was a 26 to 19% reduction. The reprocessing and maleation decreased the PP's contact angle to 75° for PP3, 74° for MAPP1 and 72° for MAPP3. The rePP3 samples had a slight increase back up to 79° is attributed to the increase in slightly shorter length compounds of the PP as well as an increase MA homopolymerization with the case of MAPP [182].

4.4.3 Thermal and physiochemical properties induced by recycling and maleation on WPCs

Examining **Figure 21(C)** and **(D)** with respect to the addition of 70 wt.% WF, it can be seen that after the addition of 70 wt.% WF there was a significant increase in the modulus from ~1,100 to a max of ~4,850 MPa (341% increase). Furthermore, the addition of WF into the polymer matrices had mostly a negative effect on the damping factor as the α-transition shifts from 22 to 13 °C. This is the result of residual bound water molecules and any filler imperfections within the wood resulting in a plasticization effect and failure as the samples are stressed. In **Figure 21(C)**, the addition of WF had a pronounced effect on the thermal stability of the WPCs as the onset temperature shifted from about 400 to 275 °C. The composites all followed a two-step degradation process with the initial mass loss starting with the hemicellulose and cellulose components (275 to 375 °C) followed by PP degradation mass loss [8]. It is noteworthy to mention that the samples with the lowest viscosities (e.g. MAPP3 and rePP3) were able to mix better with the WF (**Section 4.4.2**), which helped to shield the WF from early thermal degradation.

Figure 22(A) depicts the effect of WF loading on the rheology of the reprocessed and maleated resins. The same trend is shown here as with the neat polymers, in that, as the material is reprocessed and/or maleated the resulting composite's viscosity had decreased corroborating the loss of M_w presented earlier. The drop in viscosity is not necessarily a bad result as the decrease in viscosity from the WPCs would aid in their processability in a manufacturing setting. The yield stress (τ) of the WPCs was found by fitting the viscosity data (**Figure 22(A)** and **Table B2**) with the HB model (**Eq. 12**) [137,138]. It was noted that with the reprocessing

of MAPP1 to MAPP3 and the maleation of PP3 to rePP3 resulted in the composite's yield stress decreasing, which agrees with the mechanical properties presented in **section 4.4.4** (**Figure 23**).

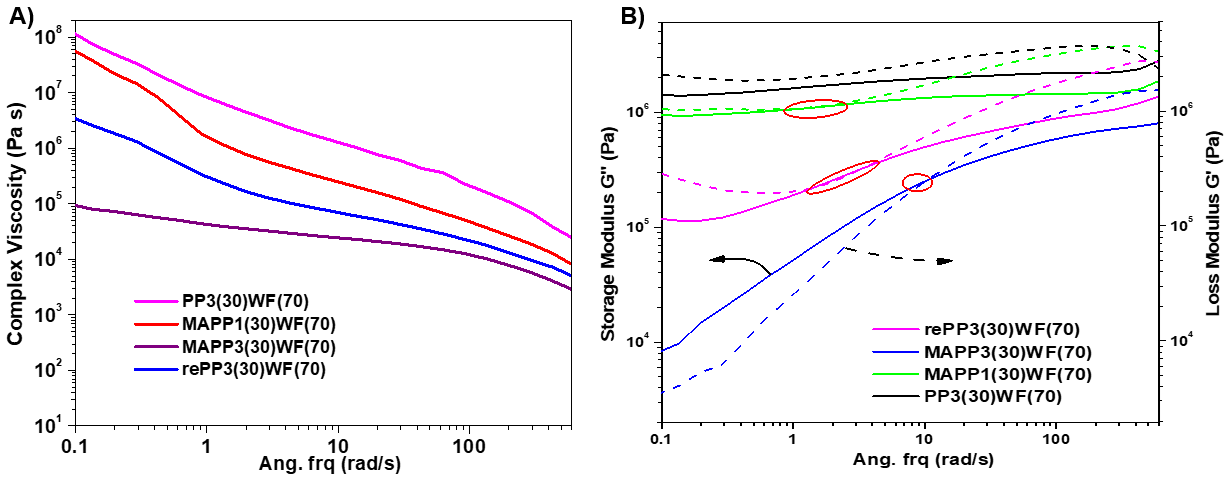

Figure 22. A) Complex viscosity profile of the reprocessed and maleated WPC specimens and **B)** Crossover modulus and frequency for reprocessed and maleated WPC specimens.

Moreover, the crossover modulus and frequencies (**Figure 22(B)**) of the WPCs are noticeably affected by both maleation and reprocessing as the crossover point is shifted down and to higher angular frequencies, indicating a narrowing of MWD and chain length, respectively. This implies that the rePP3 and MAPP3 resins have better interactions with the WF as the WPC's rheological behaviour is switching from being filler dominated to resin dominated much later. It is noteworthy to highlight that PP3(30)WF(70) has a complete absence of crossover modulus and frequency and near constant values indicate that the material is not able to flow. As well, it is shown that the loss modulus is consistently higher than the storage modulus meaning its viscous response is still the driving mechanism for this WPC.

4.4.4 Physical changes induced by recycling and maleation of PP on WPC

The effect of recycling and maleation on the fracture morphology and mechanical properties was also observed and are shown in **Figure 23**. **Figure 23(A)** displays the fracture morphologies for PP3 and rePP3 along with their WPCs. that helped to evaluate the effect of reprocessing and the effectiveness of maleation on matrix's ability to interact with the WF. Looking at PP3 and rePP3, the neat polymers had no visible changes from the effects of simulated recycling and maleation, which could be due to the absence of oxidative deterioration and a lack of severe chain scission. Only a couple of SEMs are displayed here for clarity; the others may be found within **Figure B4** in **Appendix B**.

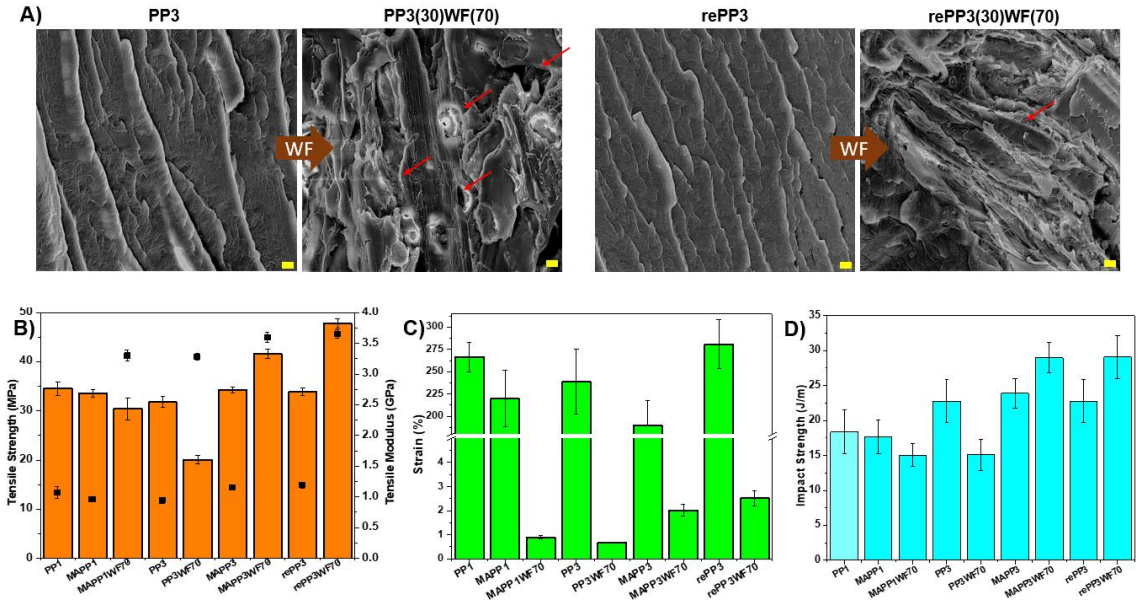

Figure 23. (A) SEM on the impact fracture surface of the PP and rePP3 polymers along with their WPCs (scale bar 10 μm at 500x); **(B)** Tensile strength (left axis) and modulus (right axis) for all samples; **(C)** Strain or Elongation at break (%) for all samples; and **(D)** Notched Izod impact strength for all samples.

Examining the WPC micrographs, the PP3(30)WF(70) micrograph shows clear boundary layers between the matrix and filler (see arrow on SEM), which is reflected in the mechanical properties. Another noteworthy observation was the non-uniformity, filler pullout,

and multiple stress concentration factors (SCF) all of which would result in the composite's catastrophic failure while under load due to poor stress transfer especially in the PP3(30)WF(70) WPC. After maleation, the boundary layers as well as the amount of pull out decreased significantly due to the enhanced interactions. Further improvements in the morphology can be seen with MAPP3(30)WF(70) and rePP3(30)WF(70), which is reflected in the mechanical properties (**Figure 23(B)** to **(D)**), due to the lower viscosity. The drastic decrease in the melt viscosity for the reprocessed and maleated specimens could have helped with the better permeation of the resin through the filler that facilitated the enhanced dispersion of the WF resulting in an improved matrix–filler adhesion and overall composite integrity. The tensile strength and modulus, presented in **Figure 23**(**B),** highlighted the effectiveness of the reprocessing and maleation processes on the WPCs mechanical properties. The reprocessing of PP to generate PP3 did not display a statistically significant ($p > 0.05$) effect on the tensile strength and modulus[29,148]. Maleation and/or a combination of reprocessing with maleation had also displayed no statistical difference from the baseline in terms of tensile strength when comparing PP1 to either MAPP1 or MAPP3 and rePP3.

The strain at break (see **Figure 23**(**C)**) also presented no statistically significant result with most having a p value of >1.0 when compared to PP1 except for MAPP3 which had a significant decrease by 56%. This result was to be expected as it was found in the literature that reprocessing of materials containing MAPP experienced more significant deterioration. The lack of significant property loss, except for strain at break, agrees with the previously presented SEM micrographs and the dynamic viscosity results. With respect to the WF, when

the filler was added into the PP3 matrix the resulting composite experienced catastrophic effects as the tensile strength drastically decreased to 21 MPa (38%) due to the lack of stress transfer between the WF and PP resin caused by the dissimilar polarities and hence poor interaction. In contrast, the MAPP1(30)WF(70) composite had a tensile strength (31 MPa) comparable to MAPP1 due to the improved interaction between the MAPP1 and the WF as shown in **Schematic 1(B)**.

MAPP3(30)WF(70) and rePP3(30)WF(70) composites also displayed significant tensile improvements from that of the PP1 based composites. This is due to the decrease in viscosity of these resins because of the reprocessing, which allowed for better resin permeation and mixing through the highly filled composite giving rise to better bonding. The rePP3(30)WF(70) composite had the greatest mechanical properties out of the composite specimens. As the tensile modulus is dependent on the amount of filler and the type of reinforcing agent, there is no significant difference in the WPC composition as they are all heavily filled with 70 wt.% reinforcement and the same WF filler. Thus, the observed property change is because of the matrix variation resulting from the fresh maleation and lower viscosity from reprocessing. Lastly, the inclusion of 70 wt.% WF had drastic effects on the composite's elongation at break due to the particle failure and poor interaction however MAPP3 and rePP3 had better elongation due to the enhanced interaction and permeability. Due to improved polymer-filler interaction, when WF filler break under stress, the encasing resin will continue to deform until complete failure resulting in the observed elongation improvement. The

notched Izod impact strength (illustrated in **Figure 23(D))** had the same trend as the tensile strength.

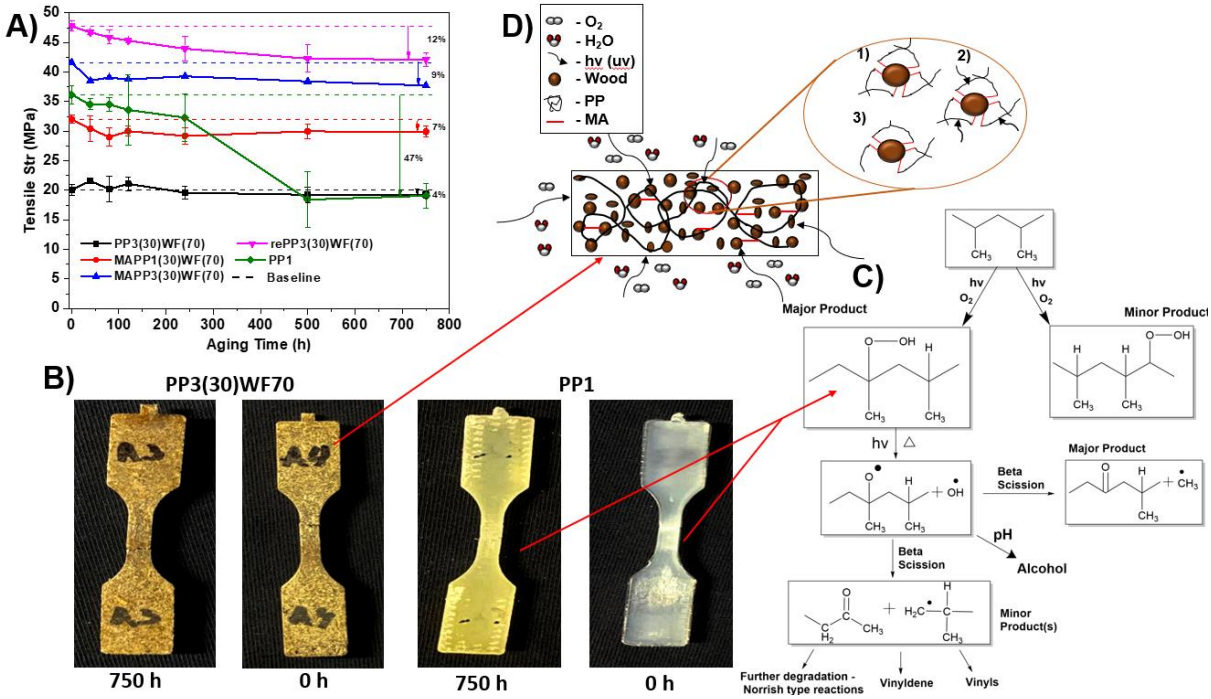

Figure 24. (A) Tensile strength results after 750h hrs of UV degradation; **(B)** Photos of before (0 h) and after (750 h) UV accelerating aging for PP3 and its WPC; **(C)** Proposed PP UV degradation mechanisms; and **(D)** Proposed mechanism for WPC UV degradation.

Figure 24(A) shows how the addition of wood aids in protecting PP from degradation concerning UV radiation. PP experienced a slight induction period of latency (≤ 80 h) in terms of tensile strength followed by a staggering reduction in the tensile strength from 80 to 500 h of radiation. When PP and most polymers are exposed to air, opposed to an inert environment, they will inevitably undergo photooxidative degradation following a radical-based autooxidation process, shown in **Figure 24(C)** [170,183]. The photooxidative degradation of polyolefins results in a variety of oxidative products throughout the polymer's altered structure, such as CO_2, CO, peroxides, peracids, and peresters which can be seen by the yellowing of PP

in **Figure 24(B)** [183,184]. The ability to form oxidative products is correlated to the polymer's oxygen diffusion limitation, and one study found that PP readily absorbed 500 mmol/kg of O_2 in 60 h. On the contrary, it took 100 h to absorb the same amount of O_2 by nylon 6 (PA6) and polybutylene terephthalate (PBT) and 230 h for polyethylene (PE). In **Figure 24(A)** it was observed that after 750 h of consistent UV radiation, there was an evident decrease in tensile strength, with the most extreme being the composite with the rePP3 (12%) polymer, while the PP1 sample displayed the least amount of deterioration (4%). However, it should be noted that PP3(30)WF(70) had no statistically significant ($p < 0.05$) change across the duration of the test. **Figure 24(B)** shows minimal changes of the WPC, expect colour changes, before and after UV aging. The colour change had been examined using ImageJ to quantify any changes and results are shown in **Table B3** in **Appendix B;** as well, the other UV aged samples are shown in Figure S5. It was found that due to the high red and green content, all WPCs were seen as yellow in colour. After UV aging, however, the colour fades slightly as observed in **Figure 24(B)**. The opposite was shown in neat PP in which it turned from bluish white to yellow color, likely due to photochemical reactions.

Comparing studies of other lignocellulosic reinforcement materials with PP, all non-modified composites degraded to various degrees when exposed to prolonged periods of UV degradation [185–190]. A proposed mechanism is presented in **Figure 24(C)** where it is illustrated that the UV rays typically caused beta chain scission in neat PP is limited by the presence of WF in the matrix as in **Figure 24(D)**. A study found that adding MA treated sisal fibres with PP increased the UV stability compared to the non-treated composites [186]. This

is contrary to what was found in **Figure 24(A)**, as the MAPP1(30)WF(70) sample had no statistically significant change from the non-maleated samples, but the reprocessed composites (rePP3 – 12% and MAPP3 – 9%) experienced a considerable amount of degradation. This trend could be correlated to the M_w and the zero-shear viscosity in **Figure 20** and **Table B3** in **Appendix B**.

4.5 Summary of Chapter 4

This work aimed to create a deeper understanding of the thermo-mechanical reprocessing of polypropylene (PP) and maleated polypropylene (MAPP) generated from single-use plastics (e.g. packaging type material). This work demonstrated a way of enhancing the compatibility between the polar lignocellulosic biomass, wood fiber, and recycled polypropylene and found that the reprocessing of MAPP with a low grafting content is viable for future application due to minimal degradation. Furthermore, maleation of recycled PP was shown to be a plausible alternative to virgin PP in WPCs as it offers a higher level of compatibility at lower M_w. After reprocessing, the viscosities of the samples all decreased, proportional to M_w loss, due to molecular fragmentation; however, the mechanical properties were only slightly affected by the reduction, indicating that the degradation was not too severe. On the contrary, MAPP3 and rePP3, displayed enhanced interaction with the WF filler that resulted in improved composite properties due to the improved flowability attributed to the reprocessing. In addition, a consistent fracture morphology with less boundary layers associated with the MAPP3 and rePP3 based WPCs has translated to superior stress transfer compared to the composite systems. The reduction in contact angle and slight change in

polarity from PP3 to MAPP3 and rePP3 also supports the improvement in the interaction between the filler and matrices that resulted in better mechanical properties when compared to the other two WPCs. Finally, while all the WPCs experienced a minimal reduction in tensile strength with UV aging (4 – 12%), it is minimal compared to the non-filled PP (PP1), which displayed a 47% reduction in tensile strength with 750 h UV aging.

Chapter 5 – Chemical modification of wood and maleation of PLA for biocomposite manufacturing[4]

5.1 Introduction

Polylactic acid (PLA) is a linear, non-toxic, aliphatic polyester that is fully bio-based and can degrade due to its susceptibility to enzymatic attacks making it more environmentally friendly compared to other thermoplastics [191,192]. PLA is produced by the polymerization of lactic acid monomers, which are derived from the fermentation of renewable polysaccharides, such as corn or rice starch, tapioca roots, potato starch, or sugarcane (see **Schematic 2 (II)**) [191,192] Typically, PLA exists in two enantiomer forms (L- and D-) due to its asymmetric carbon atom in the lactic acid and has desirable mechanical strength and transparency making it a suitable replacement for petro-based thermoplastics in several applications [193–195]. The growing interest for PLA is in the fabrication of 3D printing filaments, medical devices, and packaging industries due to its safety, reduced environmental impact in conjunction with the interest to shift away from environmentally persistent plastics [191]. Currently, the cost of PLA ranges from 2 to 6 USD/kg while the PLA manufacturing industry holds an estimated value of 1 billion USD in 2021 and is expected to grow to 1.9 billion USD at a 12% growth rate [191,196]. The main manufacturers of PLA are Total Corbion PLA (Netherlands), Natureworks LLC. (US), and Mitsubishi Chemical Corporation (Japan) [191,196].

[4] A version of this chapter has been published on peer-reviewed journal as a review article: Jubinville, D., Tzoganakis, C., & Mekonnen, T. H. (2022b). Recycled PLA – Wood flour based biocomposites: Effect of wood flour surface modification, PLA recycling, and maleation. *Construction and Building Materials*, *352*, 129026. https://doi.org/10.1016/j.conbuildmat.2022.129026.

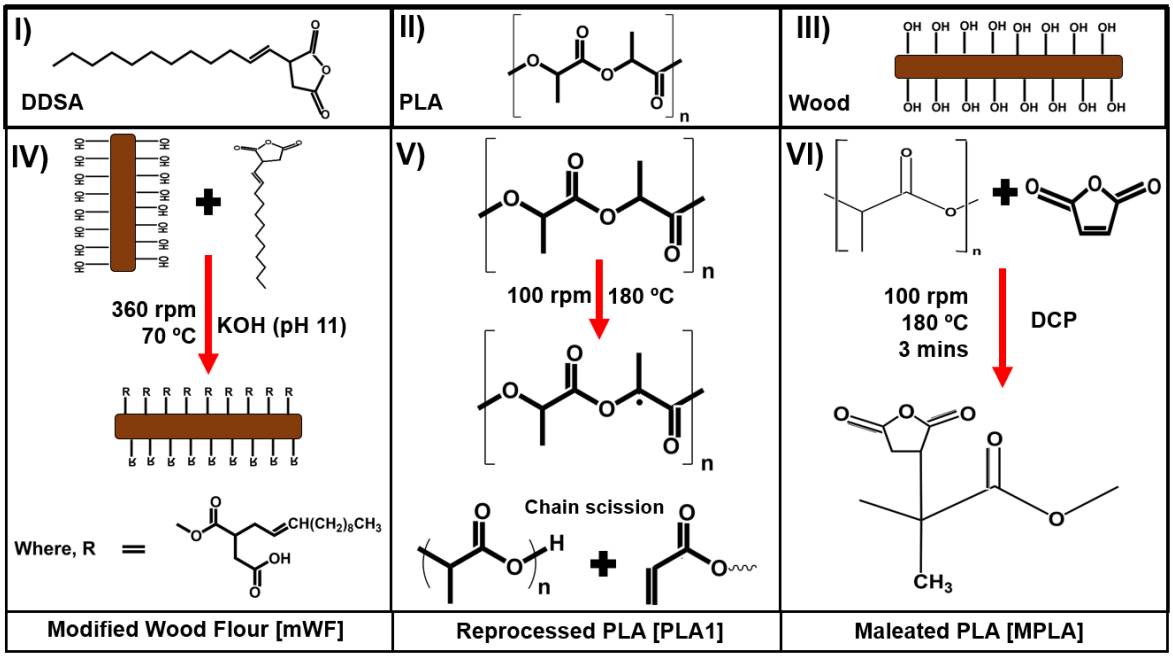

Schematic 2. The top row shows chemical structures of **(I)** Dodecenylsuccinic anhydride (DDSA); **(II)** Poly(lactic acid) (PLA); **(III)** simplified structure of wood. The bottom row shows simplified chemical reaction mechanisms **(IV)** Reaction for the modification of wood flour; **(V)** Thermo-mechanical breakdown of PLA; and **(VI)** Maleation of PLA [197,198].

Many applications of PLA, including single-use packaging, agriculture plastics, and 3D printing rely on its compostability to deal with its post-industrial and post-consumer waste. While composting of PLA like other biopolymers is an attractive attribute, it has its own limitations. For instance, PLA compostability is mostly limited to industrial composting facilities and can be as slow as 3 to 6 months, the resulting compost residue can change soil's pH (acidification) in agricultural plastic use and contribute to eutrophication and particulate matter generation; PLA's lack of degradation in water , etc. [199–201]. An appealing alternative to composting PLA is recycling [201–206]. The interest in recycling PLA, as opposed to compositing, is not only to mitigate challenges associated with composting, but also to further reduce its environmental impact resulting from biomass production that will be used as PLA feedstock. Some studies have shown that PLA can be recycled several times

without substantial disintegration [207]. For example, it was reported that after successive thermo-mechanical recycling of PLA, it has retained its tensile strength and modulus and experienced an increase in crystallinity at the cost of molecular weight (MW) and viscosity reduction [202–206]. More interestingly, it has been shown that PLA may be reprocessed up to ten times before tensile properties are significantly altered [208]. However, due to oxidative degradation besides the significant decrease in its MW, recycled PLA plastics often display yellowing. Thus, it is important to find applications that will not be affected substantially by the yellowing or the molecular weight and viscosity reductions. Wood-plastic composites (WPCs) are manufactured by compounding a polymer matrix (recycled or virgin resin bases) with wood fillers and are best used in construction materials like natural wood substitutes.

With a variety of available resins to choose from, WPCs may be divided into two broad categories that are petroleum-based or bio-based, with the latter having a lesser environmental impact from production and manufacturing [192]. More recently, the use of biodegradable polymers has also been investigated by many researchers with most reporting that the addition of wood into a brittle polymers like PLA resulted in an even more brittle material that needs to be toughened for any utilization [209]. When using a wood-based products, great consideration is placed on their dimensional stability and bio-degradability properties due to their organic nature and tendency to absorb water [210]. Controlling the moisture absorption capabilities of wood has cascading effects, in that, if the wood itself is more hydrophobic its dimensional stability and micro-organism attack/degradation can be hindered or eliminated [211–214]. Those properties may be improved upon using chemical modifications or treatments of the

wood itself. The chemical modification of wood is typically carried out by a covalent bond adjoining of a selected chemical additive with the wood's cell wall [215]. Treatment types, such as chemical impregnation, polymer inclusions, coatings, and heat treatments are usually not considered chemical modifications because they do not entail cell wall modification through reactive chemistry [211]. Most published research work on wood modification focuses on producing superhydrophobic surfaces (contact angle > 150°) that allow for enhanced abilities, such as self-cleaning, water-repelling, anti-icing, and anti-fogging [214]. Chemical modification of wood has been studied in the past with many different chemical systems, which include anhydrides (e.g. acetic, maleic, succinic), acid chlorides, isocyanates, and formaldehydes to name a few [211–216]. In the past, dodecenylsuccinic anhydride (DDSA), has been used to modify wood fractions, such as cellulose and hemicellulose, to increase the hydrophobicity but has not been investigated with wood particles in bulk. DDSA (see **Schematic 2(I)**) is a type of alkenyl succinic anhydride or an esterifying agent with similar structure to octenyl succinic anhydride (OSA) but with a carbon chain of 12 atoms [217,218].

5.2 Materials and methods

5.2.1 Materials

The PLA used in this study was produced and supplied by Total Corbion PLA under the trade name Luminy L105. The supplied PLA had a density (ρ) and melt flow index (MFI) of 1.24 g/cm^3 and 50 g/10 mins at 210 °C and 2.16 kg, respectively. The maleic anhydride (MA) (99%), dicumyl peroxide (DCP), potassium hydroxide (KOH), and dodecenylsuccinic anhydride (DDSA) were all purchased from Sigma Aldrich and all chemicals were used as

received without any further purification or modification processes. A maple (*Acer pseudoplatanus*) sawdust or wood flour (WF) with a particle size range of 0.3 to 1.0 mm (20 to 60 mesh) was obtained from Ontario Sawdust Supplies (East Gwillimbury, ON, Canada) with no further refinement or sorting. Before processing and characterization, the WF was dried overnight at 80 °C and the final moisture content of the WF was 1.5 ± 0.02%.

5.2.2 Methods

5.2.2.1 Wood modification using DDSA

DDSA was selected for this experiment due its hydrophobic long aliphatic chain and its usage has typically coincided with enhanced adhesion strength and hydrophobicity for products in the plywood industry [219]. To modify the WF (see **Schematic 2(IV)**), 250 g of the wood was dried (12 h at 80 ºC) to remove free moisture. Separately, 2 L of 0.05 M KOH solution was prepared and mixed with 50 g DDSA and homogenized (13,000 rpm for 10 s) to generate an emulsion. 250 g of WF was then soaked in the 2 L emulsion and allowed to react in a heated stirred-tank (70 ºC, 360 rpm) reactor. The reaction temperature (70 ºC) and time (12 h) were selected based on preliminary experimentation, and the caustic potash (KOH) was incorporated to facilitate ring-opening of the DDSA. After the 12 h reaction, the modified WF (mWF) was rinsed with acetone under vacuum filtration followed by re-washing with DI water to remove unreacted DDSA and neutralize it. The washed material was then dried overnight (80 ºC) and stored in an airtight container until further use.

5.2.2.2 Simulated thermo-mechanical recycling of PLA

All formulations and compositions (**Table 5**) were prepared by using a HAAKE Rheomix 3000 batch mixer (Thermo-Fisher Scientific Inc., Waltham, MA, USA) at a mixing temperature and screw speed of 190 ℃ and 100 rpm, respectively. The recycling process is shown in **Figure B1(A)** in **Appendix B**. For the simulated recycling of the PLA, the batch mixer was initially heated to the set temperature (190 ℃) and the PLA was added and melt-mixed until a constant torque was established and held for ~5 mins. This was followed by reducing the set temperature to a point below its glass transition (T_G) (< 60 ℃) to allow hardening to occur before being heated back up to the set temperature, which represents one reprocessing cycle. A more detailed explanation of the simulated recycling is provided in previous publications [8,148].

Table 5. Specimen formulation and code chart.

Specimen code	Reprocessed count	Resin (wt.%)	MA (phr)	DCP (phr)	WF (wt.%)
PLA0	0	100	-	-	-
PLA1	1	100	-	-	-
PLA1:WF30	1	70	-	-	30
PLA1:WF50	1	50	-	-	50
PLA1:mWF30	1	70	-	-	30
PLA1:mWF50	1	50	-	-	50
MPLA1:mWF30	1	70	5	0.1	30
MPLA1:mWF50	1	50	5	0.1	50

5.2.2.3 Reactive compounding of MPLA and (m)WF addition

MA was added to the formulations (shown in **Table 5**) to evaluate the interaction between the DDSA modified wood flour (mWF) and the maleated PLA (MPLA). For the reactive mixing and generation of the MPLA, 0.1 phr of DCP was added *in-situ* to the PLA (at

190 ºC) once the torque is stabilized in the batch mixer (see **Schematic 2(VI)**). The DCP was allowed to mix for 30 s before the addition of 5 phr MA and allowed to mix for another 30 s to ensure uniform dispersion and distribution in the formulation. Following the *in-situ* maleation of PLA, which lasted ~90 s, the mWF was added to the batch mixer at 30 and 50 wt.% with respect to the PLA and MPLA and mixed until the torque is equilibrated.

5.2.2.4 Injection molding

A HAAKE Mini-Jet Pro (Thermo-Fisher Scientific Inc., Waltham, MA, USA) injection molding unit was used to injection mold test specimens for the various samples. The injection molding machine had heating zones in the barrel and the mold, which were set to 200 and 70 ºC along with a pressure of 800 bar and a packing (i.e. holding) time of 5 s to produce type V tensile specimens (ASTM D638-14), impact bars (ASTM D256), and rheological discs (ASTM D4440). A set of at least five replicate test specimens were produced for each test method.

5.3 Characterization methods

5.3.1 X-ray photoelectron spectrometer (XPS)

The change in the surface chemistry of the wood because of the DDS modification was investigated using a ThermoScientific ESCALAB 250 X-ray Photoelectron Spectrometer (XPS) with Al-Kα radiation. The samples were ground into a powder (< 100 μm) using an IKA grinder for the XPS analysis. A Casa XPS and Origin software were used to extract, process, and deconvolute the collected spectra.

5.3.2 Fourier transform infrared spectroscopy (FTIR)

FTIR spectra for test samples were obtained by using a Nicolet 6700 model (Thermo-Fisher Scientific Inc., Waltham, MA, USA). To accomplish this, 5 mg of each sample was compressed with 200 mg of potassium bromide (KBr) powder for 3 min under 5 metric ton force using a Carver press. The spectra were collected in absorption mode between 600 to 2000 cm^{-1} with a resolution of 4 cm^{-1} at 64 scans.

5.3.3 Dynamic light scattering (DLS)

To evaluate the weight-average molecular weight (M_W) of the virgin PLA (PLA0) and reprocessed PLA (PLA1), dynamic light scattering (DLS) (Malvern Zetasizer, Nano ZS90) was employed. For this, the PLA0 and PLA1 samples were dissolved in chloroform (80 ℃ for 1 h) and DLS measurements were carried out. A refractive index increment (dn/dc, ml/g) of 1.45 for PLA in chloroform was used to calculate the M_W [220]

5.3.4 Melt flow index (MFI) and shear rheometry

The MFR for the unfilled specimens was measured using a Dynisco–Kayeness polymer test system (Franklin, MA, USA) in accordance with ASTM D1238 at a temperature and load of 190 °C and 2.16 kg, respectively. ASTM D4440-15 was employed to study the PLA-based WPC's rheology using a HAAKE Mars III parallel plate rheometer (Thermo-Fisher Scientific Inc., Waltham, MA, USA) with a sample thickness and diameter of 2.5 and 25 mm, respectively. A frequency sweep of 0.1 to 100 rad/s at 190 ℃ was performed on all samples under a constant strain of 0.01% (within the linear viscoelastic region (LVR)) with 1 mm plate gap.

5.3.5 Scanning electron microscopy (SEM)

The surface morphology of PLA and its WPCs were examined using an Oxford Instruments Quanta FEG 250 Environmental SEM coupled with an energy dispersive X-ray system (EDX) capability (Abingdon, Oxon, UK) without any sputter coating. The micrographs were taken from broken tensile samples to investigate the material failure under load.

5.3.6 Polarized optical microscopy (POM)

The crystal structure of all specimens was investigated using an Olympus BX53M POM (Melville, NY, USA) optical microscope equipped with a 20X objective lens and a polarized light filter as well as a Linkam heat stage, which was heated to 190 °C at 10 °C/min. All samples were prepared as 20 μm thick films from compression molding as previously described.

5.3.7 Mechanical properties

The tensile test was conducted using a Shimadzu – AGS X tensile testing unit equipped with a 10 kN load cell (Shimadzu corp., Kyoto, Japan) at a constant crosshead speed of 10 mm/min for all samples per ASTM D638-14 Type V. The notched Izod impact properties were measured using a TMI Monitor Impact Tester. All the samples were notched to a depth of 2 mm immediately following injection molding with a TMI notching device (Testing Machines, DE) at 25 °C and relative humidity of 50% in line with ASTM standard D256. All the samples were conditioned for at least 40 h in the standard laboratory environment according to ASTM D618 before the test.

5.3.8 Thermal analysis

The thermal analysis of the PLA and WPC samples was conducted using a DSC Q2000 (TA Instruments, New Castle, DE, USA). The DSC experiments were carried out under a nitrogen flow rate of 50 mL/min. About 6 mg of each sample was placed in a separate aluminum T_{zero} pan that was then heated at 10 °C/min up to 200 °C, held isothermally for 3 min before cooling down at 10 °C/min to -10 °C, and heated again at 10 °C/min up to 200 °C. The melting temperature (T_M), crystallization temperature (T_C), and melting enthalpy (H_{mPLA}) were taken during the second heating cycle to remove the thermal history of the processing. For comparison, the PLA0 specimens were all tested using the same method and conditions. The percentage crystallinity of PLA ($\%\chi_{CrPLA}$) was determined using **Eq. 13** with an $H^0_{m_{PLA}} = 93.7$ J/g which is the heat of fusion value if PLA was 100% crystalline and H_{ccPLA} is the enthalpy of cold crystallization [116].

$$\%\chi_{CrPLA} = \left(\frac{H_{m_{PLA}} - H_{cc_{PLA}}}{H^0_{m_{PLA}} * (\text{PLA wt.}\%)} \right) \cdot 100\% \qquad \textbf{Eq. 13}$$

Tan δ and the viscoelastic behaviour from all the specimens were evaluated using a DMA Q800 from TA Instruments (New Castle, DE, USA) by using a dual cantilever clamp with a frequency of 1 Hz and a strain of 0.01% (within the LVR). The width and diameter of the samples were, 11.98 ± 0.03 and 2.99 ± 0.05 mm, respectively. The tests were conducted from −35 to 100 °C with a ramp rate of 3 °C/min.

5.3.9 Water absorption kinetics and contact angle

The water absorption (%WA) and thickness swelling (%TS) for PLA1 and its WPCs were evaluated following a modified ASTM D570-98 standard. Three circular samples, with

uniform thickness (2.5 mm) and diameter (25 mm), were dried at 80 °C until a constant weight (W_0) was observed before submersion in distilled (DI) water. The dried sample's thicknesses were measured using a digital caliper with an accuracy of 0.05 mm, at four separate spots and averaged (ΣT_0) after drying. The submerged samples were kept at room temperature and monitored at various intervals for an initial 24 h to a total of three weeks. Both the weight change (W_n) and the thickness swelling (T_n) of the samples were recorded at various intervals within the pre-described period. All samples were tapped dry with blotting paper to remove any surface moisture and consequently weighed. The %WA and %TS values were then calculated using **Eq. 1** and **Eq. 2** from ***3.3.8 Water absorption (%WA) and thickness swelling (%TS)***. With the data collected from the %WA and %TS test, the diffusivity, sorption, and permeability coefficients were calculated (**Eq. 14** to **Eq. 16**) to quantify the change in rate as a direct result of the modification and maleation.

$$\text{Diffusion Coefficient (D)} = \pi\left(\frac{T^2 * m^2}{16 * W_\infty^2}\right) \qquad \textbf{Eq. 11}$$

$$\text{Sorption Coefficient (S)} = \frac{W_\infty}{W_t} \qquad \textbf{Eq. 12}$$

$$\text{Permeability Coefficient (P)} = D * S \qquad \textbf{Eq. 13}$$

Where (T) is the initial sample thickness, (m) is the slope of the linear region of the water absorption curve, and both (W_∞) and (W_t) are the percent water absorbed at saturation and at time (t), respectively [221]. For contact angle measurements, all specimens were compressed into sheets (6 metric tons for 3 min at 25 °C). The DI water contact angles were then measured by using a lab-built optical sessile drop pump system. A 5 μL water droplet was

pumped out onto the sample's surface and videos were taken to capture before, during, and after droplet has touched the surface. The contact angles of the water droplets were measured via ImageJ image analysis software with a contact angle plug-in.

5.3.10 Hydrothermal aging

The bond durability measurement of the WPCs was accomplished by soaking five tensile samples in boiling water for 2 h followed by drying until a constant weight before tensile testing. For this, all WPC samples and PLA1 were selected and dried overnight at 80 °C before testing. After the 2 h, the samples were left in an ambient environment at 50% relative humidity for 40 h before tensile testing.

5.3.11 Statistical analysis

A one-way analysis of variance (ANOVA) test was conducted to evaluate significant difference between the means between the different PLA and PLA-based WPC specimens. The difference in means was considered significant at $p \leq 0.05$.

5.4 Results

5.4.1 Confirmation of wood modification by DDSA

FTIR analysis was conducted to determine the chemical changes on the wood's surface structure as well as to evaluate the washing procedure in removing unbound DDSA. As can be seen in **Figure 25(A)**, there was a clear decrease in the peak between 3000 to 3700 cm^{-1}, which signifies a reduction of the available -OH groups from the original WF to the mWF. The reduction in the -OH moiety is indicative of the reduction in the polarity of the mWF compared

to the WF, which could subsequently reduce the hydrophilicity of the mWF. The other areas of interest include IR absorption changes at wavenumbers between 1650 to 1750 cm^{-1} and 2800 to 3000 cm^{-1}, which correlate to the formation of carbonyl ester bonds and C–H stretching, respectively. The lack of a new peak from 1790 to 1800 cm^{-1} indicated that there were no unbound succinic anhydride and the washing procedure was effective in removing free DDSA.

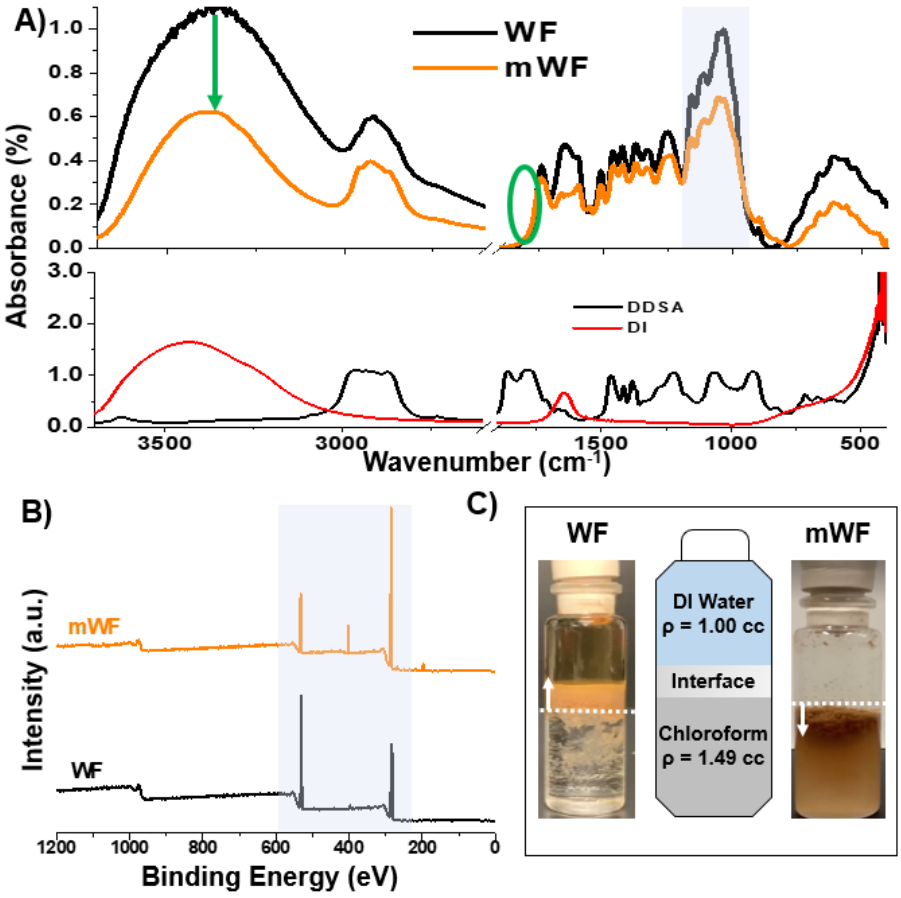

Figure 25. (A) FTIR spectra of the mWF and WF species (top) as well as the modifier (bottom) **(B)** XPS spectra comparing before and after modification for changes in the surface chemistry; and **(C)** Photos of the change in polarity from the water domain (left) to the chloroform domain due to modification.

XPS analysis is an effective technique for observing changes in the WF's surface chemistry to confirm that modification had taken place and was successful. Examination of **Figure 25(B)** and **Table 6** illustrated the presence of carbon, oxygen, and trace elements like

nitrogen, which are all elements found in wood. For the WF, the dominating elements were revealed to be C and O at 283 and 531 eV, respectively; while, the mWF had the same dominating species but at shifted values with the C and O now being 286 and 532 eV, see **Figure 25(B)**. The decrease in O/C after modification indicated a reduction in oxygen-containing functional groups, such as acetyl, hydroxyl, and carbonyl groups across the WF's surface, which agrees with the FTIR results [222]. Examining the XPS images in **Figure 26**, the carbon atom deconvolution describes the lignocellulosic structures and the three atoms change with respect to the modification. In **Figure 26(A)** and **(B)** and **Table C1 in Appendix C**, the C_1 peaks were related to C–H and C–C bonds (i.e. wood and lignin extractable); while C_2 was more closely related to a single non-carbonyl bond (e.g. derived from cellulose) [222]. The increase in the C_1 peak and the decrease in the C_2 peak, after modification indicated that some oxidation and hydrolysis of lignin structures had occurred. Finally, the C_3 peak was assigned to carbon atoms that were bound to either a carbonyl oxygen group or two non-carbonyl oxygens and the decrease in peak intensity after modification was likely related to the oxidation of cellulose [222].

Table 6. Atomic composition and O/C ratio as recorded by XPS analysis.

	Experimental Atomic Composition				
	%C	%O	%N	%Si	O/C
WF	49.82	48.72	1.46	/	0.98
mWF	64.91	26.77	5.70	2.62	0.41

Overall, the XPS information showed that oxidation and hydrolysis reactions on the surface affect all components of the wood but at different rates. XPS spectra for O_1s are also

illustrated along with their deconvolution into two separate components as well as their corresponding area in **Figure 26(C)** and **(D)** and **Table C1** in **Appendix C**.

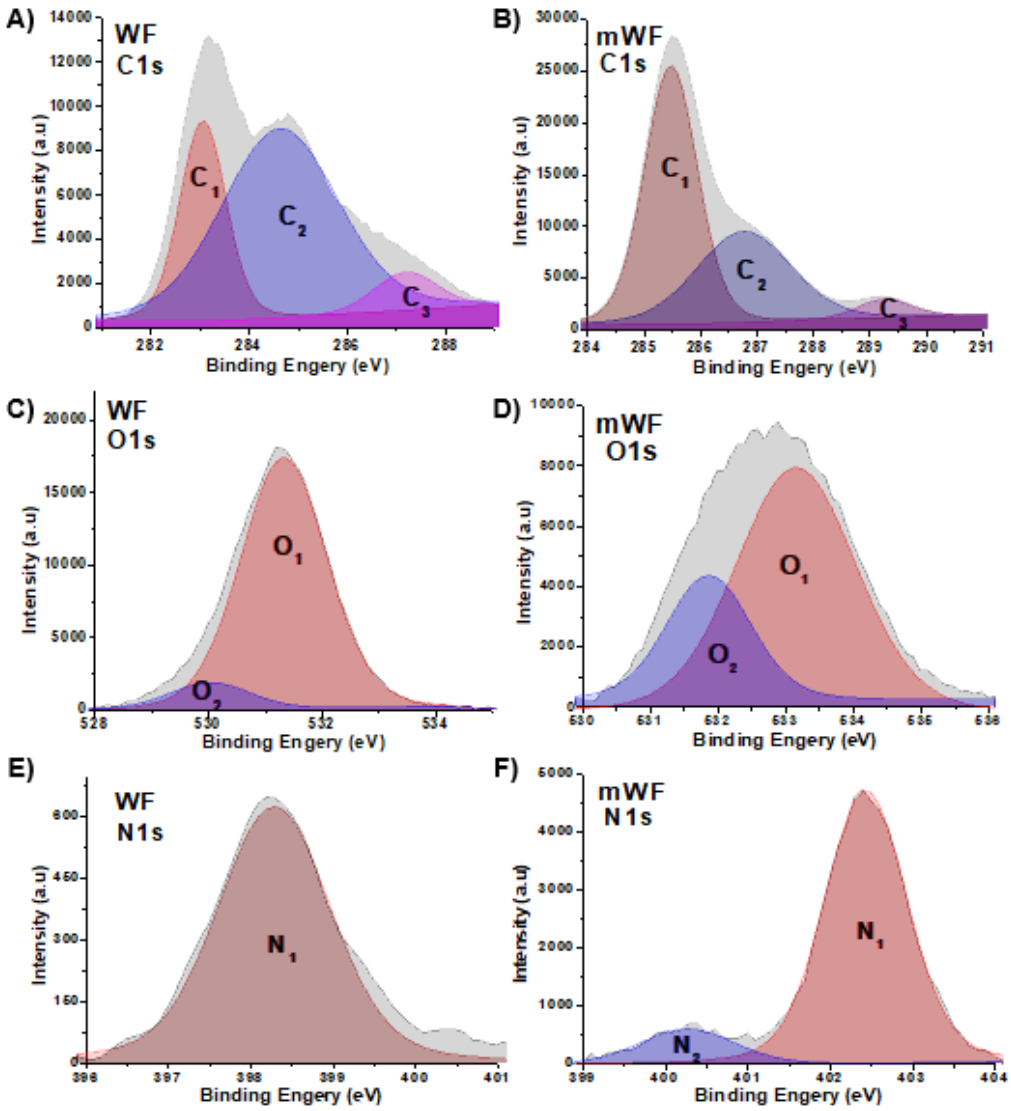

Figure 26. Atom deconvolution from XPS survey analysis for **(A)** C_1s WF; **(B)** C_1s mWF; **(C)** O_1s WF; **(D)** O_1s mWF; **(E)** N_1s WF and **(F)** N_1s mWF.

The O_1 atom is related to oxygen atoms that are linked to carbon atoms via a double or π–bond [222]. In contrast, the O_2 group is set at higher binding energy and is used to describe oxygen atoms that are bonded to a carbon atom via a σ–bond [222]. After modification, the O_1

peak increased while the O_2 peak was attributed to the extraction and elimination of lignin species. Additionally, examining the N_1s from **Figure 26(E)** and **(F)** and **Table C1** in **Appendix C**, it was shown that the N_1 peak is indicative of aliphatic C–NH (398 eV) while N_2 signifies aromatic N–H associated with the lignin component [222]. After modification, the N_1 peak decreased showing a lack of unreacted amine tail ends while an increase in the aromatic components could signify cross-linking [222]. The last mode of confirmation for successful modification is demonstrated in **Figure 25(C),** which shows two different vials that are both half-filled with DI water and chloroform as they represent two domains or phases of opposing polarities. **Figure 25(C)** clearly shows defined edges in both the chloroform and DI water domains that both separates and disperses the (m)WF particles. The mWF had a keen preference for the chloroform phase indicating a polarity shift from the baseline as WF, normally, has a strong inclination to stay in the polar water phase.

5.4.2 Effects of simulated recycling on PLA

During thermo-mechanical reprocessing of thermoplastic resins, molecular fragmentation and, in more extreme cases, chemical degradation of the backbone are common occurrences (see **Schematic 2(V)**). With successive reprocessing, the polymer's M_W can be adversely affected due to the additional heat and shear forces, which could reduce the overall chain length [204,206,223] **Figure 27(A)** shows the M_W of both the virgin and recycled PLAs, which revealed that after one reprocessing cycle there was no real statistical difference ($p = 0.25$). Moreover, the MFI did not display a statistically significant increase in agreement with the M_W measurement. Similarly, **Figure 27(B)** shows the tensile strength that also had no

significant change after one reprocessing, which has been seen in previous studies [203,205]. However, the tensile modulus had increased by 8% from PLA0 to PLA1, which was statistically significant ($p = 0.004$). The increase in modulus after one reprocessing cycle was the result of the drastic increase in the material's crystallinity and crystalline structure which is shown in **Figure 28(A)** and **(B)**. The thermal stability of the PLA0 and PLA1 was investigated using TGA, and results are shown in **Figure 27(C)**. The TGA of both the PLA0 and PLA1 samples display a single step degradation between 327 to 366 ºC and 325 to 364 ºC, respectively. This indicated that the thermal stability did not change ($P > 0.05$) with one round recycling.

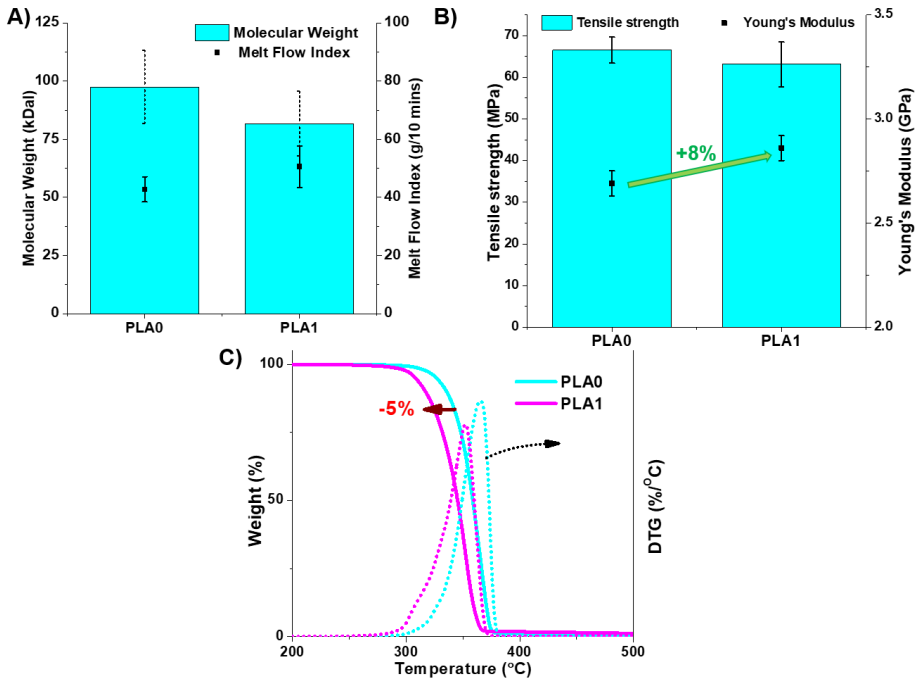

Figure 27. (A) Molecular weight determination, via DLS, correlated with PLA's MFI; **(B)** Tensile strength and modulus for the recycled and virgin PLA; and **(C)** TGA and DTG analysis of the neat PLA polymers.

Figure 28(A) and **(B)** show the DSC thermograms and the POM polarized micrographs for the neat PLA specimens. In **Figure 28(A)**, there is a clear change in the cold crystallization

behaviour, in that, before PLA is processed there was little crystallinity which could signify a re-organization of the crystal structure in perfection and/or shape after a single process. With PLA1 there were two clear cold crystallization peaks with the first appearing at 98 ºC and the second appearing right before the melting peak at 157 ºC. In contrast, the PLA0 had one broad cold crystallization peak at 138 ºC. Nevertheless, there is no change in the glass transition (T_G) or melting temperatures of the PLA because of the recycling.

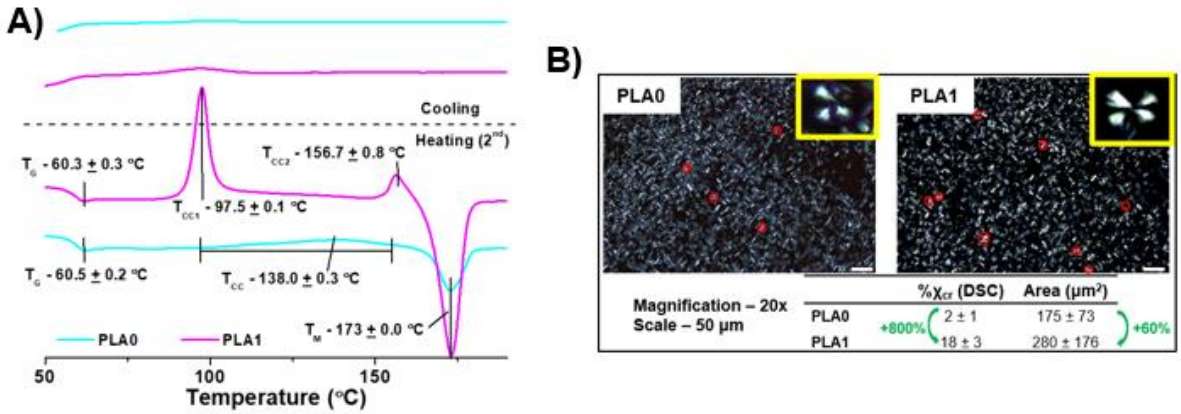

Figure 28. (A) DSC thermograms (heating and cooling) of PLA0 and PLA1 and **(B)** polarized optical microscope of melted and cooled PLA 20 µm thin films.

In **Figure 28(B)** there was a 60% increase in the "Maltese cross" formation after one processing cycle as well as there were more evident spherulites in PLA1, which showed an increase in crystal order or perfection which could have contributed to the modulus increase.

5.4.3 Influence of WF and mWF on recycled PLA WPCs

The water absorption (%WA) and thickness swelling (%TS) as a function of time at room temperature are displayed in **Figure 29(A)** and **(B)** with the linear region highlighted in **Figure C1(A)** and **(B)** in **Appendix C**. It has been extensively reported in the literature that PLA is hydrophobic and does not actively absorb water and saturates, typically, around 1%

with no noticeable swelling [224,225]. **Figure 29(A)** displays that the water absorption of the WPCs in the initial 24 h show a linear relationship, with the slope varying depending on wood content and modifications, which implies that PLA and PLA WPCs follow Fick's Law.

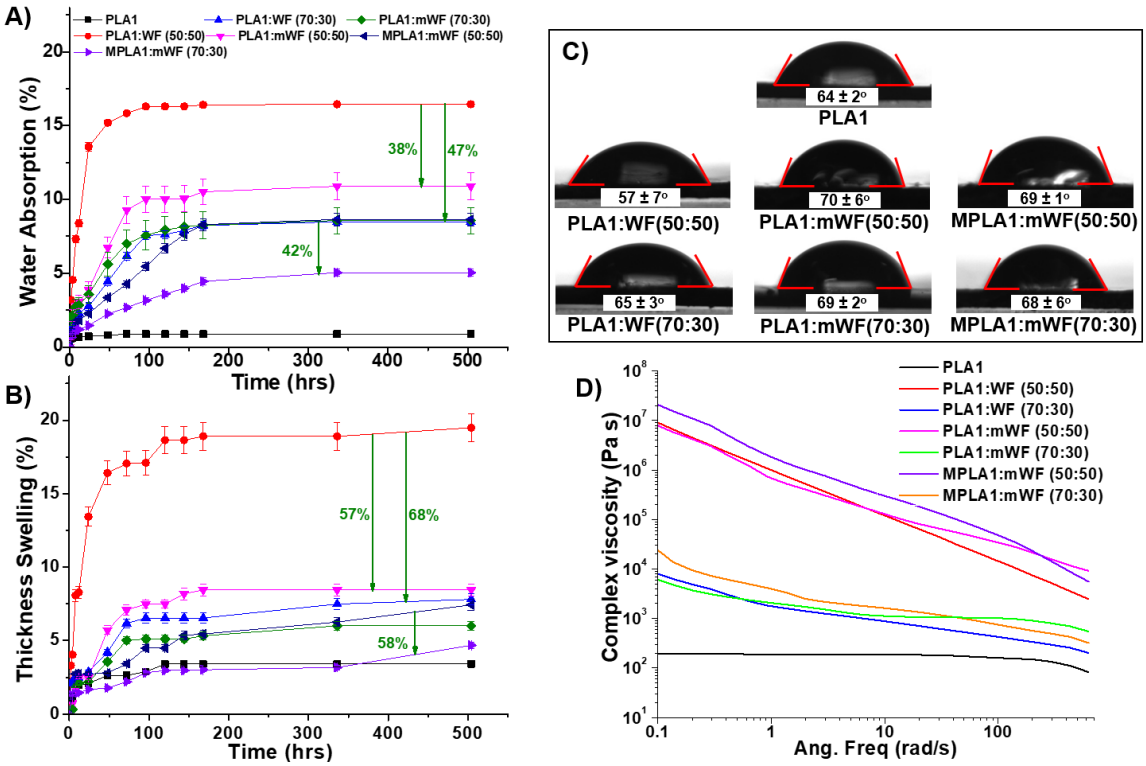

Figure 29. (A) Water absorption experiment (%WA) for the modified and not modified samples; **(B)** Thickness swelling experiment (%TS) for the modified and not modified samples; **(C)** Contact angle measurement; and **(D)** Complex viscosity of PLA and PLA based WPCs.

Apart from the 50 wt.%, WF which experienced rapid uptake in less than 10 h all started to absorb water more rapidly after the first few days before saturation at 150 to 200 h. The level of water absorption is heavily dependent on the rate of diffusion, the porosity of WF, and the permeability of water within a composite and/or polymer system [198,221,224,226–228] With the use mWF for the fabrication of the WPCs, the availability of -OH from the wood will reduce (see **Figure 25)**, which will considerably reduce the WPCs moisture absorption. For instance, in the 50 wt.% WPC, the use of mWF versus WF reduced the moisture absorption by

38% and a further 9% when MPLA was used due to the enhanced interfacial bonding between the wood fiber and the PLA matrix that prohibits moisture diffusion. In the case of the 30 wt.% mWF, it experienced a slower water uptake while the %WA value remained the same as the WF based WPC. However, with the replacement of the PLA with MPLA, the %WA saturation value has reduced by 42%. The substantial water absorption reduction with the use of MPLA is likely due to the increased interactions between the WF filler and the matrix, which aided in reducing voids of the WPC that limits water diffusion through the WPCs. %TS followed the same trend in that as water uptake increased the amount of swelling increased while controlling water absorption restricted the amount of swelling.

The water contact angle measurement (**Figure 29(C)**) was conducted to determine if the addition of mWF and MPLA influences the surface hydrophobicity and water barrier properties of the WPCs by applying DI water (5 μm) onto the WPC's surface. PLA is hydrophobic and typically has a measurable contact angle of 65 to 80º which agrees with the results reported in the literature [193,198,221,229] Since wood is inherently hydrophilic (i.e. polar functional groups that can interact with water) and hygroscopic (i.e. assimilation of moisture from the atmosphere) the addition of wood would reduce the hydrophobicity of PLA due to the increase in polar hydroxyl groups along with the formation of voids between the filler and resin. The 50 wt.% WF reduced the contact angle by 11% while the 30 wt.% is still dominated by PLA effects and the contact angle was unchanged. When mWF was switched with WF in the composites, the contact angle was considerably improved especially for the 50 wt.% composition with a 23% enhancement since there is more wood loading resulting in a greater reduction in OH^- groups from the modification with DDSA. There was no further

improvement with the addition of MPLA which was to be expected as MA is not expected to improve polarity since it actively replaces hydrogen atoms along PLA's backbone [198,223]. The addition of MA will aid more so in reducing void space by heightening the interaction between resin and filler meaning that the modification has more pronounced effects on the system.

Table 7. Thermal properties for PLA and the PLA-based WPCs from DSC, DMA, and TGA analysis.

	T_G (ºC)	T_M (ºC)	T_C (ºC)	$\%X_{cr}$	$\%W_0$ (ºC)	$\%W_{50}$ (ºC)
PLA1	60 ± 0.1	173 ± 0.0	98 ± 0.0	18 ± 3.0	325 ± 6.4	354 ± 0.9
PLA1:WF (50:50)	65 ± 1.7	171 ± 0.1	133 ± 0.2	66 ± 1.2	283 ± 2.6	328 ± 0.2
PLA1:WF (70:30)	66 ± 1.8	171 ± 0.3	130 ± 0.2	60 ± 0.2	297 ± 0.8	350 ± 0.6
PLA1:mWF (50:50)	61 ± 0.3	170 ± 0.0	132 ± 0.0	68 ± 1.2	284 ± 1.5	306 ± 0.4
PLA1:mWF (70:30)	63 ± 1.7	169 ± 0.2	123 ± 1.0	67 ± 1.8	294 ± 0.0	321 ± 2.3
MPLA1:mWF (50:50)	57 ± 1.4	169 ± 0.0	124 ± 0.0	58 ± 0.5	286 ± 0.8	310 ± 1.5
MPLA1:mWF (70:30)	58 ± 0.1	170 ± 0.0	123 ± 0.0	54 ± 0.2	292 ± 0.7	315 ± 0.0

To gain more insight into the possible water absorption kinetics of the WPCs, the diffusion, sorption, and permeability coefficients were computed using **Eq. 11** to 1**6** and compared with each other [221]. The calculated results from the aforementioned equations are shown in **Figure C1(C)**. It was noted that the 50 wt.% WF WPC had the largest diffusion and permeability coefficients due to the lack of PLA to wet all the WF that resulted in poor interaction and porosity of the WPC. There was a clear decrease in both parameters after the modification where the 50 wt.% WF based WPC displayed a reduction of 84% in permeability and 91% in diffusivity; while the 30 wt.% decreased 35 and 7% for permeability and diffusivity, respectively. The effect of maleation was also noted to be a further advantageous factor, but not to the same level as the modification of wood with DDSA. Lastly, the sorption

coefficient followed the reverse trend of the other two parameters in that the higher sorption coefficients were for the maleated and modified samples due to the difference in absorbed water at t = eight hours (8 h) and t = infinity.

Figure 29(D) depicts the effect of WF loading, WF modification, and PLA maleation on the dynamic rheological effects under an inert atmosphere. The storage and loss moduli are presented in **Figure C2** in **Appendix C**. In general, the viscosity of a polymer is linked to the irreversible deformation through means of molecular chains slipping past adjacent chains. As shown in **Figure 29(D)**, the 50 wt.% WPC has higher complex viscosity compared to 30 wt.% and neat PLA1 due to the greater restriction of polymer mobility. Except for PLA1 and 30 wt.% mWF, all specimens exhibit shear-thinning behaviour due to WF's tendency to agglomerate affecting the filler distribution and interaction with the surrounding matrix. The mWF constituent did not have any effect on the WPC viscosity at low shear rates implying. However, at higher shear rates the mWF based samples retained their viscosity compared to their non-modified counterparts. This was likely due to the improved interaction between the WF and PLA1 that within the melt that restricted chain mobility [223]. On the other hand, the maleation of PLA1 has generated a pronounced interactions between filler and resin resulting in higher viscosity as well as elevated storage and loss moduli (**Figure C2(C)**). In terms of the moduli, the addition of rigid particles into a system will increase the material's elasticity causing the storage modulus to increase; while, the loss modulus increases due to the particle-particle interaction. At higher concentrations of WF, 50 wt.%, the viscoelastic behavior is more solid-like since G' > G" while the 30 wt.% filled WPC exhibited liquid-like behaviour (G" >

G') since PLA1 is the dominant component. After modification, the gap between G' and G" has decreased indicating a better network has formed among the WF particles and the resin due to enhanced compatibility. However, due to the WF tendency to agglomerate at low frequencies G' and G" begin to diverge. [230,231]. Lastly, the PLA1 shows a G', G" crossover point around ~100 rad/s PLA1 which implies that PLA1 is fluid-like before that point [230,231]. The DSC results for the PLA and WPCs are presented in **Figure 30(A)** and **(B)** as well as **Table 7**. The crystallinity thermogram for PLA1 is typical in that there is a distinct lack of crystallization during cooling due to its cold crystallization behaviour upon heating.

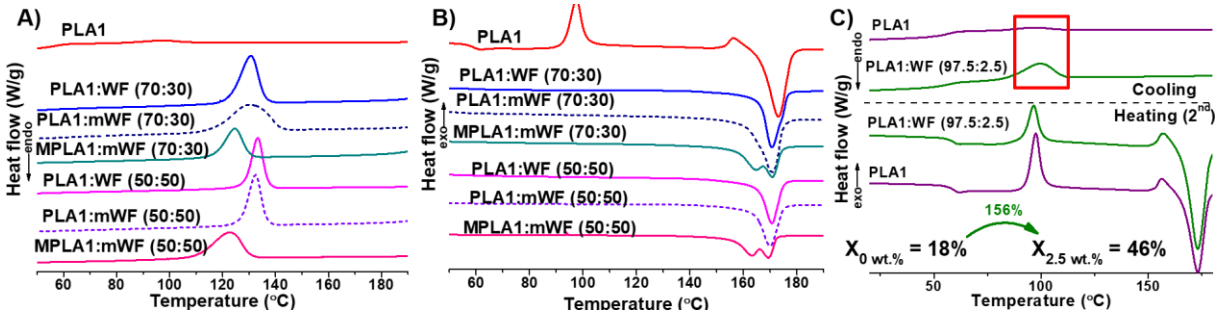

Figure 30. (A) DSC cooling thermogram for all specimens; **(B)** DSC 2nd heating thermogram for all specimens; **and (C) P**LA compared to 2.5 wt.% of wood thermogram.

It is shown that WF has an exceptional effect to cause nucleation within the PLA polymer as there is a clear crystallization peak with both 30 and 50 wt.% of (m)WF. This was verified by compounding low concentration of WF (2.5 wt.% WF) with PLA to evaluate the nucleating effect of WF in the WPCs. It was noted that with the use of only 2.5 wt.%, the crystallinity has more than doubled (from 18 to 46%) as shown in **Figure 30(C)**. A study by Behalek et al., displayed similar effects when compounding PLA with different natural fibres [232]. They found that the fibre type impacted the PLA biocomposite's ability to crystallize and its overall nucleating kinetics by eliminating PLA's cold crystallization due to the different

surface structures of the natural fibres [232]. The addition of WF and mWF caused the WPC's crystallinity to increase from 60 to 67% with 30 wt.% and 66 to 68% with 50 wt.% from WF to mWF. This is largely due to the cellulose component of wood being crystalline while hemicellulose and lignin are amorphous meaning that higher cellulose containing compounds and more wood content should result in higher crystallinity. Additionally, DDSA modified wood should have better dispersion due to the hydrocarbon chain which repels from the PLA matrix. However, with the use of MPLA, these crystallinities dropped to 54 and 58%, 30 and 50 wt.% respectively, due to the peroxide from the reaction causing chain scission of the PLA reducing its overall MW and consequently destroying the material's crystallinity [223,232–235]. The destruction of the perfect crystalline structures to secondary/ beta crystal structures is shown in the melting behaviour of **Figure 30(B)** by the formation of a secondary melting peak that appears at a lower temperature than the main melting peak of the alpha crystal structures [232–234]. No appreciable changes were observed in the overall melting temperature of the alpha crystal or changes. It should be noted that the highlighted cell in **Table 7** for PLA's T_C is its value for its cold crystallization temperature (T_{CC}). Finally, The T_G remained unchanged with the addition of wood but decreased after the maleation of PLA due to chain and crystal destruction at the cost of better interactions between the filler and matrix.

Thermogravimetric analysis (TGA) was used to investigate the thermal stability of the WPCs and PLA. **Figure C2(A)** shows the weight loss of PLA and PLA-based WPCs as a single step transition between 283 to 353 ºC for the WPC, and 318 to 361 ºC for the PLA1, which is a typical behaviour [148,236]. The loss in thermal stability was due to the addition of

WF since it has a low degradation point. Neither DDSA modification nor the maleation of PLA showed an effect on the thermal stability of the composites. **Figure C2** shows the derivative thermogravimetric curves (DTG) which display the weight fraction of the specimens. The 30 wt.% have a more intense peak which is attributed to the PLA component; while the 50 wt.% have a broader peak due to the overlapping of the weight derivative curves of the PLA and wood with all its lignocellulosic content.

5.4.4 Physical changes induced by the addition of WF and mWF

The fractured morphology of PLA1 and PLA-based biocomposites are displayed in **Figure 31(A)**. The PLA1 micrograph is typical for an unfilled PLA material since it displays a smooth fracture surface with no evident voids present. With composites, it is expected that by mixing a rigid filler into a glassy polymer matrix, the resulting composite will become more brittle. In both the 30 and 50 wt.% WF there exists boundary layers (green arrows) along with particle pull out and voids (red circles) indicating poor wettability of the filler material. The mWF samples for 30 and 50 wt.% show a much more consistent and smooth morphology when compared to the WF filler; however boundary layers and voids can still be seen with the 50 wt.% WPCs being the more extreme case. Finally, the MPLA morphologies seem to have a significant improvement in filler-matrix interactions as boundary layers are much harder to see however there still exists stress concentration factors (SCF) within the wood particles (modified or not) that will lead to failure under load. The poor compatibility or stress transfer between the PLA matrix and the WF filler along with the low inclusion of PLA in the 50 wt.%

case could result in deteriorated mechanical properties when compared to the neat polymer or modified WF based composites.

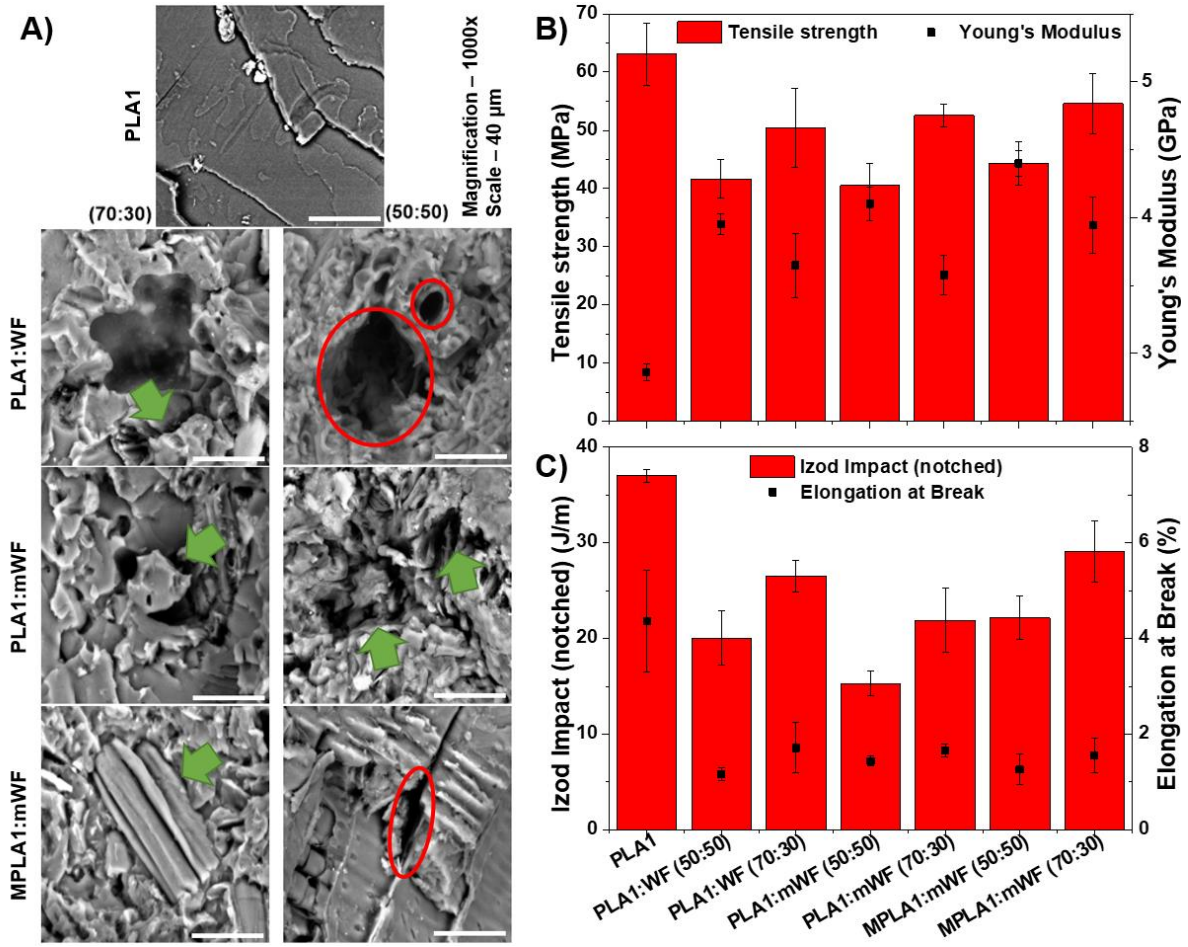

Figure 31. (A) SEM micrographs on the PLA and PLA based WPCs with and without modification at 30 (right) and 50 (left) wt.% wood; **(B)** Tensile strength and modulus of the PLA and its WPCs; and **(C)** Notched Izod impact and %strain for the PLA based WPCs and neat polymer.

The tensile strength and modulus (shown in **Figure 31(B)** of PLA1 was 63 ± 5 MPa and 2.9 ± 0 GPa, respectively which are like other reported values for PLA [198,237,238]. These values also indicate that one-time recycling does not affect the tensile properties of PLA. After the addition of 30 wt.% WF, there was a 20% decrease (50 ± 6 MPa) in tensile strength while the 50 wt.% composite decreased further by 9% ($p = 0.008$) to 45 ± 3 MPa. This

deterioration of tensile strength is likely attributed to two factors, i.e. poor compatibility and SCF within the unrefined WF itself as shown in **Figure 31(A)**. There was an overall positive effect on the modulus when the more rigid WF filler was introduced due to its effect on the chain orientation and mobility of the polymer phase and the overall crystallinity of the WPC. After WF was added to the system, the modulus increased to 3.6 and 3.9 GPa with 30 and 50 wt.% WF. When the WF was replaced with mWF, no statistically significant changes were found. Similarly, a study by Liminana et al. [239] found equivalent results when using DDSA to modify almond flour (AF) that was compounded with poly(butylene succinate) (PBS), which is also in the polyester family of polymers like PLA.

The same authors demonstrated that the modification of AF with DDSA did not also influence tensile strength when compared to the unmodified composite [239]. Lastly, the addition of MPLA appears to increase the tensile strength for both 50 and 30 wt.% mWF to 44 ± 2 and 55 ± 5 MPa, respectively, but again not significant enough or beyond the original strength of PLA [198]. This is because the wood particles are still acting more as stress concentrators rather than reinforcing agents even if the compatibility between filler and matrix is improving. The elongation at break and notched Izod impact mechanical properties are presented in **Figure 31(C)**. The elongation at break results were typical of a highly filled composite. With the more filler introduced in the composite, the more significant the WPC's ductility and toughness is hindered. While PLA1's strain was 4 ± 1%, all the WPCs exhibited a strain of 1.1 to 1.7%, representing a 73 to 58% decrease, respectively. The notched Izod impact strength of PLA was found to be 37 ± 1 J/m due to its inherent glassy/crystalline characteristics. Overall, higher WF content in the WPC restricts chain mobility along with the

aggravation of poor compatibility and SCF that drastically decreases the WPC's toughness. The MPLA specimens experienced a slight increase in impact strength due to the increased interaction. A tabulated form of the tensile and impact properties is presented in **Table C2**.

Lastly, the bond adhesion of the WPCs is shown through tensile strength, modulus, and elongation at the break in **Appendix C** in **Figure C3(A)** to **(C)**. Bond adhesion or durability testing helps to obtain insights on the applicability of the biocomposite for outdoor applications through accelerated aging, which is often coupled with Arrhenius calculations for extrapolation of the data. **Figure C3(A)** shows images taken before and after hydrothermal aging and due to the temperature of the boiling water (~100 ºC). It can be noted that the PLA was completed annealed thus the white, opaque, crystalline look. The degradation of the WF based WPC was highly dependent on the concentration of WF in the formulation. For instance, the 50 wt.% has swelled beyond the point of testing while the 30 wt.% WF based WPC was still testable. With both mWF and MPLA WPCs, the modification and compatibilization aided in preserving the 50 wt.% specimens by limiting the amount of absorbed water and consequently its swelling which is highlighted in its tensile properties. **Figure C3(B)** and **(C)** confirmed that PLA was annealed during testing as its modulus increased (7%) while its strength and elongation at break dropped significantly by 55 and 60%, respectively. As mentioned, the 50 wt.% WF was not able to be assessed; however, the 30 wt.% experienced a 91% decrease in tensile strength. The modification affected the property retention for the 50 wt.% but the 30 wt.% properties were not noticeably affected due to PLA1 being the dominant phase. The elongation at break results followed the same trend as the tensile strength.

5.5 Summary of Chapter 5

In this work, the recyclability of PLA as a juxtaposition to composting was investigated. The primary goal was to evaluate the recyclability of PLA for WPC fabrication by employing a scalable, economically, and environmentally sustainable approach. A protocol for prolonging the service life of PLA-based WPCs through the chemical modification of WF with DDSA in an effort to increase the WPCs overall hydrophobicity and dimensional instability was developed. After the successful modification of WF, this research investigated the effect of thermo-mechanical reprocessing of PLA on its structure and properties. After reprocessing, PLA was demonstrated to retain its properties while exhibiting increased crystallinity and tensile modulus (e.g., brittleness). Furthermore, the *in-situ* maleation of PLA for enhanced compatibilization between the components further aided in controlling WPCs dimensional stability by decreasing void space causing an impediment in the sorption kinetics by up to 89%. The addition of wood, in general, was found to have a significant nucleating effect on PLA even at the small inclusion of 2.5 wt.% wood. The modification of wood and maleation of PLA both aided in the compatibility of the constituents without affecting the composite's tensile strength and modulus. Finally, this work showed that the modification was more significant, compared to maleation, in enhancing the hydrothermal resistance by controlling the permeation kinetics.

Chapter 6 – Conclusion and Future Work

6.1 Conclusions

This research was an attempt to gain fundamental knowledge about opportunities and limitations for the recyclability of POs, with a specific interest in PP and LDPE, as well as polyesters, especially PLA. Furthermore, detailed investigation into the impact of recycling these thermoplastics on composite processing and fabrication, which were compounded with wood particulates (e.g. wood flour). As discussed, in the introduction chapter the limitations of wood and other natural fibers during fabrication are that they possess low thermal stabilities (< 200 °C), which hinders their usage with engineered polymers, such as polyamides, to more commodity plastics like PP.

Through this thesis, the preparation and characterization of polymer biocomposites (e.g. wood-plastic composites) were performed, where petroleum-based PP and bio-based PLA were separately compounded with a sustainable biobased reinforcement material (e.g. wood). In the first experimental study, it was discovered that PP can be thermo-mechanically reprocessed at least 6 times while maintaining its tensile strength and modulus. Additionally, it was found that process induced degradation significantly affects the materials melt flow behaviour and crystallinity as a result of molecular fragmentation being the primary mechanism of degradation. For the second part of study 1, it was found that addition of wood into PP resulted in decreased tensile strength and elongation due to the poor particle-resin interaction as well as defects within the particles themselves. With increasing the content of wood within the polymer system led to a drastic increase in the composite's viscosity resulting

in high machine torque and increased processing difficulties. Also, water absorption and thickness swelling properties are greatly affected with increased wood content. Although it was possible to compound 70 wt.% WF into recycled PP, further work is needed to optimize the process. The second experimental study revealed the potential for using simulated recycled PP as a feedstock for maleation in the production of MAPP. It was also found that the recycling of MAPP aided the composites displaying a significant tensile improvement from the virgin PP based composites. This is due to the decrease in viscosity which allowed for better resin permeation and overall mixing through the highly filled composites giving rise to better bonding and stress transfer. Finally, the last study showed that the modification of wood with DDSA was successful in prolonging and decreasing the water absorption saturation point with no effect to tensile properties from non-modified WPCs. The recycling of PLA, for one cycle, showed to have minimal influence on its properties and re-utilization for production manufacturing. The addition of maleic anhydride with recycled PLA in WPC applications aided in further reducing the water absorption while also slightly increasing tensile strength due to a reduction in void space between wood and the PLA matrix.

Two of the major scientific contributions from this work are the part of the core concepts of this thesis which were recycling of polymeric waste and sustainability. The recycling was employed as a means to alter a polymer's melt viscosity without additives all in the hopes to be able to produce highly filled WPCS (up to 70 wt.%). Additionally, the modification of wood with DDSA was another major contribution. This thesis has been the only published literature that investigated use of DDSA on a complex system (i.e. wood); while

others have used cellulous, hemi-cellulose, proteins, starches, and lignin in their extracted and purified forms. This was with hopes to create a bulk modified filler that could be compounded with recycled polymers for the same effect.

6.2 Future Works

Suggestions for future research work to assess the viability and suitability of the materials fabricated for specific applications. The future steps may be divided into two main components, short- and long-term projects that may be taken up to continue and expand upon this thesis. The first two project would fall under short term and are continuations from chapters 3 and 4. The first future work may entail obtaining real waste or 100% PP based household products to recycle and compare to the lab based simulated recycled PP. As well as investigating the recyclability of polypropylene/high density polyethylene blends. The other short-term future work project could evaluate the effect of reprocessing or recycling on higher MA grafted PPs. Moreover, the effect of PP maleation on the water/humidity absorption characteristics of WPCs is important.

The long-term project would be a follow-up to chapter 5, which one could investigate the recyclability of the composite as a whole as well as pyrolysis experiments to produce bio-charcoal for further composite development to prolong compost and landfill. Another aspect of this experiment to inquire about is the effectiveness of other chemical modifiers such as alkyl ketene dimer or octenyl succinic anhydride to evaluate effectiveness and what composite properties changes may be induced. Lastly, other manufacturing avenues could be interesting to explore would be thermoforming in order to produce food packaging containers.

References

[1] McKendry P. Energy production from biomass (part 1): overview of biomass. Bioresour Technol 2002;83:37–46. https://doi.org/10.1016/S0960-8524(01)00118-3.

[2] Bar-On YM, Phillips R, Milo R. The biomass distribution on Earth. Proceedings of the National Academy of Sciences 2018;115:6506–11. https://doi.org/10.1073/pnas.1711842115.

[3] Hornung A. Transformation of Biomass. Chichester, UK: John Wiley & Sons, Ltd; 2014. https://doi.org/10.1002/9781118693643.

[4] Manahan SE. Fundamentals of environmental and toxicological chemistry: sustainable science 2013:590.

[5] Abu Ghalia M, Dahman Y. Synthesis and utilization of natural fiber-reinforced poly (lactic acid) bionanocomposites. Lignocellulosic Fibre and Biomass-Based Composite Materials, Elsevier; 2017, p. 313–45. https://doi.org/10.1016/B978-0-08-100959-8.00015-9.

[6] Hon DNS. Chemical modification of cellulose. Chemical Modification of Lignocellulosic Materials, 2017, p. 97–127. https://doi.org/10.1201/9781315139142.

[7] Hornung A. Transformation of Biomass. Chichester, UK: John Wiley & Sons, Ltd; 2014. https://doi.org/10.1002/9781118693643.

[8] Esmizadeh E, Tzoganakis C, Mekonnen TH. Degradation Behavior of Polypropylene during Reprocessing and Its Biocomposites : Thermal and Oxidative Degradation Kinetics. Polymers (Basel) 2020;12:1627. https://doi.org/10.3390/polym12081627.

[9] Borysiak S, Doczekalska B. Influence of chemical modification of wood on the crystallisation of polypropylene. Holz Als Roh- Und Werkstoff 2006;64:451–4. https://doi.org/10.1007/s00107-006-0097-9.

[10] Mohanty AK. Natural fibers, biopolymers, and biocomposites. Edited by Amar K Mohanty, Manjusri Misra and Lawrence T Drzal. Polym Int 2006;55:1462–1462. https://doi.org/10.1002/pi.2084.

[11] Masci L. Thermoplastics materials engineering. second. Elsevier Applied Science; 1989.

[12] Gallos A, Paës G, Allais F, Beaugrand J. Lignocellulosic fibers: a critical review of the extrusion process for enhancement of the properties of natural fiber composites. RSC Adv 2017;7:34638–54. https://doi.org/10.1039/C7RA05240E.

[13] Faruk O, Bledzki AK, Fink HP, Sain M. Biocomposites reinforced with natural fibers: 2000-2010. Prog Polym Sci 2012;37:1552–96. https://doi.org/10.1016/j.progpolymsci.2012.04.003.

[14] Burgueño R, Quagliata MJ, Mehta GM, Mohanty AK, Misra M, Drzal LT. Sustainable Cellular Biocomposites from Natural Fibers and Unsaturated Polyester Resin for Housing Panel Applications. J Polym Environ 2005;13:139–49. https://doi.org/10.1007/s10924-005-2945-9.

[15] Papadopoulos AN. Advances in Wood Composites II. Polymers (Basel) 2020;12:1552. https://doi.org/10.3390/polym12071552.

[16] Jubinville D, Tzoganakis C, Mekonnen TH. Recycled PLA – Wood flour based biocomposites: Effect of wood flour surface modification, PLA recycling, and maleation. Constr Build Mater 2022;352:129026. https://doi.org/10.1016/j.conbuildmat.2022.129026.

[17] Crespell P and, Vidal M. Market and Technology Trends and Challenges for Wood Plastic Composites in North America. 51st International Convention of Society of Wood Science and Technology 2008:1–7.

[18] Zion Market Research. Global Biomass Pellets Market worth USD 15.9 Billion by 2022. 2017.

[19] Clemons CM. Woodfiber-plastic composites in the United States - History and current and future markets. The Proceedings of the 3rd International Wood and Natural Fibre Composites Symposium 2000:1–7.

[20] Klyosov AA. Wood-Plastic Composites. Hoboken, NJ, USA: John Wiley & Sons, Inc.; 2007. https://doi.org/10.1002/9780470165935.

[21] Clemons CM, Sabo RC, Kaland ML, Hirth KC. Effects of silane on the properties of wood-plastic composites with polyethylene-polypropylene blends as matrices. J Appl Polym Sci 2011;119:1398–409. https://doi.org/10.1002/app.32566.

[22] Farsi M. Wood-plastic composites: influence of wood flour chemical modification on the mechanical performance. Journal of Reinforced Plastics and Composites 2010;29:3587–92. https://doi.org/10.1177/0731684410378779.

[23] Zhang Y, Zhang SY, Choi P. Effects of wood fiber content and coupling agent content on tensile properties of wood fiber polyethylene composites. Holz Als Roh- Und Werkstoff 2008;66:267–74. https://doi.org/10.1007/s00107-008-0246-4.

[24] Dikobe DG, Luyt AS. Thermal and mechanical properties of PP/HDPE/wood powder and MAPP/HDPE/wood powder polymer blend composites. Thermochim Acta 2017;654:40–50. https://doi.org/10.1016/j.tca.2017.05.002.

[25] Mazzanti V, Mollica F. A Review of Wood Polymer Composites Rheology and Its Implications for Processing. Polymers (Basel) 2020;12:2304. https://doi.org/10.3390/polym12102304.

[26] Mazzanti V, Mollica F, El Kissi N. Rheological and mechanical characterization of polypropylene-based wood plastic composites. Polym Compos 2016;37:3460–73. https://doi.org/10.1002/pc.23546.

[27] Turku I, Kärki T, Puurtinen A. Durability of wood plastic composites manufactured from recycled plastic. Heliyon 2018;4:e00559. https://doi.org/10.1016/j.heliyon.2018.e00559.

[28] Jubinville D, Esmizadeh E, Saikrishnan S, Tzoganakis C, Mekonnen T. A comprehensive review of global production and recycling methods of polyolefin (PO) based products and their post-recycling applications. Sustainable Materials and Technologies 2020;25:e00188. https://doi.org/10.1016/j.susmat.2020.e00188.

[29] Saikrishnan S, Jubinville D, Tzoganakis C, Mekonnen TH. Thermo-mechanical degradation of polypropylene (PP) and low-density polyethylene (LDPE) blends exposed to simulated recycling. Polym Degrad Stab 2020;182:109390. https://doi.org/10.1016/j.polymdegradstab.2020.109390.

[30] Commission TE. Commission Regulation (EU) No 1272/2013. Official Journal of the European Union 2013;2013:2013–5.

[31] Nations TU. Paris Agreement. International Legal Materials 2016;55:740–55.

[32] Canada TP of. Carbon Pricing Policy in Canada. Library of Parliament 2018.

[33] PlasticsEurope. Plastics – the Facts 2017. PlasticsEurope 2017;0:0.

[34] Economics and Statistics Department ACC. 2018 Resin Situation and Trends. American Chemical Council 2019:1–4.

[35] Prieto M. Closing the loop on plastic recovery and recycling Closing the loop. 2020.

[36] PlasticsEurope. Plastics – the Facts 2019. PlasticsEurope 2019:1–42.

[37] Canada E and CC. Economic Study of the Canadian Plastic Industry, Markets, and Waste. 2019.

[38] Morten W. Ryberg, Alexis Laurent MH. Mapping of global plastics value chain and plastics losses to the environment (with a particular focus on marine environment). UN Environment 2018:1–99.

[39] Kotek R, Afshari M, Avci H, Najafi M. Production of polyolefins. Elsevier Ltd; 2017. https://doi.org/10.1016/B978-0-08-101132-4.00007-2.

[40] Lohse DJ. Polyolefins. Applied Polymer Science: 21st Century, Elsevier; 2000, p. 73–91. https://doi.org/10.1016/B978-008043417-9/50008-8.

[41] Posch W. Polyolefins. Applied Plastics Engineering Handbook 2011:23–48. https://doi.org/10.1016/B978-1-4377-3514-7.10003-0.

[42] Jordan AM, Kim K, Soetrisno D, Hannah J, Bates FS, Jaffer SA, et al. Role of Crystallization on Polyolefin Interfaces: An Improved Outlook for Polyolefin Blends. Macromolecules 2018;51:2506–16. https://doi.org/10.1021/acs.macromol.8b00206.

[43] Ojijo V, Sadiku ER. Improving wear resistance of polyolefins. Elsevier Ltd; 2017. https://doi.org/10.1016/B978-0-08-101132-4.00013-8.

[44] Agboola O, Sadiku R, Mokrani T, Amer I, Imoru O. Polyolefins and the environment. Polyolefin Fibres: Structure, Properties and Industrial Applications: Second Edition, Elsevier; 2017, p. 89–133. https://doi.org/10.1016/B978-0-08-101132-4.00004-7.

[45] Lohse DJ. Polyolefins. Applied Polymer Science: 21st Century, Elsevier; 2000, p. 73–91. https://doi.org/10.1016/B978-008043417-9/50008-8.

[46] PlasticsEurope. Plastics - the Facts 2010. PlasticsEurope 2010:1–30. https://doi.org/10.1016/j.marpolbul.2013.01.015.

[47] Posch DW. Polyolefins for Polyolefin Production. Applied Plastics Engineering Handbook 2017:27–53. https://doi.org/10.1016/B978-0-323-39040-8/00002-X.

[48] Ellen MacArthur Foundation. Towards a Circular Economy: Business Rationale for an Accelerated Transition. Ellen MacArthur Foundation (EMF) 2015:20.

[49] Will M. Towards a Sustainable Circular Economy – Remarks on plastics and wood-waste sector. The Central European Review of Economics and Management 2019;3:149–83. https://doi.org/10.29015/cerem.862.

[50] Niaounakis M. Management of Marine Plastic Debris: Prevention, Recycling, and Waste Management. 2017.

[51] Rochman CM, Brookson C, Bikker J, Djuric N, Earn A, Bucci K, et al. Rethinking microplastics as a diverse contaminant suite. Environ Toxicol Chem 2019;38:703–11. https://doi.org/10.1002/etc.4371.

[52] World Bank T. Trends in Solid Waste Management. 2020.

[53] Zhao Y-B, Lv X-D, Ni H-G. Solvent-based separation and recycling of waste plastics: A review. Chemosphere 2018;209:707–20. https://doi.org/10.1016/j.chemosphere.2018.06.095.

[54] Our world in Data. Primary plastic waste generation by polymer, 2015. Our World in Data 2017. https://ourworldindata.org/grapher/plastic-waste-polymer (accessed March 1, 2020).

[55] Canada E and CC. Economic Study of the Canadian Plastic Industry, Markets, and Waste. 2019.

[56] US EPA O. Facts and Figures about Materials, Waste and Recycling 2018.

[57] Parker L. National Geographic - Fast facts about plastic pollution. 2018.

[58] World Bank T. Trends in Solid Waste Management. 2020.

[59] Organization P. Only half of packaging waste is recycled and here's how to do better. 2018.

[60] Vanapalli KR, Samal B, Dubey BK, Bhattacharya J. Emissions and Environmental Burdens Associated With Plastic Solid Waste Management. Elsevier Inc.; 2019. https://doi.org/10.1016/b978-0-12-813140-4.00012-1.

[61] Bell JNB. Plastics, rubber and paper recycling. A pragmatic approach. Polym Int 1997;42:345–345. https://doi.org/10.1002/(SICI)1097-0126(199703)42:3<345::AID-PI696>3.0.CO;2-P.

[62] Niaounakis M. Biopolymers Reuse, Recycling, and Disposal. Oxford: Elsevier; 2013. https://doi.org/10.1016/b978-1-4557-3145-9.00006-3.

[63] Vanapalli KR, Samal B, Dubey BK, Bhattacharya J. Emissions and Environmental Burdens Associated With Plastic Solid Waste Management. Elsevier Inc.; 2019. https://doi.org/10.1016/b978-0-12-813140-4.00012-1.

[64] Ragaert K, Delva L, Van Geem K. Mechanical and chemical recycling of solid plastic waste. Waste Management 2017;69:24–58. https://doi.org/10.1016/j.wasman.2017.07.044.

[65] Singh N, Hui D, Singh R, Ahuja IPS, Feo L, Fraternali F. Recycling of plastic solid waste: A state of art review and future applications. Compos B Eng 2017;115:409–22. https://doi.org/10.1016/j.compositesb.2016.09.013.

[66] Carvalho T, Durão F, Ferreira C. Separation of packaging plastics by froth flotation in a continuous pilot plant. Waste Management 2010;30:2209–15. https://doi.org/10.1016/j.wasman.2010.05.023.

[67] Takoungsakdakun T, Pongstabodee S. Separation of mixed post-consumer PET-POM-PVC plastic waste using selective flotation. Sep Purif Technol 2007;54:248–52. https://doi.org/10.1016/j.seppur.2006.09.011.

[68] Burat F, Güney A, Olgaç Kangal M. Selective separation of virgin and post-consumer polymers (PET and PVC) by flotation method. Waste Management 2009;29:1807–13. https://doi.org/10.1016/j.wasman.2008.12.018.

[69] Fraunholcz N. Separation of waste plastics by froth flotation - A review, part I. Miner Eng 2004;17:261–8. https://doi.org/10.1016/j.mineng.2003.10.028.

[70] Pascoe RD, O'Connell B. Development of a method for separation of PVC and PET using flame treatment and flotation. Miner Eng 2003;16:1205–12. https://doi.org/10.1016/S0892-6875(03)00171-7.

[71] Drelich J, Payne T, Kim JH, Miller JD, Kobler R, Christiansen S. Selective froth flotation of PVC from PVC/PET mixtures for the plastics recycling industry. Polym Eng Sci 1998;38:1378–86. https://doi.org/10.1002/pen.10308.

[72] Carvalho T, Durão F, Ferreira C. Separation of packaging plastics by froth flotation in a continuous pilot plant. Waste Management 2010;30:2209–15. https://doi.org/10.1016/j.wasman.2010.05.023.

[73] Mantia FP La. Recycling of plastic materials. In: Mantia FP La, editor. Recycling of plastic materials, vol. 1, Toronto: ChemTec; 1993, p. 1–187.

[74] Warren LM, Burns R. Processors make a go of mixed-waste recycling. Plastic Technology 1988;34:41–2.

[75] Ecocycle - Build Zero Waste Communities. Zero Waste Creates Jobs 2011. https://www.ecocycle.org/zerowaste/jobs (accessed June 9, 2020).

[76] City of Toronto. Solid Waste Management Services (2018). City of Toronto 2017;9.

[77] Narasimhamurthy N. Development of Commercial Applications for Recycled Plastics Using Finite Element Analysis. 2005.

[78] JE G. The new science of strong materials (or why you don't fall through the floor). Princeton: Princeton University Press 1988:179.

[79] Moreno DDP, Saron C. Low-density polyethylene waste/recycled wood composites. Compos Struct 2017;176:1152–7. https://doi.org/10.1016/j.compstruct.2017.05.076.

[80] Turku I, Kärki T. Research progress in wood-plastic nanocomposites: A review. Journal of Thermoplastic Composite Materials 2014;27:180–204. https://doi.org/10.1177/0892705713486131.

[81] Gardner DJ, Han Y, Wang L. Wood–Plastic Composite Technology. Current Forestry Reports 2015;1:139–50. https://doi.org/10.1007/s40725-015-0016-6.

[82] Rosenberg B. Rapid prototyping to rapid manufacturing. Aerospace Engineering and Manufacturing 2008;28:37–9.

[83] Taylor A, Yadama V, Englund K, Harper D, Kim J. Wood Plastic Composites - A Primer -. Engineering 2012;1:11.

[84] Hietala M. Extrusion Processing of Wood-Based Biocomposites. 2012.

[85] Spear MJ, Eder A, Carus M. Wood polymer composites. Wood Composites, Elsevier Inc.; 2015, p. 195–249. https://doi.org/10.1016/B978-1-78242-454-3.00010-X.

[86] Kazemi Najafi S. Use of recycled plastics in wood plastic composites – A review. Waste Management 2013;33:1898–905. https://doi.org/10.1016/j.wasman.2013.05.017.

[87] Najafi SK, Mostafazadeh-Marznaki M, Chaharmahali M. Effect of Thermo-Mechanical Degradation of Polypropylene on Hygroscopic Characteristics of Wood Flour-Polypropylene Composites. J Polym Environ 2010;18:720–6. https://doi.org/10.1007/s10924-010-0220-1.

[88] Chaudhary SN, Borkar SP, Mantha SS. Sunnhemp Fiber-reinforced Waste Polyethylene Bag Composites. Journal of Reinforced Plastics and Composites 2009;29:2241–52. https://doi.org/10.1177/0731684409345615.

[89] Ares A, Bouza • R, Pardo • S G, Abad • M J, Barral • L. Rheological, Mechanical and Thermal Behaviour of Wood Polymer Composites Based on Recycled Polypropylene. J Polym Environ 2010;18:318–325. https://doi.org/10.1007/s10924-010-0208-x.

[90] Gregorová A, Cibulková Z, Košíková B, Šimon P. Stabilization effect of lignin in polypropylene and recycled polypropylene. Polym Degrad Stab 2005;89:553–8. https://doi.org/10.1016/j.polymdegradstab.2005.02.007.

[91] Li TQ, Ng CN, Li RKY. Impact behavior of sawdust/recycled–PP composites. J Appl Polym Sci 2001;81:1420–8.

[92] Almeida A, Capitão S, Bandeira R, Fonseca M, Picado-Santos L. Performance of AC mixtures containing flakes of LDPE plastic film collected from urban waste considering ageing. Constr Build Mater 2020;232:117253. https://doi.org/10.1016/j.conbuildmat.2019.117253.

[93] Hemmasi AH, Ghasemi I, Bazyar B, Samariha A. Influence of nanoclay on the physical properties of recycled high-density polyethylene/bagasse nanocomposite. Middle-East Journal of Scientific Research 2011;8:648–51.

[94] Tri Phuong N, Gilbert V, Chuong B. Preparation of recycled polypropylene/organophilic modified layered silicates nanocomposites part I: the recycling process of polypropylene and the mechanical properties of recycled polypropylene/organoclay nanocomposites. Journal of Reinforced Plastics and Composites 2008;27:1983–2000.

[95] Al-Maadeed MA, Shabana YM, Khanam PN. Processing, characterization and modeling of recycled polypropylene/glass fibre/wood flour composites. Mater Des 2014;58:374–80. https://doi.org/10.1016/j.matdes.2014.02.044.

[96] Pedroso AG, Rosa DS. Mechanical, thermal and morphological characterization of recycled LDPE/corn starch blends. Carbohydr Polym 2005;59:1–9. https://doi.org/10.1016/j.carbpol.2004.08.018.

[97] Najafi SK, Mostafazadeh-Marznaki M, Chaharmahali M, Tajvidi M. Effect of Thermomechanical Degradation of Polypropylene on Mechanical Properties of Wood-Polypropylene Composites. J Compos Mater 2009;43:2543–54. https://doi.org/10.1177/0021998309345349.

[98] Najafi SK, Kiaefar A, Hamidina E, Tajvidi M. Water Absorption Behavior of Composites from Sawdust and Recycled Plastics. Journal of Reinforced Plastics and Composites 2007;26:341–8. https://doi.org/10.1177/0731684407072519.

[99] Louis Lee Ray, Resty Woro Yuniar, Sri Kusmiati. Western plastics “poisoning Indonesian food chain” - BBC News. BBC Victoria Derbyshire Programme 2019.

[100] OECD. Improving plastics management: trends, policy responses, and the role of international co-operation and trade. Environmental Policy Paper No 12 2018:20.

[101] Ruvolo-Filho A, Marconcini JM. Selection criteria for recycled polyolefins from urban wastes by using TG analysis. Materials Research 2007;10:341–5. https://doi.org/10.1590/S1516-14392007000400004.

[102] Mumbach GD, de Sousa Cunha R, Machado RAF, Bolzan A. Dissolution of adhesive resins present in plastic waste to recover polyolefin by sink-float separation processes. J Environ Manage 2019;243:453–62. https://doi.org/10.1016/j.jenvman.2019.05.021.

[103] Behazin E, Rodriguez-Uribe A, Misra M, Mohanty AK. Long-term performance of β-nucleated toughened polypropylene-biocarbon composites. Compos Part A Appl Sci Manuf 2018;105:274–80. https://doi.org/10.1016/j.compositesa.2017.11.014.

[104] da Costa HM, Ramos VD, Rocha MCG. Rheological properties of polypropylene during multiple extrusion. Polym Test 2005;24:86–93. https://doi.org/10.1016/j.polymertesting.2004.06.006.

[105] Kazemi Najafi S. Use of recycled plastics in wood plastic composites – A review. Waste Management 2013;33:1898–905. https://doi.org/10.1016/j.wasman.2013.05.017.

[106] Aumnate C, Spicker C, Kiesel R, Samadi M, Rudolph N. Recycling Of PP/LDPE blend: Miscibility, thermal properties, rheological behavior and crystal structure. Annual Technical Conference - ANTEC, Conference Proceedings 2016:81–8.

[107] Ashori A. Wood–plastic composites as promising green-composites for automotive industries! Bioresour Technol 2008;99:4661–7. https://doi.org/10.1016/j.biortech.2007.09.043.

[108] World Bank T. Forests. IBRD IDA 2020. https://www.worldbank.org/en/topic/forests (accessed January 5, 2021).

[109] The World Bank. Agriculture, forestry, and fishing, value added (% of GDP) | Data. 2021.

[110] Bozdogan AM, Yarpuz-Bozdogan N. Research & Reviews in Agriculture, Forestry and Aquaculture Sciences. Gece Publishing 2019:49–64.

[111] Yeh S-K, Kim K-J, Gupta RK. Synergistic effect of coupling agents on polypropylene-based wood-plastic composites. J Appl Polym Sci 2013;127:1047–53. https://doi.org/10.1002/app.37775.

[112] Koskela K, Rowell RM, Mahlberg R, Paajanen L, Nurmi A, Kivisto A. Effect of chemical modification of wood on the mechanical and adhesion properties of wood fiber / polypropylene fiber and polypropylene / veneer composites. Holz Als Roh- Und Werkstoff 2001;59.

[113] Faruk O, Bledzki AK, Fink HP, Sain M. Biocomposites reinforced with natural fibers: 2000-2010. Prog Polym Sci 2012;37:1552–96. https://doi.org/10.1016/j.progpolymsci.2012.04.003.

[114] Shenoy A V., Saini DR. Melt flow index: More than just a quality control rheological parameter. Part II. Advances in Polymer Technology 1986;6:125–45. https://doi.org/10.1002/adv.1986.060060201.

[115] Velasco JI, Morhain C, Martínez AB, Rodríguez-Pérez MA, de Saja JA. The effect of filler type, morphology and coating on the anisotropy and microstructure heterogeneity of injection-moulded discs of polypropylene filled with aluminium and magnesium hydroxides. Part 2. Thermal and dynamic mechanical properties. Polymer (Guildf) 2002;43:6813–9. https://doi.org/10.1016/S0032-3861(02)00669-9.

[116] Gray AP. Polymer crystallinity determinations by DSC. Thermochim Acta 1970;1:563–79. https://doi.org/10.1016/0040-6031(70)80008-9.

[117] Canevarolo S V. Chain scission distribution function for polypropylene degradation during multiple extrusions. Polym Degrad Stab 2000;70:71–6. https://doi.org/10.1016/S0141-3910(00)00090-2.

[118] Waldman WR, De Paoli MA. Thermo-mechanical degradation of polypropylene, low-density polyethylene and their 1:1 blend. Polym Degrad Stab 1998;60:301–8. https://doi.org/10.1016/s0141-3910(97)00083-9.

[119] Mylläri V, Ruoko T-P, Syrjälä S. A comparison of rheology and FTIR in the study of polypropylene and polystyrene photodegradation. J Appl Polym Sci 2015;132:n/a-n/a. https://doi.org/10.1002/app.42246.

[120] Andrady AL, Pegram JE, Tropsha Y. Changes in carbonyl index and average molecular weight on embrittlement of enhanced-photodegradable polyethylenes. J Environ Polym Degrad 1993;1:171–9. https://doi.org/10.1007/BF01458025.

[121] Qin H, Zhang S, Liu H, Xie S, Yang M, Shen D. Photo-oxidative degradation of polypropylene/montmorillonite nanocomposites. Polymer (Guildf) 2005;46:3149–56. https://doi.org/10.1016/j.polymer.2005.01.087.

[122] Nasir A, Yasin T, Islam A. Thermo-oxidative degradation behavior of recycled polypropylene. J Appl Polym Sci 2011;119:3315–20. https://doi.org/10.1002/app.32918.

[123] Ferg EE, Bolo LL. A correlation between the variable melt flow index and the molecular mass distribution of virgin and recycled polypropylene used in the manufacturing of battery cases. Polym Test 2013;32:1452–9. https://doi.org/10.1016/j.polymertesting.2013.09.009.

[124] Amintowlieh Y. Rheological Modification of Polypropylene by Incorporation of Long Chain Branches Using UV Radiation. the University of Waterloo, 2014.

[125] Tzoganakis C. A rheological evaluation of linear and branched controlled-rheology polypropylenes. Can J Chem Eng 1994;72:749–54. https://doi.org/10.1002/cjce.5450720425.

[126] Maldas D, Kokta B V. Role of coupling agents on the performance of woodflour-filled polypropylene composites. International Journal of Polymeric Materials and Polymeric Biomaterials 1994;27:77–88. https://doi.org/10.1080/00914039408038294.

[127] Mijiyawa F, Koffi D, Kokta B V, Erchiqui F. Formulation and tensile characterization of wood-plastic composites: Polypropylene reinforced by birch and aspen fibers for gear applications. Journal of Thermoplastic Composite Materials 2015;28:1675–92. https://doi.org/10.1177/0892705714563120.

[128] Mirbagheri J, Tajvidi M, Hermanson JC, Ghasemi I. Tensile properties of wood flour/kenaf fiber polypropylene hybrid composites. J Appl Polym Sci 2007;105:3054–9. https://doi.org/10.1002/app.26363.

[129] Leu S-Y, Yang T-H, Lo S-F, Yang T-H. Optimized material composition to improve the physical and mechanical properties of extruded wood–plastic composites (WPCs). Constr Build Mater 2012;29:120–7. https://doi.org/10.1016/j.conbuildmat.2011.09.013.

[130] Jubinville D, Abdelwahab M, Mohanty AK, Misra M. Comparison in composite performance after thermooxidative aging of injection molded polyamide 6 with glass fiber, talc, and a sustainable biocarbon filler. J Appl Polym Sci 2020;137:48618. https://doi.org/10.1002/app.48618.

[131] Di Gianfrancesco A. Technologies for chemical analyses, microstructural and inspection investigations. Materials for Ultra-Supercritical and Advanced Ultra-Supercritical Power Plants, Elsevier; 2017, p. 197–245. https://doi.org/10.1016/B978-0-08-100552-1.00008-7.

[132] Ndiaye D, Gueye M, Diop B. Characterization, Physical and Mechanical Properties of Polypropylene/Wood-Flour Composites. Arab J Sci Eng 2013;38:59–68. https://doi.org/10.1007/s13369-012-0407-y.

[133] Cesarino I, Dias O, Negrão D, Rocha L, Leão A. Deterioration of Wood Plastics Composites by the White-Rot Fungus Pycnoporus sanguineus. Journal of Composites Science 2019;3:24. https://doi.org/10.3390/jcs3010024.

[134] Kord B. Effect of Wood Flour Content on the Hardness and Water Uptake of Thermoplastic Polymer Composites. World Appl Sci J 2011;12:1632–4.

[135] Sobczak L, Lang RW, Haider A. Polypropylene composites with natural fibers and wood – General mechanical property profiles. Compos Sci Technol 2012;72:550–7. https://doi.org/10.1016/j.compscitech.2011.12.013.

[136] Nachtigall SMB, Miotto M, Schneider EE, Mauler RS, Camargo Forte MM. Macromolecular coupling agents for flame retardant materials. Eur Polym J 2006;42:990–9. https://doi.org/10.1016/j.eurpolymj.2005.10.017.

[137] Rehman SKU, Ibrahim Z, Jameel M, Memon SA, Javed MF, Aslam M, et al. Assessment of Rheological and Piezoresistive Properties of Graphene based Cement Composites. Int J Concr Struct Mater 2018;12:64. https://doi.org/10.1186/s40069-018-0293-0.

[138] Mazzanti V, El Kissi N, Mollica F. In – line vs. off – line rheological characterization of wood polymer composites. AIP Conf Proc, vol. 1736, 2016, p. 020003. https://doi.org/10.1063/1.4949577.

[139] Bhaskar J, Haq S, Pandey AK, Srivastava N. Evaluation of properties of propylene-pine wood plastic composite. Journal of Materials and Environmental Science 2012;3:605–12.

[140] Butylina S, Martikka O, Kärki T. Comparison of water absorption and mechanical properties of wood–plastic composites made from polypropylene and polylactic acid. Wood Mater Sci Eng 2010;5:220–8. https://doi.org/10.1080/17480272.2010.532233.

[141] Mekonnen TH, Mussone PG, Choi P, Bressler DC. Adhesives from waste protein biomass for oriented strand board composites: Development and performance. Macromol Mater Eng 2014;299:1003–12. https://doi.org/10.1002/mame.201300402.

[142] Wechsler A, Hiziroglu S. Some of the properties of wood–plastic composites. Build Environ 2007;42:2637–44. https://doi.org/10.1016/j.buildenv.2006.06.018.

[143] Yeh S-K, Kim K-J, Gupta RK. Synergistic effect of coupling agents on polypropylene-based wood-plastic composites. J Appl Polym Sci 2013;127:1047–53. https://doi.org/10.1002/app.37775.

[144] Trinh BM, Ogunsona EO, Mekonnen TH. Thin-structured and compostable wood fiber-polymer biocomposites: Fabrication and performance evaluation. Compos Part A Appl Sci Manuf 2021;140:106150. https://doi.org/10.1016/j.compositesa.2020.106150.

[145] Mekonnen T, Mussone P, Alemaskin K, Sopkow L, Wolodko J, Choi P, et al. Biocomposites from hydrolyzed waste proteinaceous biomass: Mechanical, thermal and moisture absorption performances. J Mater Chem A Mater 2013;1. https://doi.org/10.1039/c3ta13560h.

[146] Baar J, Paschová Z, Čermák P, Wimmer R. Color Changes Of Various Wood Species In Response To Moisture. Wood and Fiber Science 2019;51:119–31. https://doi.org/10.22382/wfs-2019-014.

[147] Sandoval-Torres S, Jomaa W, Marc F, Puiggali J-R. Causes of color changes in wood during drying. For Stud China 2010;12:167–75. https://doi.org/10.1007/s11632-010-0404-8.

[148] Jubinville D, Esmizadeh E, Tzoganakis C, Mekonnen T. Thermo-mechanical recycling of polypropylene for the facile and scalable fabrication of highly loaded wood plastic composites. Compos B Eng 2021;219:108873. https://doi.org/10.1016/j.compositesb.2021.108873.

[149] Hansen CM, Björkman A. The Ultrastructure of Wood from a Solubility Parameter Point of View. Holzforschung 1998;52:335–44. https://doi.org/10.1515/hfsg.1998.52.4.335.

[150] Myrvold BO. The Hansen Solubility Parameters of Some Lignosulfonates. World Academy of Science, Engineering and Technology International Journal of Energy and Power Engineering 2014;1:261.

[151] Serhan M, Sprowls M, Jackemeyer D, Long M, Perez ID, Maret W, et al. Total iron measurement in human serum with a smartphone. AIChE Annual Meeting, Conference Proceedings 2019;2019-Novem. https://doi.org/10.1039/x0xx00000x.

[152] Sauerbier P, Köhler R, Renner G, Militz H. Plasma Treatment of Polypropylene-Based Wood–Plastic Composites (WPC): Influences of Working Gas. Polymers (Basel) 2020;12:1933. https://doi.org/10.3390/polym12091933.

[153] Dairi B, Djidjelli H, Boukerrou A, Migneault S, Koubaa A. Morphological, mechanical, and physical properties of composites made with wood flour-reinforced polypropylene/recycled poly(ethylene terephthalate) blends. Polym Compos 2017;38:1749–55. https://doi.org/10.1002/pc.23745.

[154] Rowell RM. Advances and Challenges of Wood Polymer Composites. Proceedings of the 8th Pacific Rim Bio-Based Composites Symposium 2006;15:2–11.

[155] Lin TA, Lin J-H, Bao L. Effect of Melting–Recycling Cycles and Mechanical Fracture on the Thermoplastic Materials Composed of Thermoplastic Polyurethane and Polypropylene Waste Blends. Applied Sciences 2020;10:5810. https://doi.org/10.3390/app10175810.

[156] Inácio ALN, Nonato RC, Bonse BC. Recycled PP/EPDM/talc reinforced with bamboo fiber: Assessment of fiber and compatibilizer content on properties using factorial design. Polym Test 2017;61:214–22. https://doi.org/10.1016/j.polymertesting.2017.05.022.

[157] Reports and Data. Maleic Anhydride Market Size Worth USD 4.70 Billion By 2027 | Growing Demand from the Polymer and Coating Industries will be the Major Factor Driving the Industry Growth, says Reports and Data. 2021.

[158] Grand View Research. U.S. Maleic Anhydride Market Size, Share & Trends Analysis Report By Product Form (Solid, Molten, Brittle), By Application (Upr, Styrene Copolymers, Specialty Products), And Segment Forecasts, 2019 - 2025. Market Analysis Report 2019:64.

[159] Chen T, Mansfield CD, Ju L, Baird DG. The influence of mechanical recycling on the properties of thermotropic liquid crystalline polymer and long glass fiber reinforced polypropylene. Compos B Eng 2020;200:108316. https://doi.org/10.1016/j.compositesb.2020.108316.

[160] Ghahri S, Najafi SK, Mohebby B, Tajvidi M. Impact strength improvement of wood flour-recycled polypropylene composites. J Appl Polym Sci 2012;124:1074–80. https://doi.org/10.1002/app.34015.

[161] Fonseca-Valero C, Ochoa-Mendoza A, Arranz-Andrés J, González-Sánchez C. Mechanical recycling and composition effects on the properties and structure of hardwood cellulose-reinforced high density polyethylene eco-composites. Compos Part A Appl Sci Manuf 2015;69:94–104. https://doi.org/10.1016/j.compositesa.2014.11.009.

[162] Van Kets K, Delva L, Ragaert K. Structural stabilizing effect of SEBSgMAH on a PP-PET blend for multiple mechanical recycling. Polym Degrad Stab 2019;166:60–72. https://doi.org/10.1016/j.polymdegradstab.2019.05.012.

[163] McNeill IC, Polishchuk AYa, Zaikov GE. Thermal degradation studies of alternating copolymers: I—maleic anhydride-vinyl acetate. Polym Degrad Stab 1992;37:223–32. https://doi.org/10.1016/0141-3910(92)90164-Z.

[164] Back RA, Parsons JM. The thermal and photochemical decomposition of maleic anhydride in the gas phase. Can J Chem 1981;59:1342–6. https://doi.org/10.1139/v81-197.

[165] O'Mara JH, McIntyre D. Temperature Dependence of the Refractive Index Increment of Polystyrene in Solution. J Phys Chem 1959;63:1435–7. https://doi.org/10.1021/j150579a025.

[166] Fujimatsu H, Ideta Y, Nakamura H, Usami H, Ogasawara S. Coloration of Polypropylene Gel and Temperature Conditions for Gel Formation. Polym J 2001;33:543–6. https://doi.org/10.1295/polymj.33.543.

[167] Osswald T, Rudolph N. Polymer Rheology: Fundamentals and Applications. vol. 37. 2015.

[168] Marcovich NE, Reboredo MM, Kenny J, Aranguren MI. Rheology of particle suspensions in viscoelastic media. Wood flour-polypropylene melt. Rheol Acta 2004;43:293–303. https://doi.org/10.1007/s00397-003-0349-0.

[169] Sclavons M, Carlier V, De Roover B, Franquinet P, Devaux J, Legras R. The anhydride content of some commercial PP-g-MA: FTIR and titration. J Appl Polym Sci 1996;62:1205–10. https://doi.org/10.1002/(SICI)1097-4628(19961121)62:8<1205::AID-APP10>3.0.CO;2-6.

[170] Rajakumar K, Sarasvathy V, Thamarai Chelvan A, Chitra R, Vijayakumar CT. Natural Weathering Studies of Polypropylene. J Polym Environ 2009;17:191–202. https://doi.org/10.1007/s10924-009-0138-7.

[171] Bonelli CMC, Martins AF, Mano EB, Beatty CL. Effect of recycled polypropylene on polypropylene/high-density polyethylene blends. J Appl Polym Sci 2001;80:1305–11. https://doi.org/10.1002/app.1217.

[172] Sclavons M, Franquinet P, Carlier V, Verfaillie G, Fallais I, Legras R, et al. Quantification of the maleic anhydride grafted onto polypropylene by chemical and viscosimetric titrations, and FTIR spectroscopy. Polymer (Guildf) 2000;41:1989–99. https://doi.org/10.1016/S0032-3861(99)00377-8.

[173] Rengarajan R, Parameswaran VR, Lee S, Vicic M, Rinaldi PL. N.m.r. analysis of polypropylene-maleic anhydride copolymer. Polymer (Guildf) 1990;31:1703–6. https://doi.org/10.1016/0032-3861(90)90188-5.

[174] Yang L, Zhang F, Endo T, Hirotsu T. Microstructure of Maleic Anhydride Grafted Polyethylene by High-Resolution Solution-State NMR and FTIR Spectroscopy. Macromolecules 2003;36:4709–18. https://doi.org/10.1021/ma020527r.

[175] Bettini SHP, Agnelli JAM. Grafting of maleic anhydride onto polypropylene by reactive extrusion. J Appl Polym Sci 2002;85:2706–17. https://doi.org/10.1002/app.10705.

[176] Heinen W, Van Duin M. C13 NMR Study of the Grafting Of C13 Labeled Maleic Anhydride Onto PE, PP and EPM. Macromol Symp 1998;129:119–25. https://doi.org/1022-1360/98/$ 10.00.

[177] Heinen W, Rosenmöller CH, Wenzel CB, de Groot HJM, Lugtenburg J, van Duin M. 13 C NMR Study of the Grafting of Maleic Anhydride onto Polyethene, Polypropene, and Ethene−Propene Copolymers. Macromolecules 1996;29:1151–7. https://doi.org/10.1021/ma951015y.

[178] Zhang R, Zhu Y, Zhang J, Jiang W, Yin J. Effect of the initial maleic anhydride content on the grafting of maleic anhydride onto isotactic polypropylene. J Polym Sci A Polym Chem 2005;43:5529–34. https://doi.org/10.1002/pola.21038.

[179] Canevarolo S. Chain scission distribution function for polypropylene degradation during multiple extrusions. Polym Degrad Stab 2000;70:71–6. https://doi.org/10.1016/S0141-3910(00)00090-2.

[180] Beg M, Pickering K. Reprocessing of wood fibre reinforced polypropylene composites. Part I: Effects on physical and mechanical properties. Compos Part A Appl Sci Manuf 2008;39:1091–100. https://doi.org/10.1016/j.compositesa.2008.04.013.

[181] Xu J, Reiter G, Alamo RG. Concepts of nucleation in polymer crystallization. Crystals (Basel) 2021;11:1–19. https://doi.org/10.3390/cryst11030304.

[182] Oromiehie A, Ebadi-Dehaghani H, Mirbagheri S. Chemical Modification of Polypropylene by Maleic Anhydride: Melt Grafting, Characterization and Mechanism. International Journal of Chemical Engineering and Applications 2014;5:117–22. https://doi.org/10.7763/IJCEA.2014.V5.363.

[183] Gijsman P, Meijers G, Vitarelli G. Comparison of the UV-degradation chemistry of polypropylene, polyethylene, polyamide 6 and polybutylene terephthalate. Polym Degrad Stab 1999;65:433–41. https://doi.org/10.1016/S0141-3910(99)00033-6.

[184] Baumhardt-Neto R, De Paoli M-A. Mechanical degradation of polypropylene: Effect of UV irradiation. Polym Degrad Stab 1993;40:59–64. https://doi.org/10.1016/0141-3910(93)90191-K.

[185] Kaczmarek H, Ołdak D, Malanowski P, Chaberska H. Effect of short wavelength UV-irradiation on ageing of polypropylene/cellulose compositions. Polym Degrad Stab 2005;88:189–98. https://doi.org/10.1016/j.polymdegradstab.2004.04.017.

[186] Joseph PV, Rabello MS, Mattoso LHC, Joseph K, Thomas S. Environmental effects on the degradation behaviour of sisal fibre reinforced polypropylene composites. Compos Sci Technol 2002;62:1357–72. https://doi.org/10.1016/S0266-3538(02)00080-5.

[187] Beg MDH, Pickering KL. Accelerated weathering of unbleached and bleached Kraft wood fibre reinforced polypropylene composites. Polym Degrad Stab 2008;93:1939–46. https://doi.org/10.1016/j.polymdegradstab.2008.06.012.

[188] Seldén R, Nyström B, Långström R. UV aging of poly(propylene)/wood-fiber composites. Polym Compos 2004;25:543–53. https://doi.org/10.1002/pc.20048.

[189] Kuka E, Andersons B, Cirule D, Andersone I, Kajaks J, Militz H, et al. Weathering properties of wood-plastic composites based on heat-treated wood and polypropylene. Compos Part A Appl Sci Manuf 2020;139:106102. https://doi.org/10.1016/j.compositesa.2020.106102.

[190] Soccalingame L, Perrin D, Bénézet JC, Mani S, Coiffier F, Richaud E, et al. Reprocessing of artificial UV-weathered wood flour reinforced polypropylene composites. Polym Degrad Stab 2015;120:313–27. https://doi.org/10.1016/j.polymdegradstab.2015.07.013.

[191] PR Newswire. Polylactic Acid (PLA) Market worth $1.9 billion by 2026 - Exclusive Report by MarketsandMarkets™ - Bloomberg. Bloomberg 2022.

[192] Kamau-Devers K, Kortum Z, Miller SA. Hydrothermal aging of bio-based poly(lactic acid) (PLA) wood polymer composites: Studies on sorption behavior, morphology, and heat conductance. Constr Build Mater 2019;214:290–302. https://doi.org/10.1016/j.conbuildmat.2019.04.098.

[193] Taib N-AAB, Rahman MR, Huda D, Kuok KK, Hamdan S, Bakri MK bin, et al. A review on poly lactic acid (PLA) as a biodegradable polymer. Polymer Bulletin 2022. https://doi.org/10.1007/s00289-022-04160-y.

[194] Ncube LK, Ude AU, Ogunmuyiwa EN, Zulkifli R, Beas IN. Environmental Impact of Food Packaging Materials: A Review of Contemporary Development from Conventional Plastics to Polylactic Acid Based Materials. Materials 2020;13:4994. https://doi.org/10.3390/ma13214994.

[195] Sinclair RG. The Case for Polylactic Acid as a Commodity Packaging Plastic. Journal of Macromolecular Science, Part A 1996;33:585–97. https://doi.org/10.1080/10601329608010880.

[196] Markets and Markets. Polylactic Acid (PLA) Market Global Forecast to 2026 | MarketsandMarkets. MarketsandMarkets 2020.

[197] Ozdemir E, Hacaloglu J. Thermal degradation of polylactide and its electrospun fiber. Fibers and Polymers 2016;17:66–73. https://doi.org/10.1007/s12221-016-5679-5.

[198] Trinh BM, Ogunsona EO, Mekonnen TH. Thin-structured and compostable wood fiber-polymer biocomposites: Fabrication and performance evaluation. Compos Part A Appl Sci Manuf 2021;140:106150. https://doi.org/10.1016/j.compositesa.2020.106150.

[199] Sun C, Wei S, Tan H, Huang Y, Zhang Y. Progress in upcycling polylactic acid waste as an alternative carbon source: A review. Chemical Engineering Journal 2022;446:136881. https://doi.org/10.1016/j.cej.2022.136881.

[200] Rosli NA, Karamanlioglu M, Kargarzadeh H, Ahmad I. Comprehensive exploration of natural degradation of poly(lactic acid) blends in various degradation media: A review. Int J Biol Macromol 2021;187:732–41. https://doi.org/10.1016/j.ijbiomac.2021.07.196.

[201] Goto T, Kishita M, Sun Y, Sako T, Okajima I. Degradation of Polylactic Acid Using Sub-Critical Water for Compost. Polymers (Basel) 2020;12:2434. https://doi.org/10.3390/polym12112434.

[202] Åkesson D, Fazelinejad S, Skrifvars V-V, Skrifvars M. Mechanical recycling of polylactic acid composites reinforced with wood fibres by multiple extrusion and hydrothermal ageing. Journal of Reinforced Plastics and Composites 2016;35:1248–59. https://doi.org/10.1177/0731684416647507.

[203] Fazelinejad S, Åkesson D, Skrifvars M. Repeated Mechanical Recycling of Polylactic Acid Filled With Chalk. vol. 33. 2017.

[204] Beltrán FR, Infante C, de la Orden MU, Martínez Urreaga J. Mechanical recycling of poly(lactic acid): Evaluation of a chain extender and a peroxide as additives for upgrading the recycled plastic. J Clean Prod 2019;219:46–56. https://doi.org/10.1016/j.jclepro.2019.01.206.

[205] Zenkiewicz M, Richert J, Rytlewski P, Moraczewski K, Stepczyńska M, Karasiewicz T. Characterisation of multi-extruded poly(lactic acid). Polym Test 2009;28:412–8. https://doi.org/10.1016/j.polymertesting.2009.01.012.

[206] Beltrán FR, Lorenzo V, Acosta J, de la Orden MU, Martínez Urreaga J. Effect of simulated mechanical recycling processes on the structure and properties of poly(lactic acid). J Environ Manage 2018;216:25–31. https://doi.org/10.1016/j.jenvman.2017.05.020.

[207] Freeland B, McCarthy E, Balakrishnan R, Fahy S, Boland A, Rochfort KD, et al. A Review of Polylactic Acid as a Replacement Material for Single-Use Laboratory Components. Materials 2022;15:2989. https://doi.org/10.3390/ma15092989.

[208] Żenkiewicz M, Richert J, Rytlewski P, Moraczewski K, Stepczyńska M, Karasiewicz T. Characterisation of multi-extruded poly(lactic acid). Polym Test 2009;28:412–8. https://doi.org/10.1016/j.polymertesting.2009.01.012.

[209] Petchwattana N, Naknaen P, Narupai B. A circular economy use of waste wood sawdust for wood plastic composite production: effect of bio-plasticiser on the toughness. International Journal of Sustainable Engineering 2020;13:398–410. https://doi.org/10.1080/19397038.2019.1688422.

[210] Dalu M, Temiz A, Altuntaş E, Demirel GK, Aslan M. Characterization of tanalith E treated wood flour filled polylactic acid composites. Polym Test 2019;76:376–84. https://doi.org/10.1016/j.polymertesting.2019.03.037.

[211] Kumar S. Chemical Modification of Wood. Wood and Fibre Science 1994;26:270–80.

[212] Rowell RM. Chemical Modification of Wood. Handbook of wood chemistry and wood composites. , Foresty Products Laboratory - CRC press; 2005, p. 381–420.

[213] Rowell RM. Chemical Modification of Wood. In: Fakirov S, Bhattacharyya D, editors. Handbook of Engineering Biopolymers Homopolymers, Blends, and Composites, Cincinnati: Hanser; 2007, p. 673–91.

[214] Arminger B, Gindl-Altmutter W, Keckes J, Hansmann C. Facile preparation of superhydrophobic wood surfaces via spraying of aqueous alkyl ketene dimer dispersions. RSC Adv 2019;9:24357–67. https://doi.org/10.1039/C9RA03700D.

[215] Rowell RM. Chemical modification of wood: A short review. Wood Mater Sci Eng 2006;1:29–33. https://doi.org/10.1080/17480270600670923.

[216] Teacă C-A, Bodîrlău R, Spiridon I. Maleic Anhydride Treatment of Softwood-Effect on Wood Structure and Properties. CELLULOSE CHEMISTRY AND TECHNOLOGY Cellulose Chem Technol 2014;48:863–8.

[217] Ramaswamy R, Shine KG. Some Aspects on the Synthesis and Characterization of Dodecenyl Succinic Anhydride (DDSA)-a Curing Agent for Epoxy Resins. J Appl Polym Sci 1987;33:49–65.

[218] Li G, Xu X, Zhu F. Physicochemical properties of dodecenyl succinic anhydride (DDSA) modified quinoa starch. Food Chem 2019;300:125201. https://doi.org/10.1016/j.foodchem.2019.125201.

[219] Atifi S, Miao C, Hamad WY. Surface modification of lignin for applications in polypropylene blends. J Appl Polym Sci 2017;134:45103. https://doi.org/10.1002/app.45103.

[220] Hutchinson MH, Dorgan JR, Knauss DM, Hait SB. Optical Properties of Polylactides. J Polym Environ 2006;14:119–24. https://doi.org/10.1007/s10924-006-0001-z.

[221] Gupta M, Singh R. PLA-coated sisal fibre-reinforced polyester composite: Water absorption, static and dynamic mechanical properties. J Compos Mater 2019;53:65–72. https://doi.org/10.1177/0021998318780227.

[222] Sun H, Yang Y, Han Y, Tian M, Li B, Han L, et al. X-ray Photoelectron Spectroscopy Analysis of Wood Degradation in Old Architecture. Bioresources 2020;15:6332–43.

[223] Jubinville D, Tzoganakis C, Mekonnen TH. Simulated Recycling of Polypropylene and Maleated Polypropylene for the Fabrication of Highly-Filled Wood Plastic Composites. ACS Appl Polym Mater 2021. https://doi.org/10.1021/ACSAPM.1C01671/SUPPL_FILE/AP1C01671_SI_001.PDF.

[224] Yew GH, Mohd Yusof AM, Mohd Ishak ZA, Ishiaku US. Water absorption and enzymatic degradation of poly(lactic acid)/rice starch composites. Polym Degrad Stab 2005;90:488–500. https://doi.org/10.1016/j.polymdegradstab.2005.04.006.

[225] Wang H, Sun X, Seib P. Strengthening blends of poly(lactic acid) and starch with methylenediphenyl diisocyanate. J Appl Polym Sci 2001;82:1761–7. https://doi.org/10.1002/app.2018.

[226] Ayrilmis N, Kariz M, Kwon JH, Kitek Kuzman M. Effect of printing layer thickness on water absorption and mechanical properties of 3D-printed wood/PLA composite materials. The International Journal of Advanced Manufacturing Technology 2019;102:2195–200. https://doi.org/10.1007/s00170-019-03299-9.

[227] Butylina S, Martikka O, Kärki T. Comparison of water absorption and mechanical properties of wood–plastic composites made from polypropylene and polylactic acid. Wood Mater Sci Eng 2010;5:220–8. https://doi.org/10.1080/17480272.2010.532233.

[228] Chung T-J, Park J-W, Lee H-J, Kwon H-J, Kim H-J, Lee Y-K, et al. The Improvement of Mechanical Properties, Thermal Stability, and Water Absorption Resistance of an Eco-Friendly PLA/Kenaf Biocomposite Using Acetylation. Applied Sciences 2018;8:376. https://doi.org/10.3390/app8030376.

[229] Hassan MM, le Guen MJ, Tucker N, Parker K. Thermo-mechanical, morphological and water absorption properties of thermoplastic starch/cellulose composite foams reinforced with PLA. Cellulose 2019;26:4463–78. https://doi.org/10.1007/s10570-019-02393-1.

[230] Bek M, Gonzalez-Gutierrez J, Kukla C, Pušnik Črešnar K, Maroh B, Slemenik Perše L. Rheological Behaviour of Highly Filled Materials for Injection Moulding and Additive Manufacturing: Effect of Particle Material and Loading. Applied Sciences 2020;10:7993. https://doi.org/10.3390/app10227993.

[231] Mazzanti V, Mollica F. Rheological behavior of wood flour filled poly(lactic acid): Temperature and concentration dependence. Polym Compos 2019;40:E169–76. https://doi.org/10.1002/pc.24559.

[232] Běhálek L, Maršálková M, Lenfeld P, Habr J, Bobek J, Seidl M. Study of Crystallization of Polylactic Acid Composites and Nanocomposites with Natural Fibres by DSC Method. NanoCon 2013;18:1–6.

[233] Yoo HM, Jeong S-Y, Choi S-W. Analysis of the rheological property and crystallization behavior of polylactic acid (Ingeo™ Biopolymer 4032D) at different process temperatures. E-Polymers 2021;21:702–9. https://doi.org/10.1515/epoly-2021-0071.

[234] Ecker JV, Haider A, Burzic I, Huber A, Eder G, Hild S. Mechanical properties and water absorption behaviour of PLA and PLA/wood composites prepared by 3D printing and injection moulding. Rapid Prototyp J 2019;25:672–8. https://doi.org/10.1108/RPJ-06-2018-0149.

[235] Chow W, Tham W, Seow P. Effects of maleated-PLA compatibilizer on the properties of poly(lactic acid)/halloysite clay composites. Journal of Thermoplastic Composite Materials 2013;26:1349–63. https://doi.org/10.1177/0892705712439569.

[236] Nurazzi NM, Asyraf MRM, Rayung M, Norrrahim MNF, Shazleen SS, Rani MSA, et al. Thermogravimetric Analysis Properties of Cellulosic Natural Fiber Polymer Composites: A Review on Influence of Chemical Treatments. Polymers (Basel) 2021;13:2710. https://doi.org/10.3390/polym13162710.

[237] Qiang T, Yu D, Gao H, Wang Y. Polylactide-Based Wood Plastic Composites Toughened with SBS. Polym Plast Technol Eng 2012;51:193–8. https://doi.org/10.1080/03602559.2011.618518.

[238] González-López ME, Pérez-Fonseca AA, Cisneros-López EO, Manríquez-González R, Ramírez-Arreola DE, Rodrigue D, et al. Effect of Maleated PLA on the Properties of Rotomolded PLA-Agave Fiber Biocomposites. J Polym Environ 2019;27:61–73. https://doi.org/10.1007/s10924-018-1308-2.

[239] Liminana P, Garcia-Sanoguera D, Quiles-Carrillo L, Balart R, Montanes N. Development and characterization of environmentally friendly composites from poly(butylene succinate) (PBS) and almond shell flour with different compatibilizers. Compos B Eng 2018;144:153–62. https://doi.org/10.1016/j.compositesb.2018.02.031.

Appendices

Appendix A

Supporting Information from Chapter 3

Table A1. One-way ANOVA of the tensile properties of neat PP and the WPCs.

Sample	Cycle #	Tensile strength (MPa)	p value	Young's modulus (GPa)	p value	%Strain	p value
PP100W00	1	35.35 ± 1.065	0.42 > 0.05	1.28 ± 0.040	0.17 > 0.05	313.76 ± 34.84	0.01 < 0.05*
	3	36.31 ± 1.251		1.31 ± 0.044		266.40 ± 29.96	
	6	36.06 ± 1.159		1.33 ± 0.043		238.39 ± 13.48	
PP60W40	1	32.10 ± 0.91	0.00 < 0.05*	2.72 ± 0.10	0.60 > 0.05	2.30 ± 0.23	0.00 < 0.05*
	3	33.29 ± 1.02		2.78 ± 0.07		2.19 ± 0.04	
	6	33.56 ± 0.63		2.75 ± 0.08		1.69 ± 0.13	
PP50W50	1	27.56 ± 0.74	0.01 < 0.05*	3.16 ± 0.10	0.78 > 0.05	2.05 ± 0.44	0.00 < 0.05*
	3	25.59 ± 0.84		3.15 ± 0.06		1.41 ± 0.11	
	6	25.07 ± 1.63		3.20 ± 0.15		1.14 ± 0.12	
PP40W60	1	27.70 ± 1.11	0.00 < 0.05*	3.44 ± 0.13	0.54 < 0.05	1.59 ± 0.11	0.00 < 0.05*
	3	31.68 ± 1.76		3.48 ± 0.05		1.39 ± 0.13	
	6	30.77 ± 1.58		3.52 ± 0.20		1.16 ± 0.09	
PP30W70	3	19.15 ± 0.58	0.00 < 0.05*	3.58 ± 0.15	0.51 > 0.05	0.81 ± 0.06	0.00 < 0.05*
	6	16.89 ± 0.80		3.52 ± 0.11		0.64 ± 0.04	

*-denotes significant change with respect to one way ANOVA p-value (0.05)

Appendix B

Supporting Information from Chapter 4

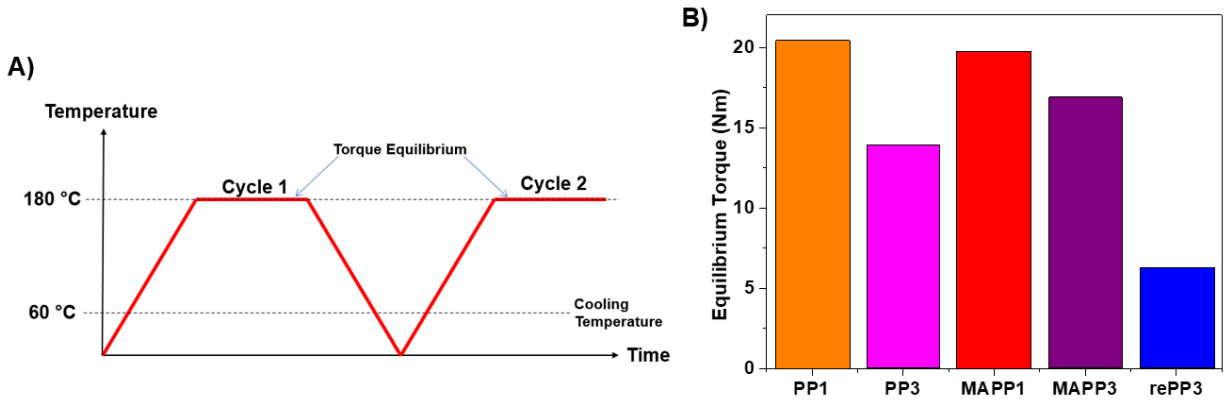

Figure B1. (A) Reprocessing protocol for both the PP and MAPP specimens and **(B)** Equilibrium torque values.

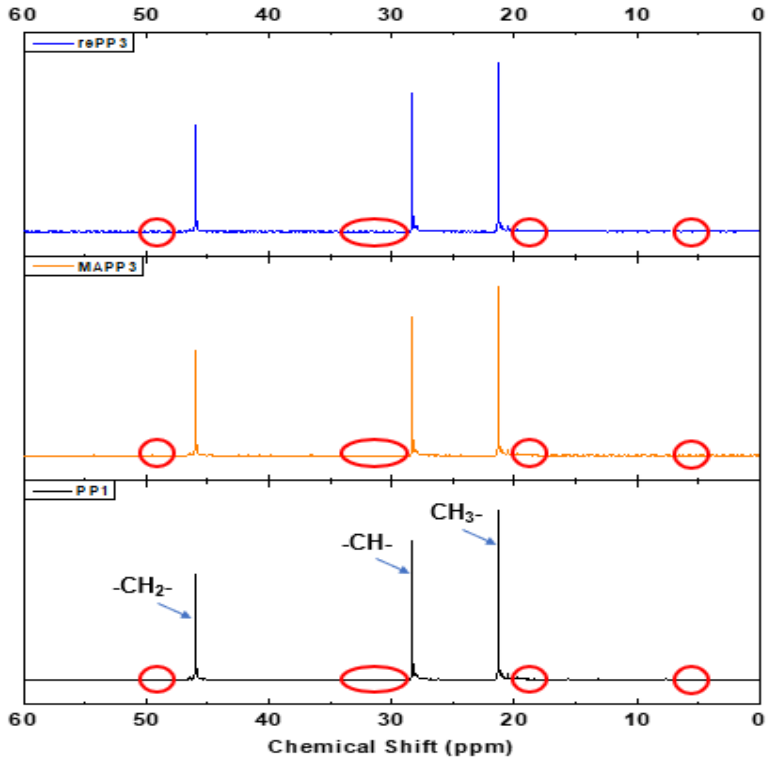

Figure B2. C^{13} NMR spectra of PP, MAPP3 and rePP3 from 0 to 60 ppm.

Table B1. Zero-shear viscosity and power law values from unfilled specimens.

	Zero shear viscosity [η_0] Pa▪s	Consistency index [m] KPa▪s^n	Power Index [n]
PP1	2831	6050	0.42
MAPP1	2410	4082	0.45
PP3	711.9	1252	0.31
MAPP3	1588	2912	0.39
rePP3	392.5	714	0.24

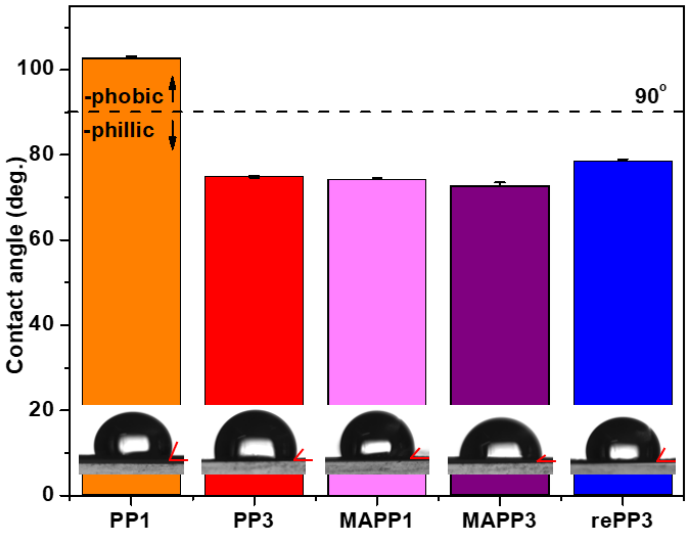

Figure B3. Contact angle determination for the reprocessed and maleated species.

Table B2. Shear stress and power law values from WPC specimens.

	Yield stress [τ_0] Pa	Consistency index [m] KPa▪s^n
PP3(30)WF(70)	1.02×10^7	1.05×10^7
MAPP1(30)WF(70)	5.72×10^6	3.32×10^6
MAPP3(30)WF(70)	3.97×10^5	6.21×10^5
rePP3(30)WF(70)	6.21×10^5	1.63×10^5

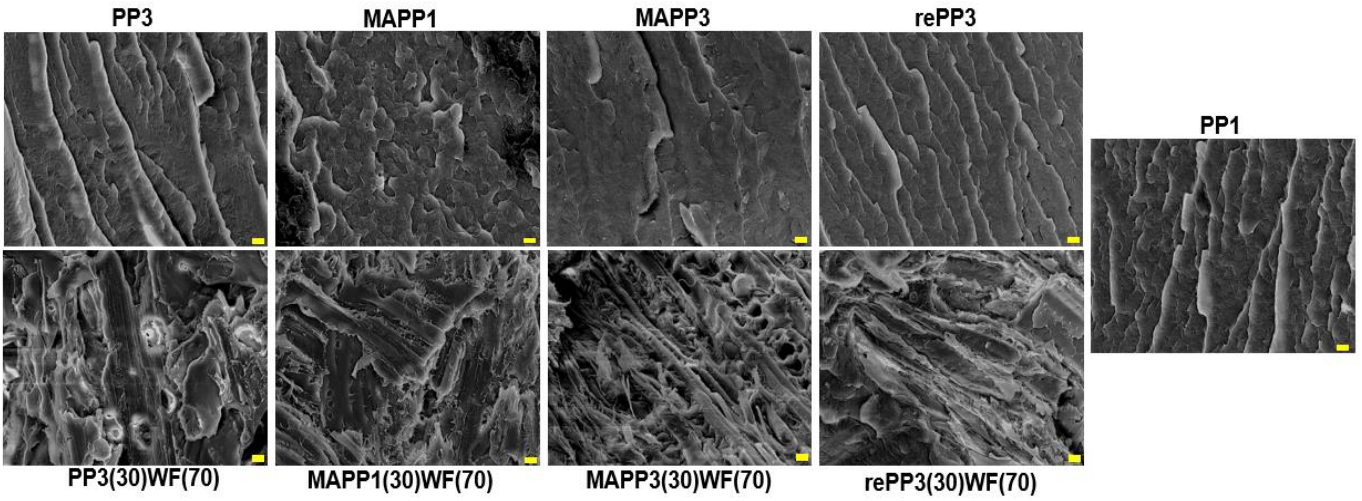

Figure B4. SEM on the impact fracture surface of the PP and rePP3 along with their WPCs (scale bar 10 μm at 500x).

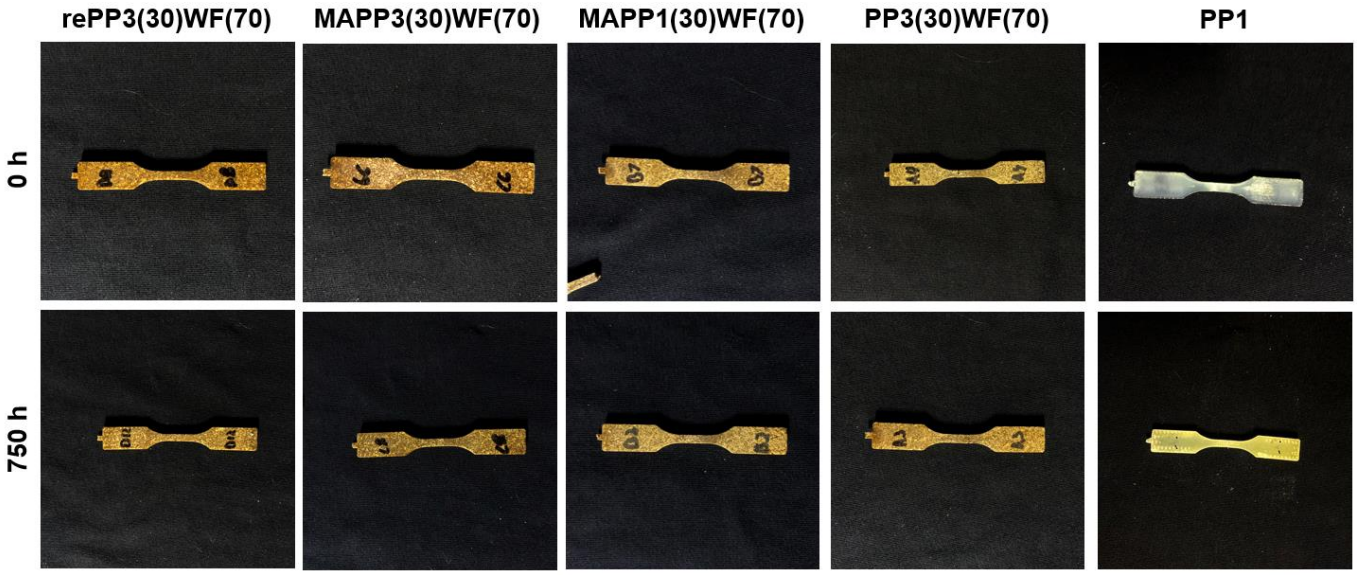

Figure B5. Before (0 h) and After (750 h) UV aging.

Table B3. Colour scale for WPCs and neat PP before and after UV aging.

Material	Colour	0 h	750 h
rePP3(30)WF(70)	Red	196.9	190.2
	Green	147.3	141.5
	Blue	46.9	65.1
MAPP3(30)WF(70)	Red	213.8	147.7
	Green	170.3	112.9
	Blue	45.1	48.7
MAPP1(30)WF(70)	Red	199.5	191.4
	Green	158.5	156.1
	Blue	72.2	78.4
PP3(30)WF(70)	Red	192.7	188.2
	Green	158.8	145.8
	Blue	72.6	63.1
PP1	Red	176.4	192.8
	Green	183.7	185.5
	Blue	166.1	95.3

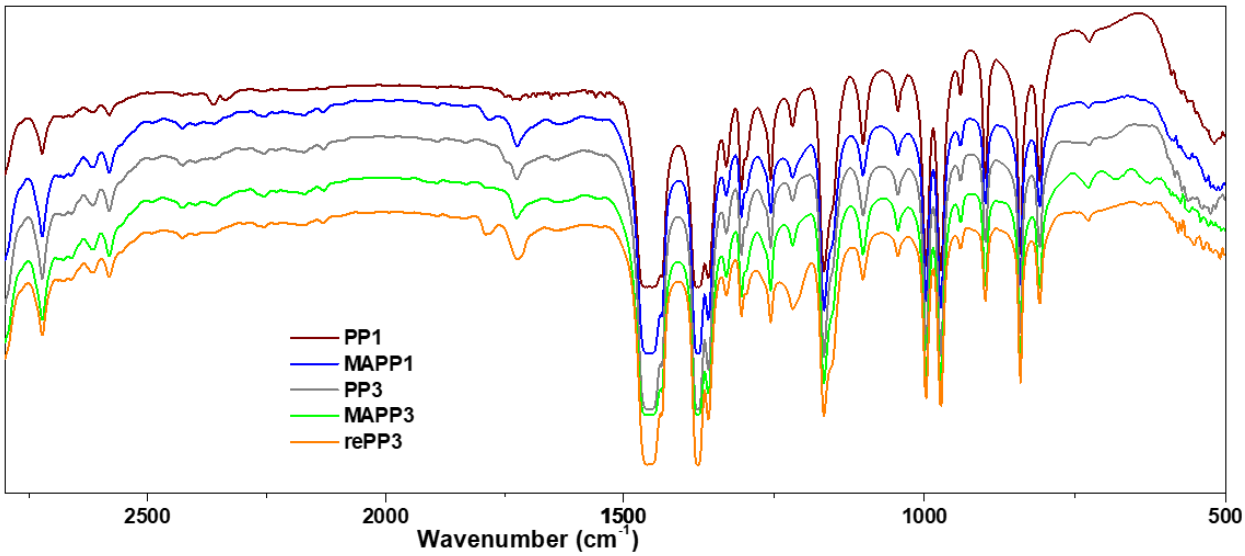

Figure B6. Complete FTIR spectra a PP and its recycled and maleated derivatives.

Appendix C

Supporting Information from Chapter 5

Table C1. Carbon, oxygen, and nitrogen atom breakdown including binding energies, intensities, and relative composition.

Atom Type	Binding Energy (eV)	Intensities (CPS)	Area (%)
WF (Baseline)			
C1	283	13,195	42.8
C2	284	8,956	36.0
C3	286	2,483	21.3
mWF (20 wt.% DDSA)			
C1	285	28,245	58.8
C2	286	9,431	36.9
C3	289	3,162	4.3
WF			
O1	529	1,875	6.20
O2	531	17,326	93.80
mWF			
O1	532	4,342	26.4
O2	533	7,914	73.7
WF			
N1	398	624	90.7
N2	400	45	9.3
mWF			
N1	400	595	87.6
N2	402	4,680	12.4

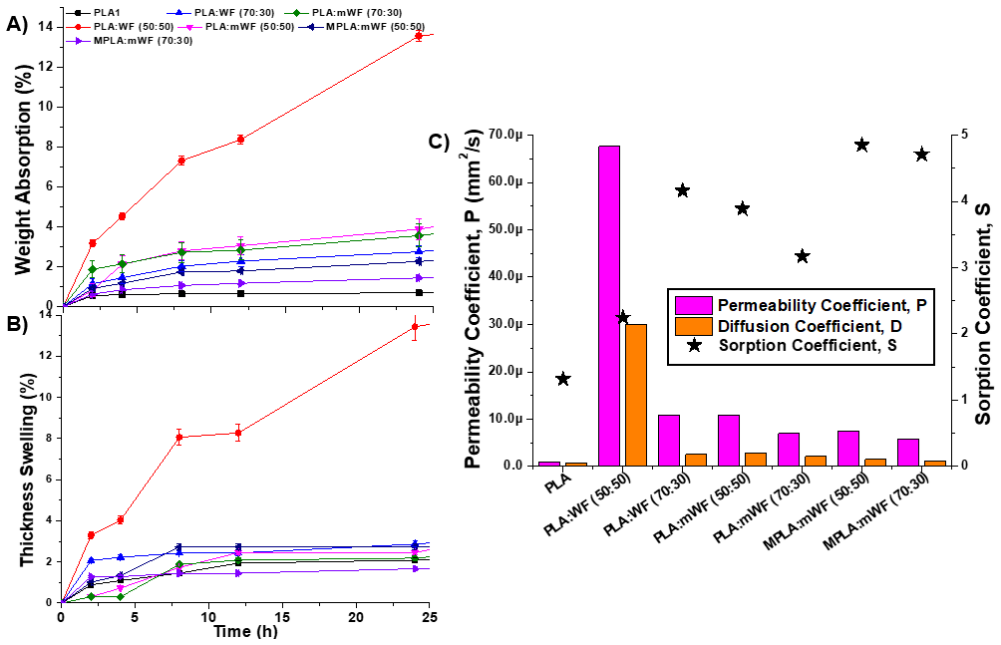

Figure C1. (A) Linear region of the water absorption test for PLA and PLA based WPCs; **(B)** Thickness swelling for PLA based composites; and **(C)** The diffusion, sorption, and permeability coefficients calculated from the linear region of the %WA experiment.

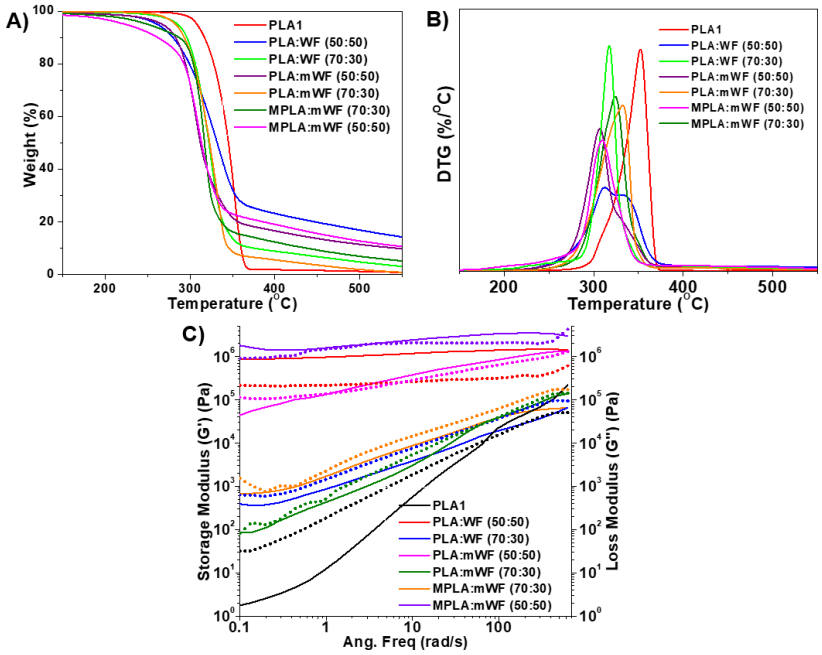

Figure C2. (A) TGA thermograms of the PLA based composites; **(B)** Weight derivative thermogram for the respective WPCs; and **(C)** Storage and loss moduli for the PLA and PLA based WPCs.

Table C2. Recorded tensile strength, modulus, elongation at break, and impact results for all specimens.

	Tensile Strength (MPa)	Young's Modulus (GPa)	Elongation at break (%)	Notched Izod Impact Strength (J/m)
PLA0	66.5 ± 3.1	2.7 ± 0.1	4.5 ± 1.1	39 ± 2.5
PLA1	63.1 ± 5.4	2.9 ± 0.1	4.4 ± 1.1	37 ± 0.7
PLA:WF (50:50)	41.6 ± 3.4	3.9 ± 0.1	1.2 ± 0.1	20.1 ± 2.8
PLA:WF (70:30)	50.4 ± 6.8	3.6 ± 0.2	1.7 ± 0.5	26.5 ± 1.6
PLA:mWF (50:50)	40.5 ± 3.8	4.1 ± 0.1	1.4 ± 0.1	15.3 ± 1.3
PLA:mWF (70:30)	52.5 ± 2.0	3.6 ± 0.1	1.7 ± 0.1	21.9 ± 3.4
MPLA:mWF (50:50)	44.3 ± 2.2	4.4 ± 0.2	1.3 ± 0.3	22.2 ± 2.3
MPLA:mWF (70:30)	54.6 ± 5.1	3.9 ± 0.2	1.6 ± 0.4	29.1 ± 3.2

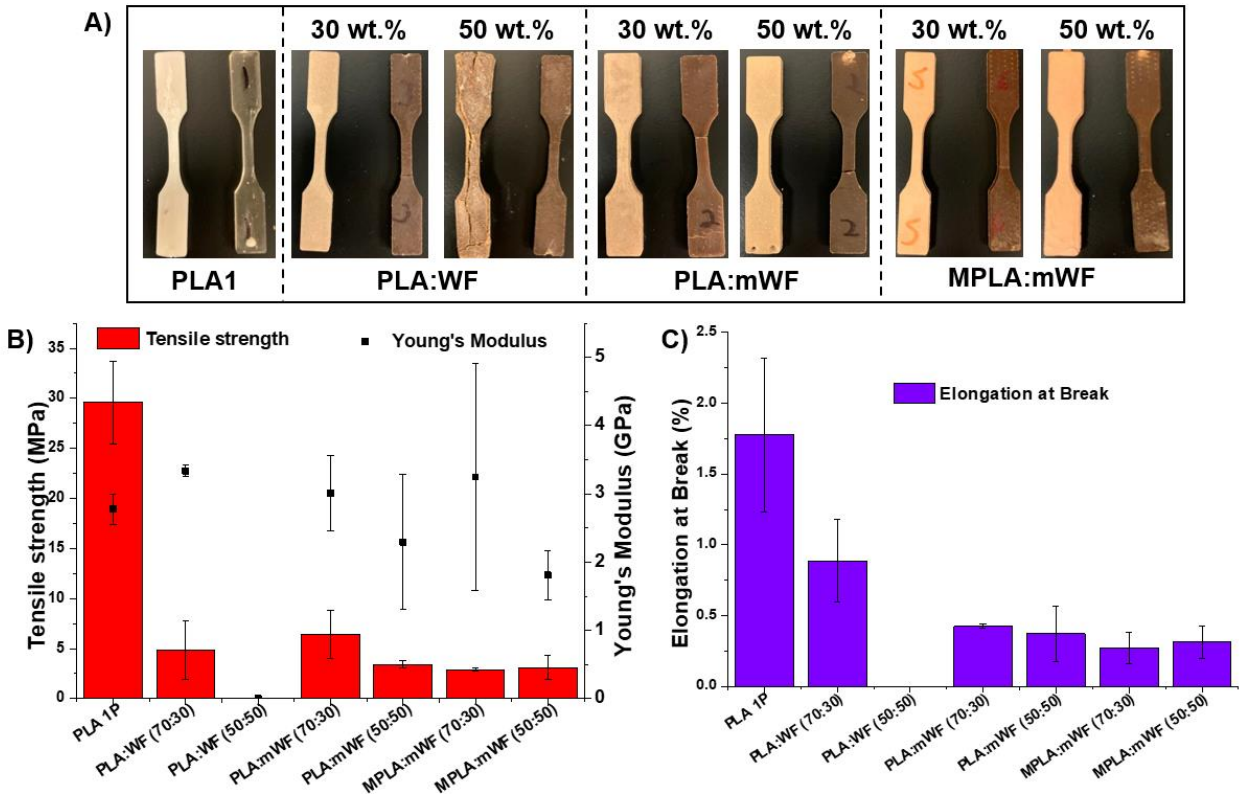

Figure C3. Bond Adhesion testing of the PLA and WPCs. **(A)** Images before (right) and after (left) of tensile bars; **(B)** Tensile strength and modulus for PLA and its WPCs after bond adhesion; and **(C)** Elongation at break results after boiling water test.

Table C3. Testing species geometry.

	Thickness, mm	Length overall, mm	Width overall, mm
Tensile Bar	3	115	19
Impact Bar	3	64	13
Rheology Disc	1	/	25 (Diameter)

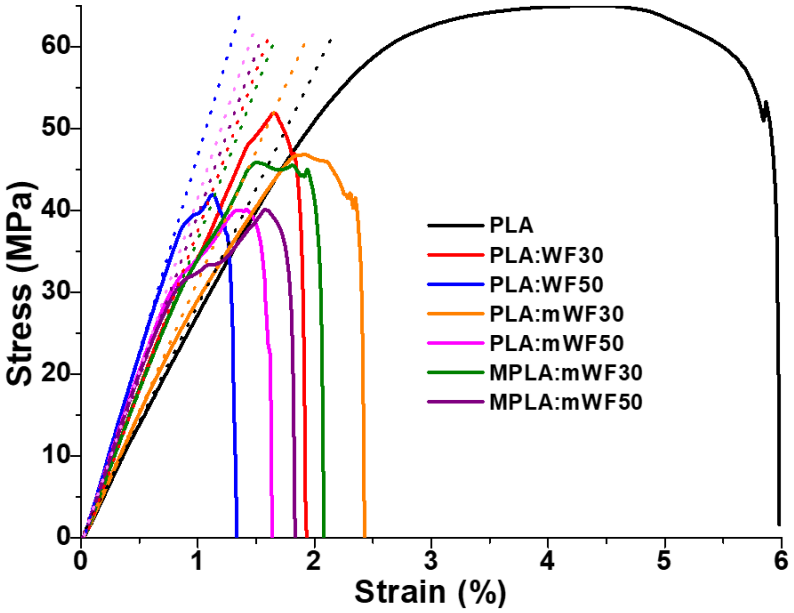

Figure C4. Stress/Strain curve for chapter 5 showing an example from each PLA WPC. The dotted line is showing the Modulus tangent determination.